INVESTIGATION OF ANCHOR NUT LOOSENING IN HIGH-MAST LIGHT POLES USING FIELD MONITORING AND FINITE ELEMENT ANALYSIS

FINAL PROJECT REPORT

by

David Hoisington
Scott Hamel
University of Alaska
Anchorage

for
Pacific Northwest Transportation Consortium (PacTrans)
USDOT University Transportation Center for Federal Region 10
University of Washington
More Hall 112, Box 352700
Seattle, WA 98195-2700

In cooperation with US Department of Transportation-Research and Innovative Technology Administration (RITA)

Disclaimer

The contents of this report reflect the views of the authors, who are responsible for the facts and the accuracy of the information presented herein. This document is disseminated under the sponsorship of the U.S. Department of Transportation's University Transportation Centers Program, in the interest of information exchange. The Pacific Northwest Transportation Consortium, the U.S. Government and matching sponsor assume no liability for the contents or use thereof.

Technical Report Documentation Page

1. Report No.	2. Government Accession No.	3. Recipient's Catalog No.
2012-S-UAF-0014	01538101	

4. Title and Subtitle

Investigation of Anchor Nut Loosening in High-Mast Light Poles Using Field Monitoring and Finite Element Analysis

5. Report Date

September 15, 2014

6. Performing Organization Code

7. Author(s)

David Hoisington, Scott Hamel

8. Performing Organization Report No.

14-739439

9. Performing Organization Name and Address

PacTrans

Pacific Northwest Transportation Consortium, University Transportation Center for Region 10

University of Washington More Hall 112
Seattle, WA 98195-2700

University of Alaska Anchorage

10. Work Unit No. (TRAIS)

11. Contract or Grant No.

DTRT12-UTC10

12. Sponsoring Organization Name and Address

United States of America

Department of Transportation

Research and Innovative Technology Administration

13. Type of Report and Period Covered

Research 9/1/2012-7/31/2014

14. Sponsoring Agency Code

15. Supplementary Notes

Report uploaded at www.pacTrans.org

16. Abstract

High mast lighting poles (HMLPs) are cost effective structures for lighting highways and intersections. They are 100 to 250 feet (30m to 76m) tall, and can hold a variety of lamp configurations. They are commonly used at highway interchanges because a single unit effectively covers more area than the typical, approximately 30 foot (10m) tall, light poles. The AKDOT&PF maintains 104 such poles in the greater Anchorage area.

One issue that has been observed by the Alaska Department of Transportation and Public Facilities (AKDOT&PF) with HMLPs is anchor nut loosening. Anchor rods and their associated nuts are used to secure the HMLP base plate to the pole's foundation. When they're tight, they allow the rods to transfer load from the HMLP to the foundation. The anchor nuts have been loosening on many HMLPs regardless of foundation type, pole height, lamp configuration, date of installation, number of anchor rods, rod diameter, or temperature during the time of installation. Any poles that have loose nuts undergo a re- tightening procedure outlined by the American Association of Highway Transportation Officials (AASHTO). From 2007-2011, 177 inspections were done on 104 poles. 54 of these inspections revealed loose anchor nuts. This program is too costly for the Department to continue indefinitely. The need for solutions for existing and yet to be installed poles is evident.

To understand the behavior of HMLP foundations during tightening, strains were monitored in the anchor rods of two HMLPs. The first was tightened according to existing AASTHO provisions. The second modified those provisions based on the conclusions drawn from the first tightening. The strains in the rods of both HMLPs were monitored after their tightening procedures to try to capture anchor nuts loosening.

The tightening procedures did not result in rod pretension magnitudes below existing recommendations. Some of the rods in the initial tightening procedure resulted in rods tightened above yield. Existing literature suggests that the recommended pretension magnitudes are adequate to prevent nearly all loosening in dynamic loading scenarios of low magnitude. This is how traditional loosening manifests itself, with the nut rotating due to vibratory effects. There are reports by AKDOT&PF personnel who indicated that nuts that were "loose" didn't rotate from a position which was marked after tightening. The loss of clamp load without rotation of either clamping nut has been quantified in previous studies which showed that to simulate this nonlinear post-yield behavior, a complex model is required.

This model must allow for contact interactions, friction between parts, nonlinear behavior, displacement based tightening, and force based loading. Finite-element (FE) modelling satisfies all these requirements in the most accurate way possible. An FE model was created of several HMLP foundation configurations, including the two whose tightening was monitored in the field. In addition to these scenarios, the effects of thickening the base plates, adding stiffeners to the poles, and using high strength anchor rods were analyzed. Significant clamp load loss due to post-yield effects was recreated in all of the scenarios. One such scenario had complete clamp load loss in five rods with a single application of a design wind load. Other scenarios were highly resistant to this type of clamp load loss.

A number of conclusions were drawn from these studies. It is shown that large diameter fasteners with short grip lengths are snug tightened without controlling the torque, they are likely to exceed the recommended snug tight pretension range. Final bolt pretensions would be more likely to fall within the desired range if the degree of rotation in the turn- of-the-nut method were adjusted for the grip length/rod diameter ratio. Clamp load loss due to permanent rod deformation is not affected by pretension magnitude (in F1554 grade 55 rods). The difference between the magnitude of external load required to cause complete clamp load loss in one rod, and that required to cause complete clamp load loss in several rods, is relatively small. Rods in double nut moment connections and high strength rods are less likely to experience clamp load loss due to permanent deformation. Recommendations for existing and yet to be installed HMLPs are presented based on these conclusions

17. Key Words	18. Distribution Statement
High mast lighting poles, anchor nut, loosening, model	No restrictions.

19. Security Classification (of this report)	20. Security Classification (of this page)	21. No. of Pages	22. Price
Unclassified.	Unclassified.		NA

Abstract

High mast lighting poles (HMLPs) are cost effective structures for lighting highways and intersections. They are 100 to 250 feet (30m to 76m) tall, and can hold a variety of lamp configurations. They are commonly used at highway interchanges because a single unit effectively covers more area than the typical, approximately 30 foot (10m) tall, light poles. The AKDOT&PF maintains 104 such poles in the greater Anchorage area.

One issue that has been observed by the Alaska Department of Transportation and Public Facilities (AKDOT&PF) with HMLPs is anchor nut loosening. Anchor rods and their associated nuts are used to secure the HMLP base plate to the pole's foundation. When they're tight, they allow the rods to transfer load from the HMLP to the foundation. The anchor nuts have been loosening on many HMLPs regardless of foundation type, pole height, lamp configuration, date of installation, number of anchor rods, rod diameter, or temperature during the time of installation. Any poles that have loose nuts undergo a re-tightening procedure outlined by the American Association of Highway Transportation Officials (AASHTO). From 2007-2011, 177 inspections were done on 104 poles. 54 of these inspections revealed loose anchor nuts. This program is too costly for the Department to continue indefinitely. The need for solutions for existing and yet to be installed poles is evident.

To understand the behavior of HMLP foundations during tightening, strains were monitored in the anchor rods of two HMLPs. The first was tightened according to existing AASTHO provisions. The second modified those provisions based on the conclusions drawn from the first tightening. The strains in the rods of both HMLPs were monitored after their tightening procedures to try to capture anchor nuts loosening.

The tightening procedures did not result in rod pretension magnitudes below existing recommendations. Some of the rods in the initial tightening procedure resulted in rods tightened above yield. Existing literature suggests that the recommended pretension magnitudes are adequate to prevent nearly all loosening in dynamic loading scenarios of

low magnitude. This is how traditional loosening manifests itself, with the nut rotating due to vibratory effects. There are reports by AKDOT&PF personnel who indicated that nuts that were "loose" didn't rotate from a position which was marked after tightening. The loss of clamp load without rotation of either clamping nut has been quantified in previous studies which showed that to simulate this nonlinear post-yield behavior, a complex model is required.

This model must allow for contact interactions, friction between parts, nonlinear behavior, displacement based tightening, and force based loading. Finite-element (FE) modelling satisfies all these requirements in the most accurate way possible. An FE model was created of several HMLP foundation configurations, including the two whose tightening was monitored in the field. In addition to these scenarios, the effects of thickening the base plates, adding stiffeners to the poles, and using high strength anchor rods were analyzed. Significant clamp load loss due to post-yield effects was recreated in all of the scenarios. One such scenario had complete clamp load loss in five rods with a single application of a design wind load. Other scenarios were highly resistant to this type of clamp load loss.

A number of conclusions were drawn from these studies. It is shown that large diameter fasteners with short grip lengths are snug tightened without controlling the torque, they are likely to exceed the recommended snug tight pretension range. Final bolt pretensions would be more likely to fall within the desired range if the degree of rotation in the turn-of-the-nut method were adjusted for the grip length/rod diameter ratio. Clamp load loss due to permanent rod deformation is not affected by pretension magnitude (in F1554 grade 55 rods). The difference between the magnitude of external load required to cause complete clamp load loss in one rod, and that required to cause complete clamp load loss in several rods, is relatively small. Rods in double nut moment connections and high strength rods are less likely to experience clamp load loss due to permanent deformation. Recommendations for existing and yet to be installed HMLPs are presented based on these conclusions.

Table of Contents

Page

Signature Page i
Title Page iii
Abstract v
Table of Contents vi
List of Figures xi
List of Tables xiii
List of Appendices xv
Acknowledgments xvii
CHAPTER 1: General Introduction 1
References 4
CHAPTER 2: Measured Anchor Rod Tightening of High-mast Light Poles in Alaska 5
2.1 Abstract 5
2.2 Introduction 6
2.3 Background 8
2.3.1 General Bolted Joint Interaction 8
2.3.2 Acceptable pretension ranges 10
2.3.3 Fatigue loading 10
2.3.4 HMLPs Foundation Types 11
2.4 Methodology 12
2.4.1 Calibrating Strain Gages 13
2.4.2 Bolt Installation and Tightening 14
2.5 Results 16
2.5.1 Effect of the Tightening Procedure 19
2.6 Conclusions 22
2.7 Acknowledgments 22
2.8 References 23
CHAPTER 3: Evaluating the Behavior of Anchor Rod Foundations for High-mast Light Poles (HMLPs) using Nonlinear Finite-element Analysis 25

Page

3.1 Abstract 25
3.2 Introduction 26
3.2.1 Background 27
3.2.2 Mechanics of Pre-tensioned Joints 29
3.2.3 Acceptable pretension ranges 29
3.2.4 Monitoring Tightening of Mild Steel Rods 29
3.2.5 External Tensile Loading 30
3.2.6 Fatigue Loading 32
3.2.7 Post Yield Behavior of Bolted Joints 32
3.2.8 Finite-Element Modeling Of Bolted Joints 35
3.2.9 Objectives 36
3.3 Methodology 37
3.3.1 Pole Configurations for Modeling 37
3.3.2 HMLP Geometry 39
3.3.3 Material Behavior 39
3.3.4 Element Description 40
3.3.5 Interaction Definitions 41
3.3.6 Boundary Conditions 41
3.3.7 Applied Loads 42
3.4 Results 44
3.4.1 Flange-Flange Twelve 1.5 inch Rods 44
3.4.2 Flange-Flange Twenty-four 1.5 inch Rods 46
3.4.3 Double Nut Moment Connection Twelve 1.5 inch Rods 46
3.4.4 Effect of Pretension Magnitude 47
3.4.5 High Strength Rods 48
3.4.6 Clamp Load Losses due to Localized Stress 48
3.4.7 Effect of Thicker Plates and Stiffeners 50
3.4.8 Clamp Loss for all Configurations 51
3.5 Summary and Conclusions 51

Page

3.6 References 54
CHAPTER 4: General Conclusions 55
4.1 Conclusions 55
4.2 Limitations 56
4.3 Recommendations 57
4.4 Additional Research 59
References 60
Appendices 60

List of Figures

Page

Figure 2.1: 12 Bolt Group Tightening Sequence 7
Figure 2.2: Force-Displacement Diagram of a Preloaded Bolted Joint's Behavior. 8
Figure 2.3: Force-Displacement Diagram of a Preloaded Joint's Response to Compressive Load. 9
Figure 2.4: Flange-Flange Foundation Type 12
Figure 2.5: Rod Blohm (AKDOT&PF Bridge Crew) turning an Anchor Nut 20 Degrees 15
Figure 2.6: Axial Force in Anchor Rods during the Tightening Procedure and Re-tightening 17
Figure 2.7: Tightening of Anchor Rod #3 18
Figure 2.8: Effect of Adjacent Rods in Rod #3 During Tightening 21
Figure 3.1: HMLP Foundation Types; A: Flange-Flange B: Double Nut C:Cast in Place Concrete 28
Figure 3.2: Mild Steel Response to Tensile Load in (A) low pretension bolts, (B) high pretension bolts 31
Figure 3.3: Clamp Load Loss in High Strength Bolts 33
Figure 3.4: Clamp Loss in Mild Steel Bolts 34
Figure 3.5: Flange-Flange Pretension FEM 36
Figure 3.6: HMLP Assemblies 38
Figure 3.7: Stress-strain Relationship of F1554 Rods Used in FE Models 40
Figure 3.8: Scenario A Load (6800 k*in Moment) 44
Figure 3.9: Scenario A Unload (6800 k*in Moment) 45
Figure 3.10: Scenario C Load (6800 k*in Moment) 46
Figure 3.11:Scenario C Unload (6800 k*in Moment) 47
Figure 3.12:Scenario A Unload (6000 k*in) 49
Figure 3.13:Scenario A with Stiffeners Load (6800 k*in) 50
Figure 3.14:Scenario A with 4.5 Inch Thick Plates Load (6800 k*in) 51

Page

Figure A.1: Type ‘B’ Tightening Sequence 62
Figure A.2: Type ‘B’ Rod Assembly 62
Figure B.1: Tightening Sequence 68
Figure B.2: Rod Assembly 68
Figure C.1: Peters Creek Tightening of Strain Gauges(1) 74
Figure C.2: Peters Creek Tightening of Strain Gauges(2) 75
Figure D.1: Weigh Station HMLP cRIO DAQ 77
Figure D.2: Weigh Station cRIO Long Term Data(1) 78
Figure D.3: Weigh Station cRIO Long Term Data(2) 78
Figure D.4: Weigh Station Custom DAQ Build 79
Figure D.5: Peter’s Creek HMLP Custom DAQ Build 80
Figure D.6: Peter's Creek Time Data (1) 81
Figure D.7: Peter's Creek Time Data (2) 82
Figure E.1: CIP Concrete Pretension (..... 83
Figure E.2: CIP Concrete Load (9500 k*in Moment) 84
Figure E.3: CIP Concrete Unload (9500 k*in Moment) 85
Figure E.4: CIP Concrete Load (18000 k*in Moment) 86
Figure E.5: CIP Concrete Unload (18000 k*in Moment) 86
Figure F.1: F1554 Specimen Tested to Fracture 89

List of Tables

Page

Table 2-1: Axial Loads in Anchor Rods as measured by the strain gages (kips) 19
Table 3-1: HMLP Dimensions for all Scenarios 39
Table 3-2: HMLP Dimensions for Specified FE Models 39
Table 3-3: Abaqus Interaction Definitions for all Scenarios 41
Table 3-4: Minimum Clamp Loss & Separation Moments (All Scenarios) 51
Table C-1: Pretensions in SG Rods 76
Table G-1: RCSC Table 8.1, Minimum Bolt Pretension for High Strength Bolts 91
Table G-2: RSCS Table 8.2, Turn-of-the-Nut Rotation for High Strength Bolts 92
Table H-1: Scenario A Nodes/Element 93
Table H-2: Scenario B Nodes/Elements 94
Table H-3: Scenario C Nodes/Elements 95
Table H-4: Scenario D Nodes/Elements 96
Table K-1: AKDOT&PF HMLP Inspection Reports, 2007-2011 127
Table M-1: FHWA Recommended Turn-of-the-Nut Rotation 135
Table N-1: ASCE 7-10 Moment Calculation Scenarios A & C 138
Table N-2: ASCE 7-10 Moment Calculation Scenario B 139

List of Appendices

Page

Appendix A: Weighstation Tightening Procedure 61
Appendix B: Tightening Procedure for Peter's Creek HMLP 67
Appendix C: Results of Peter's Creek Tightening 73
Appendix D: Long Term Monitoring Data 77
Appendix E: FEA of CIP Concrete HMLP Sixteen 2 Inch Rods 83
Appendix F: ASTM E8 Specimen Test to Fracture 89
Appendix G: RCSC Suggested Minimum Pretension & Rotation for High Strength Bolts 91
Appendix H: FEA Element Descriptions 93
Appendix I: Weighstation DAQ Python Code 97
Appendix J: Peter's Creek Daq Python Code 111
Appendix K: Inspection Reports 127
Appendix L: Strain gauging Procedure 133
Appendix M: Turn-of-the-Nut Rotation Table 135
Appendix N: ASCE 7-10 Design Wind Calculations 137

Acknowledgments

First and foremost, I'd like to thank Scott Hamel, my advisor and co-author for his guidance, expertise, and patience during my time as a graduate student. Without him providing this opportunity, none of this would have been possible.

I'd like to thank Daniel King for his great contribution. He helped in many ways, dealing with LabView, helping during the tightening procedures, and assembling the Data Acquisition Systems.

I'd like to thank Sava White for his contribution to programming and assembling our custom Data Acquisition System.

Thanks to UAA and assisting faculty including Anthony Paris, John Lund, Todd Peterson, Jeff Hoffman, Aaron Doston, and Zlata Lokteva for the help they provided

If my father were another man, I doubt I would have made it this far. His work ethic is a constant reminder that we are always capable of more. My mother has been there for me, as most mothers are, with unconditional love.

This thesis is dedicated to my parents who somehow always knew I was capable of getting through graduate school, even when I didn't.

CHAPTER 1: GENERAL INTRODUCTION

High mast lighting poles (HMLPs) are cost effective structures for lighting highways and intersections. They are 100 to 250 feet (30m to 76m) tall, and can hold a variety of lamp configurations. They are commonly used at highway interchanges because a single unit effectively covers more area than the typical, approximately 30 foot (10m) tall, light poles. Because each HMLP covers more area, they can be placed further from the edge of the roadway. The Alaska Department of Transportation and Public Facilities (AKDOT&PF) maintains 104 such poles in the greater Anchorage area.

There have been problems with HMLPs in the past, including a collapse of a 140' lighting tower in Iowa in 2003. An investigation by Connor et al. (1) showed that the collapse was due to fatigue cracking at the base of the pole. The study concluded that the fracture surfaces were due to weld discontinuities and improper implementation of fatigue based design. The recommendations included a thicker pole base, a thicker pole base plate, and full penetration welds. The HMLPs that the AKDOT&PF currently uses have base plates with thicknesses of 2.25" (compared to 1.25" thickness of the collapsed Iowa pole), backer plates to increase the effective thickness at the pole's base, and full penetration welds. AKDOT&PF inspections have not revealed any signs of fatigue cracking.

The major issue that has been observed by the AKDOT&PF with HMLPs is anchor nut loosening. Anchor rods and their associated nuts are used to secure the HMLP base plate to the pole's foundation. When they're tight, they allow the rods to transfer load from the HMLP to the foundation. The anchor nuts have been loosening on many HMLPs regardless of foundation type, pole height, lamp configuration, date of installation, number of anchor rods, rod diameter, or temperature during the time of installation. Since the issue was discovered in 2007, AKDOT&PF has instituted pole inspections on a 5 year cycle. Any poles that have loose nuts undergo a re-tightening procedure outlined by the American Association of Highway Transportation Officials (AASHTO). From

2007-2011, 177 inspections were done on 104 poles. 54 of these inspections revealed loose anchor nuts. This program is too costly for the Department to continue indefinitely. The need for solutions for existing and yet to be installed poles is evident.

It has been suggested by Garlich and Koonce *(1)* that nut loosening is primarily caused by failure to follow proper tightening procedures as outlined by AASHTO. However, proper tightening procedures have been carefully followed and observed during installation and re-tightening, and the phenomenon of loosening persists.

To uncover the mechanism behind loosening, two methods were used in this study to examine HMLP foundation behavior. First, HMLP behavior was monitored in the field. Strain gauges were inserted into threaded rods which were placed on two HMLPs to record axial strain in the anchor rods during and after installation. One HMLP was tightening according to an AASHTO tightening procedure. Chapter 2 contains this study entitled *Measured Anchor Rod Tightening of High-Mast Lighting Poles in Alaska* which was published in the Transportation Research Record. In this study, the strains are measured and expressed as elastic axial force, which is recorded while the anchor rods of an HMLP are being tightened.

A second HMLP was tightened according to a modified tightening procedure, which was developed from the conclusions reached in chapter 2. The tightening procedure and the data recorded during the tightening of the second HMLP that followed this procedure can be found in the Appendix B and Appendix C, respectively. The strain and wind data gathered from the HMLPs over time after their tightening procedures can also be found in Appendix D.

The second method to investigate HMLP behavior was to analyze Finite-Element (FE) models of various HMLP foundations. Chapter 3 contains a study entitled *Evaluating the Behavior of Anchor Rod Foundations for High Mast Lighting Poles (HMLPs) Using Nonlinear Finite Element Analysis*, which will be submitted for publication in the ASCE Journal of Structural Engineering. In this study, multiple HMLP configurations are

analyzed using the Finite Element Analysis (FEA) program ABAQUS. Three foundation scenarios are examined by applying load in multiple steps. The anchor rods are pre-tensioned to recommended values in the 1st step, then a moment that represents external wind loading is applied to a pole in the 2nd step, and the moment is removed in the 3rd step. Both the design wind moment, and a moment required to cause nuts to "loosen" are applied to each scenario.

One probable mechanism behind anchor rod loosening in Alaska is demonstrated through this study. Conclusions, limitations of the study, recommended further research, as well as recommendations for existing and future designs are presented in chapter 4.

References

[1] M. J. Garlich and J. W. Koonce, "Anchor Rod Tightening for Highmast Light Towers and Cantilever Sign Structures," in *Transportation Research Board 90th Annual Meeting*, Washington, D.C., 2011, vol. 11–2030.

[2] Robert J Connor, Steven H Collicott, Allen M. DeSchepper, Ryan J. Sherman, and Jaime A Ocampo. *Fatigue Loading and Design Methodology for High-Mast Lighting Towers*. Publication NCHRP 718. Transportation Research Board, Washington, D.C., 2012.

CHAPTER 2: MEASURED ANCHOR ROD TIGHTENING OF HIGH-MAST LIGHT POLES IN ALASKA[1]

2.1 Abstract

The Alaska Department of Transportation and Public Facilities owns and maintains 124 high-mast light poles (HMLP) in south-central Alaska. Some of the anchor nuts that secure these 100'+ tall poles to their foundations have been found to loosen without apparent cause. In this study, the axial force was measured in the 1½ inch (38mm) diameter anchor rods of one HMLP during the tightening of new rods. These rods had a relatively low grip-length/diameter ratio of approximately 3. The force was measured using strain gages mounted in a small hole along the anchor rod axis and a computer controlled data acquisition system. The FHWA tightening procedure was followed, including a "snug-tight" condition, followed by 60 degrees of turn-of-the-nut method. The "snug-tight" condition was created by the full force of a workman pulling on a 24 inch (610mm) wrench. A specified verification torque was applied to the nuts after one week to ensure adequate tension in the anchor rods.

It was found that after the tightening procedure, the axial force in several of the twelve rods exceeded their yield capacity. In each rod that yielded, the axial force caused by the "snug-tight" condition was higher than the anticipated values. It was concluded that several variables contributed to the yielding including snug-tight axial loads that were higher than expected, effects of low grip-length/diameter ratios, and an unnecessarily large verification torque.

[1] D. Hoisington, S. Hamel, & J. Hoffman, "*Measured Anchor Rod Tightening of High-Mast Light Poles In Alaska*," in Transportation Research Board 93rd Annual Meeting, Washington, D.C., 2014, vol. 14–0776.

2.2 Introduction

High mast lighting poles (HMLPs) are cost effective structures for lighting highways and intersections. They are 100 to 250 feet (30m to 76m) tall, and can hold a variety of lamp configurations. They are commonly used at highway interchanges because a single unit effectively covers more area than the typical, approximately 30 foot (10m) tall, light poles. Because each HMLP covers more area, they can be placed further from the edge of the roadway.

One issue that has been observed by the Alaska Department of Transportation and Public Facilities (AKDOT&PF) with HMLPs is anchor nut loosening. Anchor rods and their associated nuts are used to secure the HMLP base plate to the pole's foundation. When they're tight, they allow the rods to transfer load from the HMLP to the foundation. The anchor nuts have been loosening on many HMLPs regardless of foundation type, pole height, lamp configuration, date of installation, number of anchor rods, rod diameter, or temperature during the time of installation. It has been suggested by Garlich and Koonce *(1)* that nut loosening is caused by not following proper tightening procedures as outlined by the American Association of Highway Transportation Officials (AASHTO). However, proper tightening procedures have been carefully followed during installation and the phenomenon of loosening persists. Since the issue was discovered in 2007, AKDOT&PF has instituted pole inspections on a 5 year cycle. This program is too costly for the Department to continue indefinitely. The need for solutions for existing and yet to be installed poles is evident. Installation and re-tightening are conducted according to the FHWA publication "Guidelines for the Installation, Inspection, Maintenance and Repair of Structural Supports for Highway Signs, Luminaires and Traffic Signals" *(2)*, which prescribes the "turn-of-the-nut method" used in an alternating star pattern, as shown in Figure 2.1.

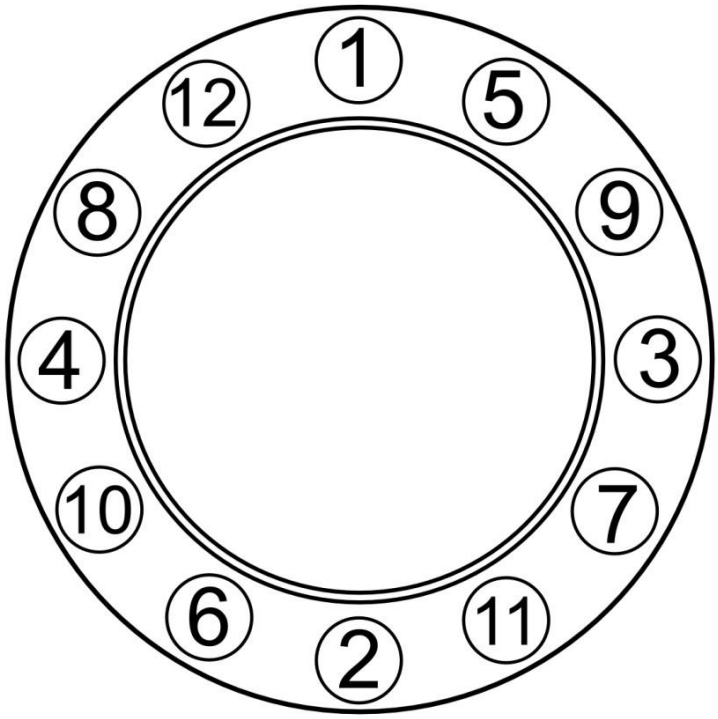

Figure 2.1: 12 Bolt Group Tightening Sequence

Initially, the nuts are all tightened to the "snug tight" condition, to ensure that the nut-plate interface is in contact. The FHWA guidelines define snug tight as the nuts tightened to a pretension between 20-30% of the the final pretension *(2)*. Snug tight is also accepted as the full effort of an average workman on an open-ended wrench with a length equal to 14 times the rod diameter, but not less than 18 inches *(3)*. After the nuts are in the snug-tight condition, they are then tightened past snug tight a portion of a full rotation. As per FHWA recommendations, the 1½ in (38mm) and 2 in (51mm) anchor rods, which are ASTM F1554 Grade 55, are tightened $1/6^{th}$ of a turn. This rotation is accomplished in 3 stages, each comprised of a 20° turn. After this procedure is complete, there must be a follow-up retightening at least 48 hours and at most 2 weeks later. This retightening torque is equal to 110% of the torque used previously in the 20° turns. Re-tightening is to counter any self-loosening and relaxation experienced by the rods.

2.3 Background

2.3.1 General Bolted Joint Interaction

The purpose of the threaded fasteners at the base of HMLPs is to clamp the pole to its foundation through a bolted joint interface. The clamping force is equal to the compression applied to the joint, which is equal and opposite to the tension load in the fastener group. The initial clamping load at each anchor rod is generally achieved by rotating one of its nuts to induce tension in the rod. This tension is referred to as "pre-tension", because it exists before external load is applied.

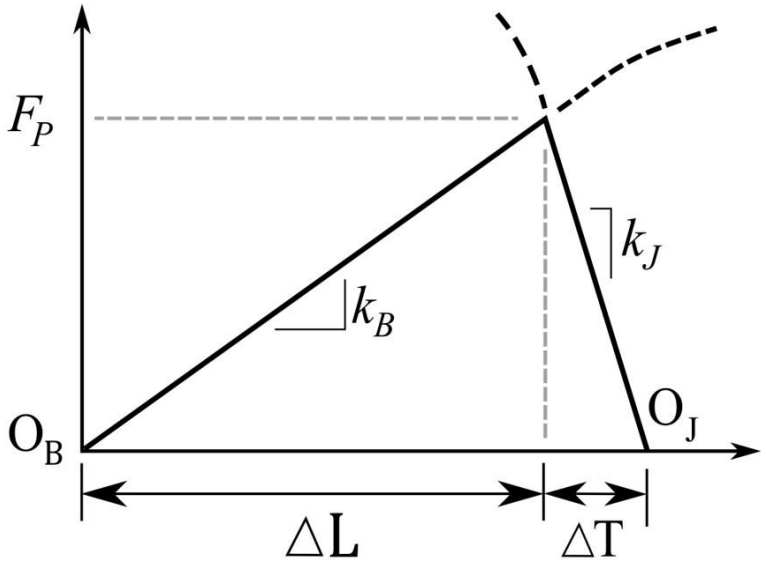

Figure 2.2: Force-Displacement Diagram of a Preloaded Bolted Joint's Behavior.

While the bolt and joint are subject to equal and opposite forces, they do not undergo equal changes in length (or strain). This is due to the difference in stiffness between the bolt and the joint. Generally, the bolt will have 1/3rd to 1/5th of the stiffness of the joint. Figure 2.2 is a diagram from Bickford *(4)* that illustrates the behavior of bolted joints with an applied pre-tension. is the initial length of the bolt, is the initial thickness of the joint, is the pretension magnitude, is the change in length of the bolt, is

the change in thickness of the joint. The figure illustrates that the joint compresses less than the bolt elongates because of its higher stiffness.

When a preloaded bolted joint undergoes external loading, the resulting forces in the bolt and joint depend on the nature of that loading. Tensile loading will increase the load in the bolt while simultaneously decreasing the load in the joint. Compressive loading will increase the load in the joint while simultaneously decreasing the load in the bolt. In other words, the the load applied to the bolt is opposite to that of the joint. Figure 2.3 is a diagram from Bickford *(4)* that illustrates the behavior of bolted joints with an applied external load.

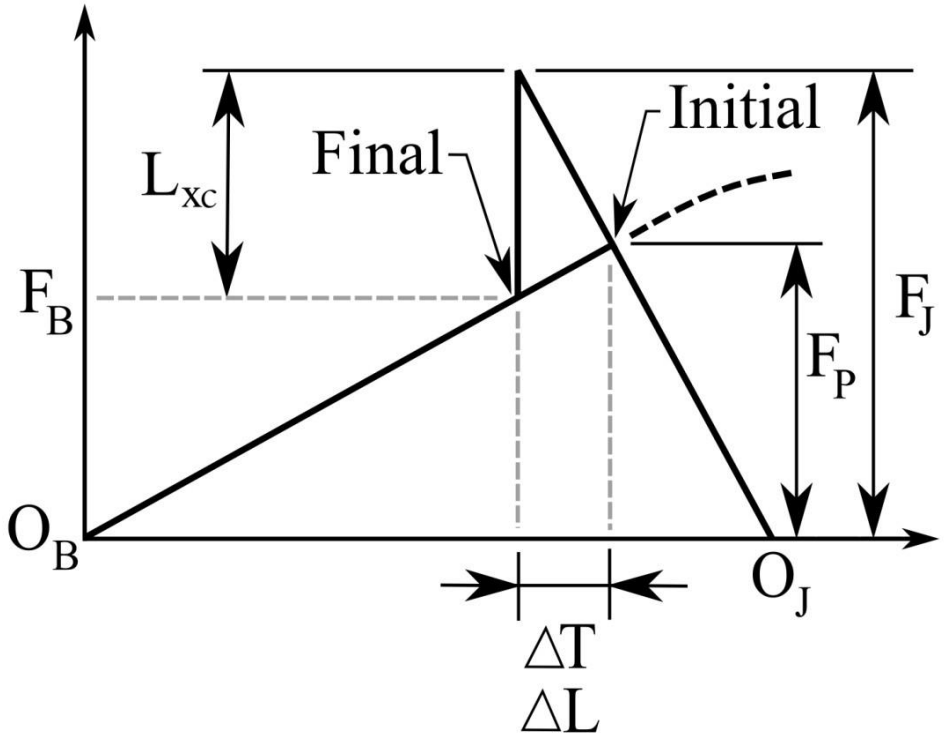

Figure 2.3: Force-Displacement Diagram of a Preloaded Joint's Response to Compressive Load.

F_p is the initial preload, which is equal and opposite in the bolt and the joint. As the external load is applied, the compression will increase in the joint, while the bolt

simultaneiously loses some of its tension load. F_j becomes the force in the joint, F_b is the new force in the bolt, and L_{xc} is the magnitude of the external compressive load. Because the joint is stiffer than the bolt, it experiences a larger change in force than the bolt, while the magnitude of their deflections, (joint compression) and (bolt relaxation) will be equal and opposite.

Most external loads are transferred through moments induced by wind on the pole. For every moment-induced external load, a portion of the bolted joint interface will experience a tensile load and, the remainder will experience compression.

2.3.2 Acceptable pretension ranges

The Research Council on Structural Connections (RCSC) *Specification for Structural Joints Using High-Strength Bolts (5)* recommends that the minimum pretension in high strength bolts should be equal to 70% of their minimum tensile strength. Table 8.2 in this specification dictates the amount of rotation beyond snug tight recommended to reach this minimum pretension. Non high-strength bolts are outside the scope of this standard because the pretension would cause yielding. For these lower-strength bolts, Garlich *(1)* recommends pretension between 50%-60% of the minimum tensile strength. This keeps the pre-tension force high enough to avoid loosening, but low enough to avoid yielding or fatigue failure. Using this recommendation, F1554 Grade 55 rods with a diameter of 1½ in (38mm) and a minimum tensile strength of 75 ksi (517 MPa) have an acceptable pretension range of 53-63kips (247-280kN).

2.3.3 Fatigue loading

A fatigue load is any load that is repeated many times in succession. Fatigue life describes the number of fatigue loading cycles a bolted joint can sustain before failure and is strongly correlated to the peak stress and mean stress that occurs in each cycle. Fatigue failure eventually occurs when an imperfection initiates a crack that propagates with each cycle until rupture occurs. Because the expected number of wind load cycles is unkown, the AASHTO specification for light poles *(6)* recommends an infinite fatigue

life to avoid fatigue failure. A study by James et al. *(7)*, however, found that fatigue did not loosen any nuts, even if they were only tightened to the snug tight condition. The study also concluded that since small alternating stresses due to vortex shedding are the primary alternating fatigue loads in HMLPs, and mean stresses in large diameter anchor rods are generally small, these rods will seldom undergo fatigue failure. James suggests that highly concentrated stresses due to incorrect bolt alignment are more critical than bolt preload when considering fatigue behavior in the elastic range. AKDOT&PF is not aware of any anchor rods that have failed due to rupture, or large cracks that are generally manifested by fatigue failure.

2.3.4 HMLPs Foundation Types

There are several HMLP foundation designs in service in Alaska. For all types, thick base plates that are welded to the pole are attached to the foundation using F1554 Grade 55 anchor rods. These rods have a diameter of are either 1½ inch (38 mm) or 2 inch (50 mm), and are arranged in groups of 12, 16, or 24. The base plates are attached to a foundation pile in two different ways. In the flange-flange type, a flange plate is welded to the top of steel pile, and then clamped to the HMLP's base plate with a short threaded rod and two nuts, as shown in Figure 2.4. In the other type, a concrete cap is cast at the top of the pile with long, approximately 90 inch (2.3m), anchor rods cast in that protrude from the top. The base plate of the HMLP is then positioned above the cap with leveling nuts and secured with top nuts on these anchor rods. This study focused on HMLPs with the double-plate type illustrated in Figure 2.4.

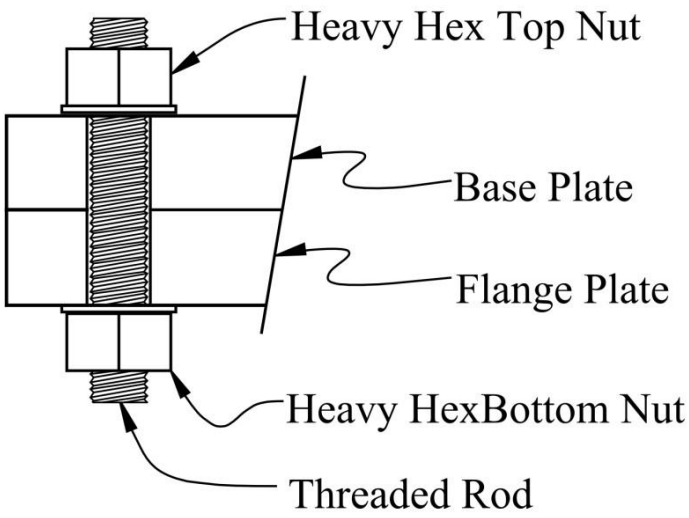

Figure 2.4: Flange-Flange Foundation Type

2.4 Methodology

In order to examine the pretensions in an HMLP bolt group, field testing of an in-service pole during and after the turn-of-the-nut method was utilized. The five year inspection reports from the AKDOT&PF were compiled and reviewed to find a pole that had the following characteristics:

1) The HMLP had a history of nut loosening.
2) The same foundation and bolt group type had a history of loosening in other poles.
3) The HMLP had a flange to flange foundation design.
4) The HMLP has unobstructed location nearby to record wind speed & direction.

For these reasons, the 150 foot (46 m) tall HMLP designated GW1 was chosen. The 43 inch (1092 mm) diameter flange connection consists of twelve 1½ in (38mm) diameter F1554 grade 55 steel threaded rods. These rods clamp the 2.25 in (57 mm) base plate of the HMLP to the 2.25 in (57 mm) flange plate of the driven steel pile. The replacement rods were of the same grade as the existing ones.

To record the tightening procedure, the resulting pretensions, and the axial force in the rods for several months, the measurement system had to meet the following requirements:

1) Rain and snow contact must be avoided in all exposed electronics
2) Faying surfaces and threads must be free of wires
3) Preload measurements should have an accuracy of +/- 1 kip (4.4 kN)
4) The system should be relatively economical so that it could be replicated for all twelve anchor rods

The best method to meet these requirements was to employ strain gages positioned along the central axis of the anchor rods. A 6 inch (150mm) deep, 0.079 inch (2mm) diameter hole was drilled via Electrical Discharge Machining (EDM) into the middle of each bolt. A strain gauge (Texas Measurements BTM-6C-1LDA Bolt Gages) and strain gauge epoxy (Micro-Measurements M-Bond AE15) with an acceptable minimum temperature of -20°F (-29°C) were inserted in the hole. The strain gauge was inserted 5.5 inches (140 mm) into the hole while the epoxy was extruded through a syringe & spinal needle into the hole. The epoxy extrusion continued while slowly pulling the needle out, until the entire volume of the hole was filled with the epoxy. The strain gauge is designed to float in the epoxy, while the epoxy bonds to walls of the hole.

2.4.1 Calibrating Strain Gages

A hydraulic MTS universal testing machine with a 110 kip (500 kN) capacity was used to calibrate the voltage output of the embedded strain gages to a applied axial load on the anchor rods. Custom built steel adapters were used to mount the anchor rods to the test machine. Once mounted in the machine, the load on the anchor rod was increased in a displacement controlled ramp at 0.05 in/min up to approximately 15 kips (67 kN). The strain gauges were connected to a Wheatstone bridge using a ¼ bridge configuration and excited with 10 volts DC. The output voltage was monitored using an NI-9205 cDAQ module. The resulting linear relationship between load and the strain gage output voltage

was determined for each anchor rod and subsequently used in the field to calculate the pre-yield axial force applied during tightening.

2.4.2 Bolt Installation and Tightening

The anchor rods installed in the field were monitored using an NI-9205 CompactDAQ module, which was mounted in a cRIO-9111 Chassis attached to a cRIO-9012 Controller, all products of National Instruments. The data acquisition system recorded output voltages from the strain gages, as well as the air temperature using an EI-1022 thermometer from Labjack Inc.

The anchor rods were tightened according to the "turn-of-the-nut-method" in a four stage process using the "star pattern" for a 12 bolt group specified by FHWA. Each existing anchor rod was loosened, replaced with a strain gauged rod, and the new rod was then tightened to the "snug tight" condition. After all the rods were replaced, each nut was turned 20 degrees with a hydraulic wrench. Figure 2.5 shows Rod Blohm (AKDOT bridge crew) rotating one of the anchor nuts 20 degrees.

Figure 2.5: Rod Blohm (AKDOT&PF Bridge Crew) turning an Anchor Nut 20 Degrees

The tightening process was repeated two more times for a total of 60 degrees of rotation as specified by the FHWA Guidelines *(2)*. After one week, as recommended by NCHRP Report 469 *(8)*, the rods were tightened with a verification torque equal to 110% of the installation torque. The installation torque, as defined by the Guidelines *(2)* is specified as

(1)

T_i=Installation Torque

d_b=Nominal bolt diameter (inches)

P_i=Installation Pretention (kips), which is calculated using a stress equal to 60% of the minimum tensile strength of Grade 55 rods and the minimum cross-sectional area of the bolt.

The 0.12 coefficient in Equation (1) is an approximation that is used to replace the contact diameter constants and friction coefficients. This constant was suggested by Till

and Lefke *(9)*. Equation 1 utilizes a pretension of 79 kips and resulted in a final torque of 1150 ft-lbs (1.56 kN-m) for the anchor rods in this study. After one week, as per FHWA recommendations, a verification torque of 1300 ft-lbs (1.76 kN-m), which is 110% of the final torque, was applied. These torque values, which were published in the existing AKDOT&PF tightening procedure, were mistakenly based on the nominal cross-sectional area of the rods, 1.76 in^2 (1142 mm^2). The correct usage of equation 1, as outlined in NCHRP 469 *(8)*, utilizes the tensile stress area, 1.41 in^2 (906 mm^2), which is calculated from the minimum diameter. This results in a pretension force of 63 kips, and the correct torque values for the final and verification torques are 945 ft-lbs (1.28 kN-m) and 1040 ft-lbs (1.41 kN-m), respectively.

2.5 Results

The installation of the strain-gaged threaded rods was conducted in February of 2013, the ambient air temperature was approximately 25^{o}F (-4^{o}C). The temperature, and the large number of wires, caused the installation to be slower than usual, and took about 3 hours. In some cases, heat was used to unfreeze the existing rods for removal. Four of the twelve rods produced unreliable results either due to electronic hardware components (broken connections) or thermal issues.

The results of the tightening procedure, along with the retightening a week later, can be seen in Figure 2.6. The nominal yield load of 55ksi (379 MPa), based on the tensile stress area is shown. In addition, one bolt was machined to a dogbone specimen and tested to failure according to ASTM E8. The results of this test are shown in 0. The magnitude of the load associated with the measured yield stress from that test of 63 ksi (434 MPa) is shown. It is clear from this figure that at least one anchor rod, #3, exceeded its yield stress during tightening. This matches the experience in the field, where the nut turned with seemingly little resistance when the verification torque was applied. A closer look at rod #3 is shown in Figure 2.7. The rods have a specified yield stress of 55ksi (379 MPa), which combined with a tensile stress area of (910), results in

yielding at an axial force of 77kips (343 kN). Rod #3 is around its yield point at the end of the tightening procedure. Upon returning a week later, the rod was tightened with the verification torque, seen in Figure 2.6.

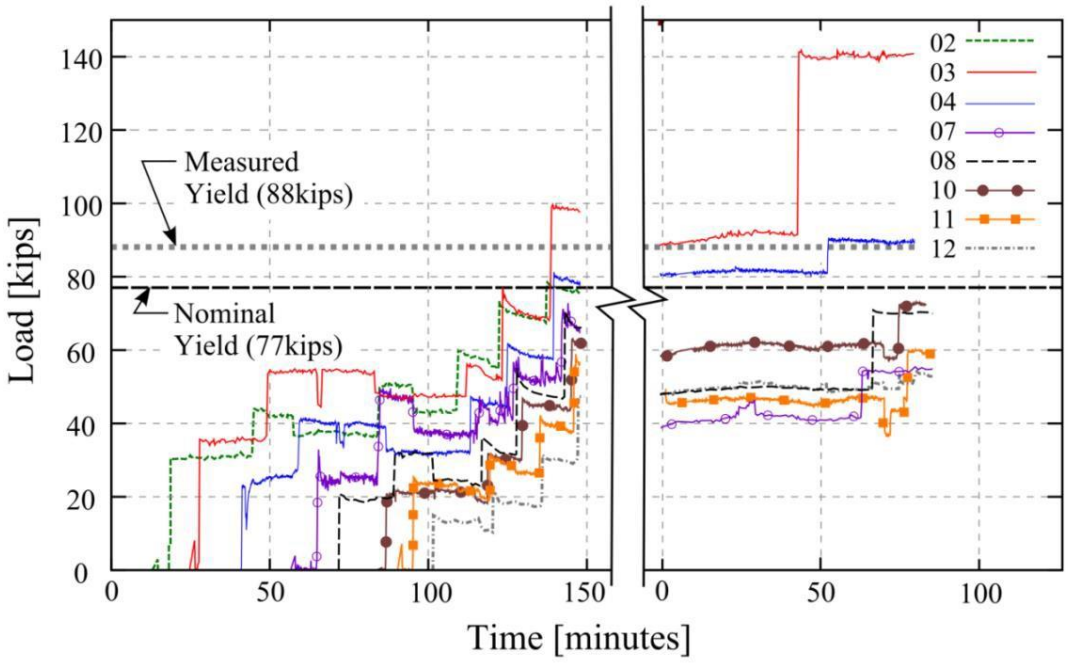

Figure 2.6: Axial Force in Anchor Rods during the Tightening Procedure and Re-tightening

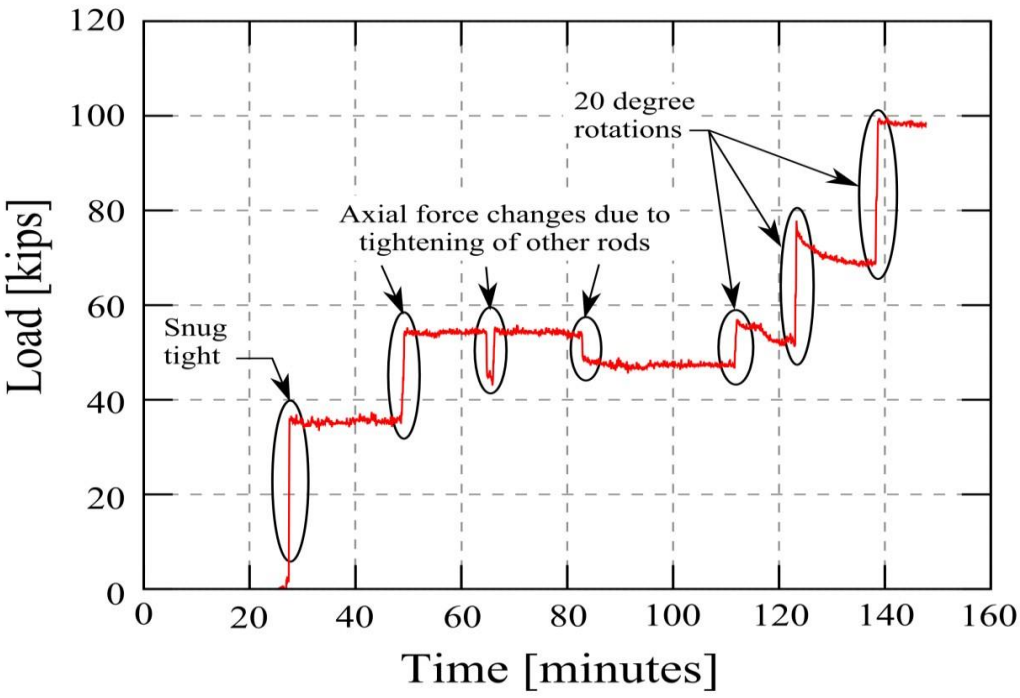

Figure 2.7: Tightening of Anchor Rod #3

Rod #3 has clearly yielded in this figure. Since the load has been extrapolated from strain based on the elastic modulus of the bolt, any load above the yield stress is inaccurate. It is a reasonable representation of the strain in the bolt as a percentage of the yield strain. In the case of Rod #3, the fastener was stretched about 40% beyond its yield strain.

As mentioned above, eight of the twelve strain gauges returned complete data during the tightening procedure. Table 2-1 shows the values returned by each strain gauge at the end of each stage of tightening. It also shows the total pretension developed during the $1/6^{th}$ of a turn and recorded rotation experienced by each tension nut during re-tightening. FIGURE 6 shows the pretension in each of the 8 strain gauges over time. The break in the data indicates the one week wait before re-tightening with the verification torque.

Table 2-1: Axial Loads in Anchor Rods as measured by the strain gages (kips)

Bolt #	Snug Tight	20 degrees	40 degrees	60 degrees	Verif. Torque	Pretension turn-of the-nut	Rotation during Verification (deg)
1**	--	--	--	58	--	--	45+
2	31	59	73	76	358*	46	60+
3	36	56	76	99*	141*	63	30+
4	23	47	58	80*	90*	57	8
7	25	41	52	65	55	40	8
8	21	36	53	66	70	45	20
9**	--	--	--	--	--	--	5
10	21	31	44	62	72	41	12
11	25	31	41	57	59	32	10
12	15	21	31	48	53	33	10

*Indicates yielded Anchor Rod

+Rotation was halted

** Signal was lost in Rods 1 and 9 due to severed electrical connections

2.5.1 Effect of the Tightening Procedure

Using 20-30% of final pretension, which is 60% of minimum tensile strength, as a target for snug tight results in a range of 12-19 kips (57-84 kN) for the rods used in this study. The average force in the rods from the snug-tight procedure was 25 kips (111 kN), and most of the rods were tensioned beyond the recommended range.

The rods used in this study had a grip length of 4.5 inches (114.3mm), which is 3 times the bolt diameter (d_b). Table 2-1 shows the change in pretension the rods experience after the nuts have been rotated 1/6th of a turn. In "Guidelines for the Installation, Inspection, Maintenance and Repair of Structural Supports for Highway Signs, Luminaires and Traffic Signals" *(2)*, the FHWA recommends that nuts be rotated 1/6th of a turn for all bolt diameters greater than 1½ inch (38.1mm). The turn-of-the-nut method resulted in an

average of 45kips (198 kN) of axial force developed above the snug tight tension. 1½ inch (38.1mm) diameter rods on HMLPs in service in Alaska are as low as $1.5d_b$, and as high as $4.5d_b$. If a nut on a 1½ inch (38.1mm) diameter rod with a grip length of $1.5d_b$, were rotated the same $1/6^{th}$ of a turn, the rod would develop significantly more preload.

Returning and applying the verification torque used in the turn–of-the-nut method resulted in the yield of four rods, three of which had not yielded prior to re-tightening. Table 2-1 shows the rotations the nuts experienced during this re-tightening. Note that the nut tightening of rods #1, #2, & #3 were stopped after excessive rotation. The rods that were brought close to yield during snug tight and turn-of-the-nut resulted in yielding when re-tightened. The correct verification torque is expected to result in 70 kips (311kN) of pretension, which is equal to 90% of the yield strength.

Isolating changes in the axial force of an individual rod during the tightening sequence demonstrates that the axial load can be affected by adjacent rods in the group. Figure 2.8 shows anchor rods that affected the axial tension in rod #3.

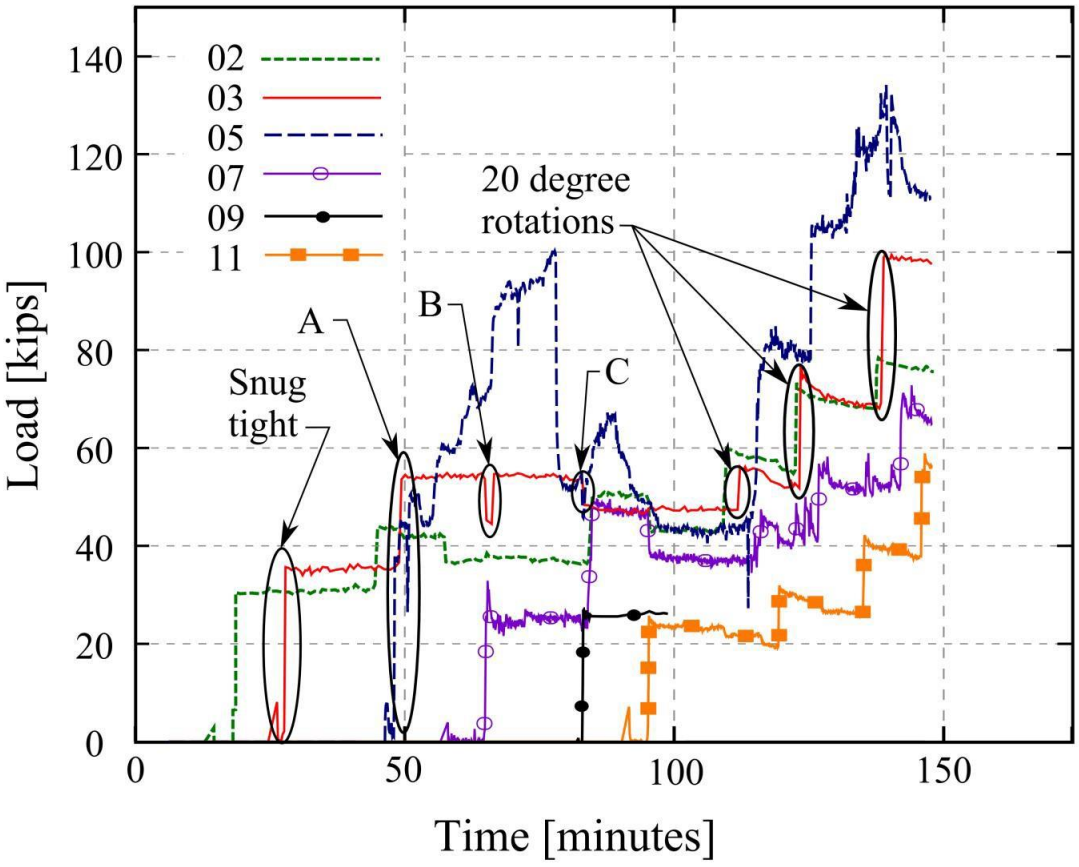

Figure 2.8: Effect of Adjacent Rods in Rod #3 During Tightening

Jump ‘A’ is due to rod #5 being tightened to snug tight. The loss and jump in ‘B’ is due to existing rod #7 being removed (it is adjacent to bolt #3) and then the new rod #7 being tightened to snug tight. The loss in ‘C’ is due to existing rod #9 being loosened and removed. Existing pretension in the original rods likely exceeds snug tight, which when removed affects the surrounding anchor rods. Rods #7 & #9 are adjacent to rod #3, and rods #5 & #11 are two positions away. These four rods are the ones in which a change in pretension is most likely to affect rod #3 and, as shown in the figure, the time at which these rods are brought to snug tight aligns with the pretension changes in rod #3.

2.6 Conclusions

In this study, the axial force was measured in the anchor rods of a high-mast light pole during the tightening of new rods on an existing pole. This was done using strain gages mounted in the center of the anchor rods and a computer controlled data acquisition system. The FHWA tightening procedure was followed, including a snug-tight condition, followed by 60 degrees of turn-of-the-nut method. It was determined that several of the anchor rods yielded during the tightening procedure. It was also noted that the rods that yielded were largely tightened beyond the target loads during the initial step (snug-tight) of the procedure. Based on the foundation type, anchor rod geometry, and data acquired during this study, three primary conclusions were drawn:

1) Large diameter fasteners with short grip lengths that are snug tightened without controlling the torque are likely to exceed the recommended snug tight pretension range.
2) If the degree of rotation in the turn-of-the-nut method were adjusted for the grip length/rod diameter ratio, in addition to existing recommendations about bolt diameter and grade, then final bolt pretensions would be more likely to fall within the desired range.
3) If the verification torque were reduced from 60% to 50% of the minimum tensile stress of F1554 Grade 55, as is the case with F1554 grade 36, the rods would be less likely to yield.

2.7 Acknowledgments

Funding for this project was provided by The Pacific Northwest Transportation Consortium (PACTRANS) through the Alaska University Transportation Center (AUTC), and by the Alaska Department of Transportation and Public Facilities (AKDOT&PF). A large amount of assistance in the experimental setup and data analysis was provided by Daniel King. Assistance in testing was provided by Anthony Paris, Ph.D.,P.E., and John Lund, Ph.D.

2.8 References

1. Michael J. Garlich, and Jeremy W. Koonce. Anchor Rod Tightening for Highmast Light Towers and Cantilever Sign Structures. In *Transportation Research Board 90th Annual Meeting*, No. 11-2030, Washington, D.C., 2011.
2. Michael J. Garlich, and Eric R. Thorkildsen. *Guidelines for the Installation, Inspection, Maintenance and Repair of Structural Supports for Highway Signs, Luminaires, and Traffic Signals*. Publication FHWA NHI 05-036. Federal Highway Administration, Washington, D.C., Mar. 2005.
3. Robert J Connor, Steven H Collicott, Allen M. DeSchepper, Ryan J. Sherman, and Jaime A Ocampo. *Fatigue Loading and Design Methodology for High-Mast Lighting Towers*. Publication NCHRP 718. Transportation Research Board, Washington, D.C., 2012.
4. Bickford, J. H. *An Introduction to the Design and Behavior of Bolted Joints*. CRC Press, 1995.
5. Research Council on Structural Connections. *Specification for Structural Joints Using High-Strength Bolts*. AISC, Chicago, Il, 2009.
6. American Association of State Highway and Transportation Officials. *Standard Specifications for Structural Supports for Highway Signs, Luminaires, and Traffic Signals*. AASHTO, 2009.
7. James, R. W., P. B. Keating, R. W. Bolton, F. C. Benson, D. E. Bray, R. C. Abraham, and J. B. Hodge. *Tightening Procedures for Large-Diameter Anchor Bolts*. Publication 1472-1F. Texas Transportation Institute, Texas A&M University System, College Station, TX, 1997.
8. R. J. Dexter, and M. J. Ricker. *Fatigue-Resistant Design of Cantilever Signal, Sign, and Light Supports*. Publication NCHRP 469. Transportation Research Board, Washington, D.C., 2002.
9. R. D. Till, and N.A. Lefke. *The Relationship Between Torque, Tension, and Nut Rotation of Large Diameter Anchor Bolts*. Publication R-1330. Michigan Dept. of Transportation, Lansing, MI, Oct. 1994.

CHAPTER 3: EVALUATING THE BEHAVIOR OF ANCHOR ROD FOUNDATIONS FOR HIGH-MAST LIGHT POLES (HMLPS) USING NONLINEAR FINITE-ELEMENT ANALYSIS[1]

3.1 Abstract

This study examines the behavior of High Mast Lighting Pole (HMLP) foundations through the use of nonlinear finite-element modeling. HMLPs utilize nuts & threaded rods to clamp the light pole structure's base plate to the foundation. Inspections by the Alaska Department of Transportation and Public Facilities (AKDOT&PF) have revealed widespread loosening of the nuts used on HMLPs. The threaded rods used are F1554 Grade 55, which are heat treated from mild steel rods (=36ksi) to gain additional yield strength. This study briefly highlights the difference in post yield behavior in mild steel and high strength steel and proposes a probable mechanism behind the clamp load loss experienced by Alaska's HMLPs. Because the HMLPs are much taller than traditional lighting poles, they experience larger external wind loading. This wind load is potentially stressing threaded rods into the post yield range. A previous study shows that the current tightening procedure is likely not under-tightening nuts, which could be a major culprit behind loosening. Due to this and previous research it is believed that the nuts aren't "loosening" in the traditional sense of losing clamp because they are rotating on the threads during external load. Instead, this study concludes that during external loading, threaded rods undergo significant post yield strain. This strain translates into plastic deformation, which is large enough in magnitude to make the bolted joint interface lose clamp load when the external force is removed. This clamp loss mechanism is examined by applying wind loads to three pre-tensioned HMLP configurations using finite element analysis software (ABAQUS). The analysis uses 3-D solid elements, contact surfaces that allow for separation, bonding surfaces where contact

[1] D. Hoisington, S. Hamel, "*Evaluating The Behavior Of Anchor Rod Foundations For High Mast Light Poles (HMLPs) Using Nonlinear Finite Element Analysis*", prepared for ASCE Journal of Structural Engineering

surfaces aren't required, boundary conditions that approximate reality, displacement controlled pretension, and external wind loading represented by coupled moments. The FE model produces clamp load loss due to permanent deformation of threaded rods in all HMLP scenarios.

3.2 Introduction

High mast lighting poles (HMLPs) are cost effective structures for lighting highways and intersections. They are 100 to 250 feet (30m to 76m) tall, and can hold a variety of lamp configurations. They are commonly used at highway interchanges because a single unit effectively covers more area than the typical, approximately 30 foot (10m) tall, light poles. Because each HMLP covers more area, they can be placed further from the edge of the roadway.

One issue that has been observed by the Alaska Department of Transportation and Public Facilities (AKDOT&PF) with HMLPs is anchor nut loosening. Anchor rods and their associated nuts are used to secure the HMLP base plate to the pole's foundation. When they're tight, they allow the rods to transfer load from the HMLP to the foundation. The anchor nuts have been loosening on many HMLPs regardless of foundation type, pole height, lamp configuration, date of installation, number of anchor rods, rod diameter, or temperature during the time of installation. It has been suggested by Garlich and Koonce [1] that nut loosening is caused by failure to follow proper tightening procedures as outlined by the American Association of Highway Transportation Officials (AASHTO). However, proper tightening procedures have been carefully followed during installation and the phenomenon of loosening persists. Since the issue was discovered in 2007, AKDOT&PF has instituted pole inspections on a 5 year cycle. This program is too costly for the Department to continue indefinitely. The need for solutions for existing and yet to be installed poles is evident.

3.2.1 Background

There are three general HMLP foundation types currently in service in Alaska. These are shown in Figure 3.1.

- A flange-flange connection where the pole's base plate is connected to the pile's flange plate (Figure 3.1A).
- A double nut moment connection where the base and flange plate are clamped separately (Figure 3.1B).
- A cast in place concrete configuration where the pole's base plate is clamped using anchor rods that are embedded in concrete (Figure 3.1C).

The majority of AKDOT poles are either flange-flange foundations or cast in place concrete foundations. Inspections have revealed loose nuts in both of these connections.

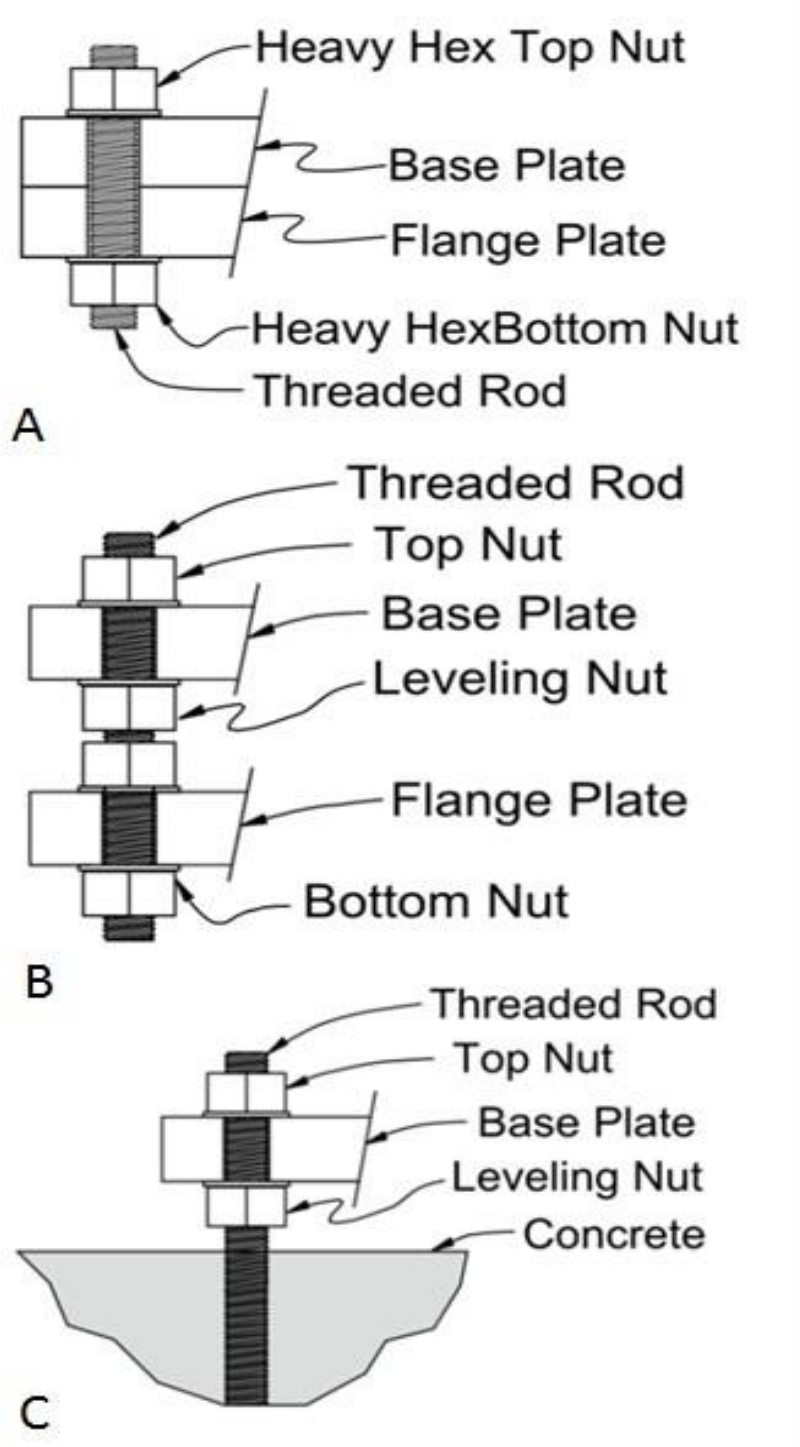

Figure 3.1: HMLP Foundation Types; A: Flange-Flange B: Double Nut C:Cast in Place Concrete

3.2.2 Mechanics of Pre-tensioned Joints

The purpose of the threaded fasteners at the base of HMLPs is to clamp the pole to its foundation through a bolted joint interface. The clamping force is equal to the compression applied to the joint, which is equal and opposite to the tension load in the fastener group. The initial clamping load at each anchor rod is generally achieved by tightening one of its nuts to induce tension in the rod. This tension is referred to as "pre-tension", because it exists before external load is applied.

While the bolt and joint are subject to equal and opposite forces, they do not undergo equal changes in length (or strain). This is due to the difference in stiffness between the bolt and the joint. Generally, the bolt will have $1/3^{rd}$ to $1/5^{th}$ of the stiffness of the joint, and stretch 3-5 times more than the joint for a given pretension [3] .

3.2.3 Acceptable pretension ranges

The Research Council on Structural Connections (RCSC) *Specification for Structural Joints Using High-Strength Bolts* [3] recommends that the minimum pretension in high strength bolts should be equal to 70% of their minimum tensile strength (Also known as "ultimate strength" or "rupture strength"). RCSC also dictates the amount of rotation beyond snug tight recommended to reach this minimum pretension. Non high-strength bolts are outside the scope of this standard because the pretension could cause yielding. For these lower-strength bolts, Garlich [4] recommends pretension between 50%-60% of the minimum tensile strength. Based on research by James [6], this should keep the pre-tension high enough to avoid loosening.

3.2.4 Monitoring Tightening of Mild Steel Rods

The bolts modeled in this study are F1554 Gr. 55 (=55ksi, =75-95ksi). The study in chapter 2 monitored the forces in the anchor rods during a tightening procedure that followed FHWA turn-of-the-nut guidelines. This procedure produced pretensions in the rods between 50-80% of their minimum tensile strength. Appendix C contains data

collected during a modified tightening procedure on a second HMLP that attempted to control pretension scatter. This tightening procedure produced pretensions in the rods between 50-60% of their minimum tensile strength. Because neither procedure resulted in under-tightened rods, low pretension is likely not a factor behind loosening in HMLPs with flange-to-flange connections.

3.2.5 External Tensile Loading

The pre-tensioned bolted joint interface will absorb external force based on the stiffness ratio of the bolt and the joint, and how close the bolt is to yield. In Figure 3.2, a graph modified from Bickford [3], it can be seen that the mild steel bolt has a range on the stress-strain curve where its post yield stiffness is equal to zero. In this figure, F_p is the magnitude of pretension, is the force in the bolt, is the force in the joint, is the external tensile load applied to the interface, is the external tensile load that will completely unload the joint, and is the external load that will result in the bolt absorbing additional load post yield. The negative Y axis shows the force in the joint, while the positive Y axis shows the force in the bolt. The X axis represents an external tensile load, increasing in value.

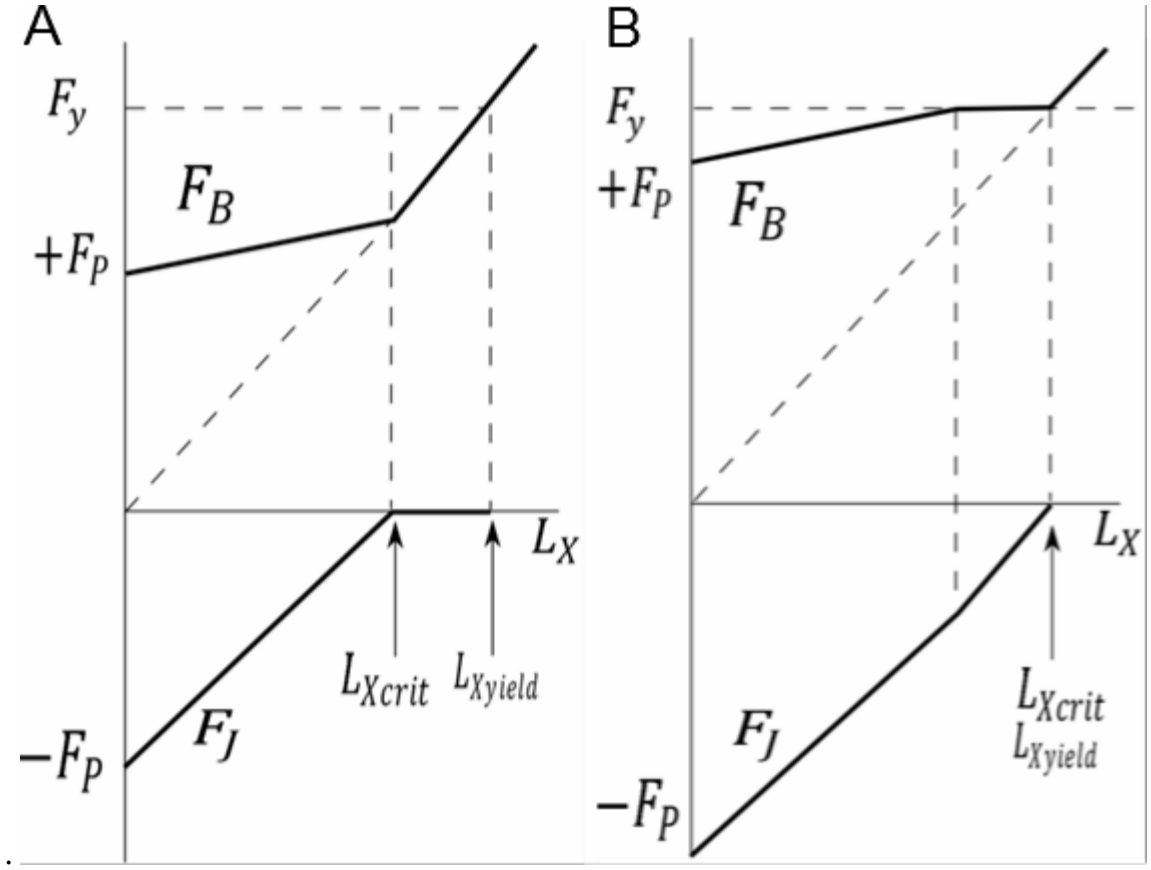

Figure 3.2: Mild Steel Response to Tensile Load in (A) low pretension bolts, (B) high pretension bolts

Figure 3.2A shows load absorption of a bolted joint where the bolt yields after the plate is unloaded because it has lower pretension. Figure 3.2B shows load absorption of a bolted joint where the bolt yields before the plate is unloaded because it has higher pretension.

Inspecting the two graphs, it can be seen that pre yield, the joint can only absorb a force equal to , while the bolt can absorb a force equal to . Adding the two together shows that pre yield, the bolted joint interface can only absorb a force equal to . Because of this, the value Lxyield will always be equal to of the bolt, regardless of .

3.2.6 Fatigue Loading

A fatigue load is any load that is repeated many times in succession. Fatigue life describes the number of fatigue loading cycles a bolted joint can sustain before failure and is strongly correlated to the peak stress and mean stress that occurs in each cycle. Fatigue failure eventually occurs when an imperfection initiates a crack that propagates with each cycle until rupture occurs. Because the expected number of wind load cycles is unknown, the AASHTO specification for light poles [5] recommends an infinite fatigue life to avoid fatigue failure. A study by James et al. [6] found that fatigue did not loosen any nuts, even if they were only tightened to 15% of their minimum tensile strength. James also suggests that highly concentrated stresses due to incorrect bolt alignment are more critical than bolt preload when considering fatigue behavior in the elastic range. AKDOT&PF is not aware of any anchor rods that have failed due to rupture, or large cracks that are generally caused fatigue failure.

3.2.7 Post Yield Behavior of Bolted Joints

Nassar & Matin [7] examined clamp load loss in high strength steel bolts. They showed that the permanent deformation that occurs when a bolt is loaded beyond yield will result in a loss of clamp load. Figure 3.3, modified from Nassar & Matin shows how a high strength bolt loses clamp load when it is loaded beyond yield.

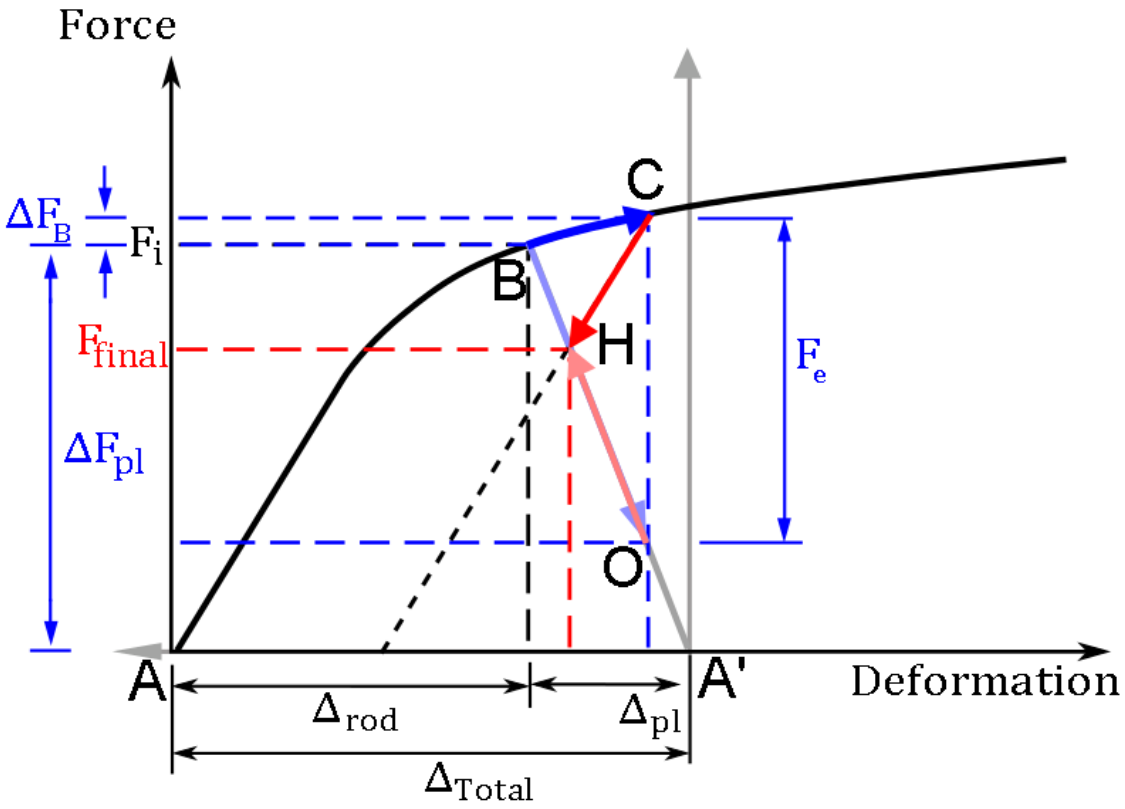

Figure 3.3: Clamp Load Loss in High Strength Bolts

Figure 3.3 shows a bolted joint interface, represented by a rod and a plate, being pre-tensioned past yield, undergoing an external wind load, and then having that load removed. The pretension develops in the rod through its stress-strain curve from point A to point B. The plate must absorb an equal and opposite compressive force, travelling from point A' to point B. They both carry the same force magnitude , but have different deformation magnitudes because the plate is stiffer than the rod. When an external tensile load of magnitude is applied, the bolt absorbs a portion of the load equal to , travelling up its stress-strain curve from point B to point C. The plate absorbs a larger portion of the load equal to because its stiffness is much higher than the bolt's, which is in its post yield region. The plate's compressive force is decreased from point B to point O. When the external load is removed, the plate regains some of its

compressive force on a slope equal to its elastic modulus, while the bolt loses some of its tensile force on a slope equal to its elastic modulus. This rebound occurs in both parts until these slopes meet at point H. The bolted joint interface is now at an equilibrium point equal to . Due to permanent deformation of the rod, the bolted joint interface has a clamp load loss equal to .

In mild steel bolts, the fundamental behavior is similar. The difference lies in the post yield behavior. Figure 3.4 shows a mild steel rod and plate interface being pre-tensioned past yield, undergoing an external wind load, and then having that load removed.

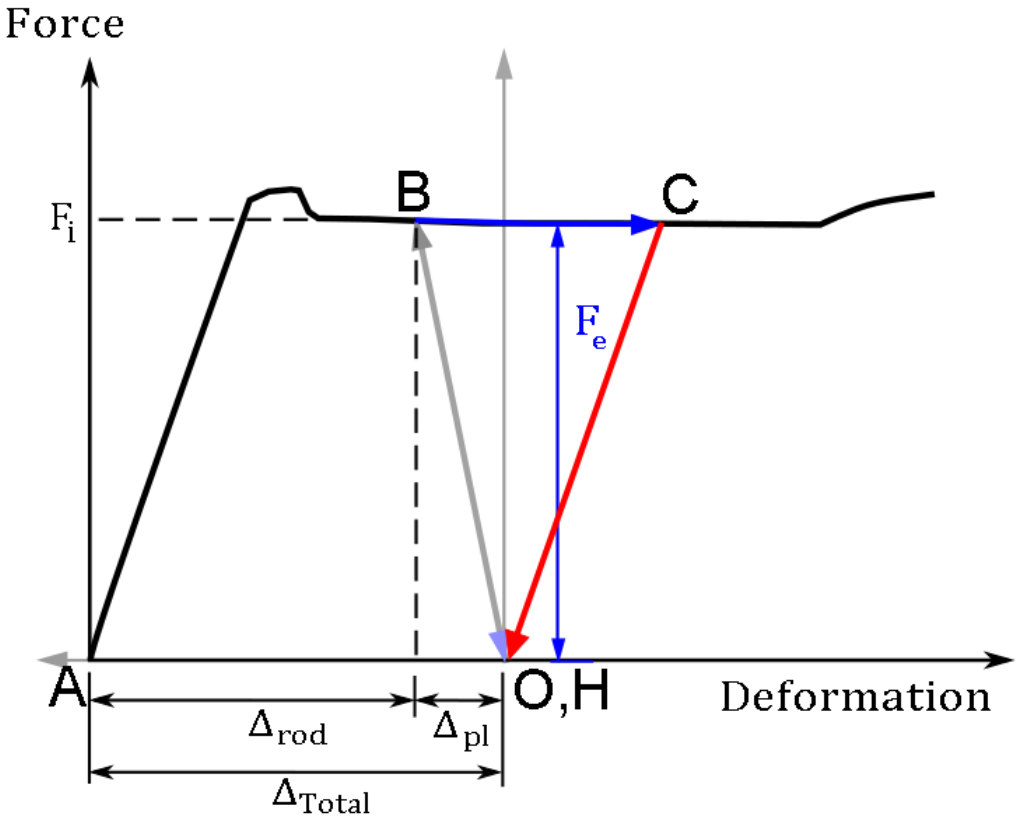

Figure 3.4: Clamp Loss in Mild Steel Bolts

The pretension develops in the rod during tightening through its stress-strain curve from point A to point B. The plate absorbs an equal and opposite compressive force, travelling

from point O to point B. When an external tensile load is applied to the pre-tensioned interface, the plate absorbs all of it because the rod's stiffness is zero. If is greater than or equal to , the plate is completely unloaded to point O. During this external load, the rod will stretch depending on the stiffness of the plate and condition of adjacent bolts. When the load is removed, the rod relaxes down a slope equal to its elastic modulus until it meets the plate at point H. In this case, because exceeded , the rod was forced to undergo permanent strain large enough to remove its pretension. Due to this permanent deformation, this bolted joint interface will have no clamp load left after the external load is removed.

3.2.8 Finite-Element Modeling Of Bolted Joints

A finite element model can't perfectly model reality, but techniques can be used to approximate true mechanical behavior. Montgomery [9] discusses different methods that can be used to model a bolted joint interface. The different parts of the interface can be bonded, or represented by surface-surface contact. The plates can be represented by plate elements or 3D solid elements. The bolt can be represented by a line element or 3D solid elements. Accuracy and calculation time are the primary considerations behind choosing a method. Also, the interface must be allowed to separate when pretension is exceeded.

To allow for separation in a typical flange-flange bolted connection, the top flange and bottom flange can't be bonded. Instead, they must be represented by a surface-surface contact interaction that will allow for separation. The nut-top flange interface and the nut-bottom flange interface are bonded to reduce calculation time. Modelling the bolt and plate as 3D solid elements instead of line and plate elements allows for higher accuracy and a more easily visualized stress distribution. Figure 3.5 shows the cross section of a pre-tensioned bolted joint where all parts are 3D solid elements and flange-flange interaction is represented by surface-surface contact.

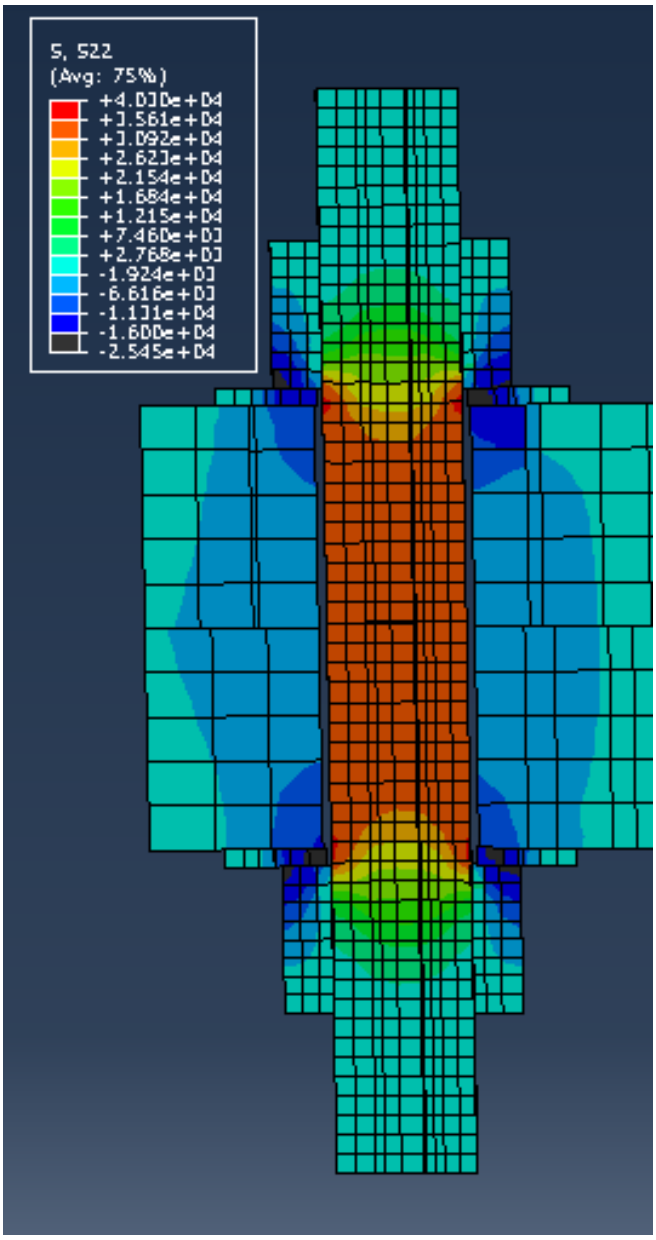

Figure 3.5: Flange-Flange Pretension FEM

3.2.9 Objectives

In this study, FE software was used to examine the behavior of several high mast lighting pole base plate-foundation connections. In theory, because the bolts are mild steel, if an external force imposes an axial force on one bolt/joint interface at least equal to of the

rod, the interface should lose clamp load as seen in Figure 3.4. External loads that represent wind gusts were applied to the HMLP in the model to determine the following:

- The magnitude and frequency of applied load required to cause clamp load loss.
- The effect of pretension on clamp load loss.
- The effect of different foundation configurations on clamp load loss.
- The effect of the presence and distance of adjacent bolts.

3.3 Methodology

ABAQUS was used for all finite element modeling done in this study. The Newton-Raphson method is used to solve non-linear calculations in ABAQUS implicit, the incremental solver used in this study.

3.3.1 Pole Configurations for Modeling

Three different model scenarios were chosen to encompass the majority of HMLPs in service from the three general configurations described in Chapter 3.1, which can be seen in Figure 3.6:

A. Flange-Flange, 12 rods, 150' height (Weigh-station HMLP)
B. Flange-Spacer-Flange, 24 rods, 155' height (Peter's Creek HMLP)
C. Double Nut Moment, 12 rods, 150' height

Configuration B is atypical, and is representative of newly installed poles which utilized design changes to prevent anchor nut updates based on the loosening problem. Configuration C is also atypical in Alaska. A CIP concrete scenario was not included due to the inability to experimentally determine the pretension load in those foundations. High strength rods were used in scenarios A & C to determine their effects. Thicker plates and stiffeners were used in scenario A to determine their effects.

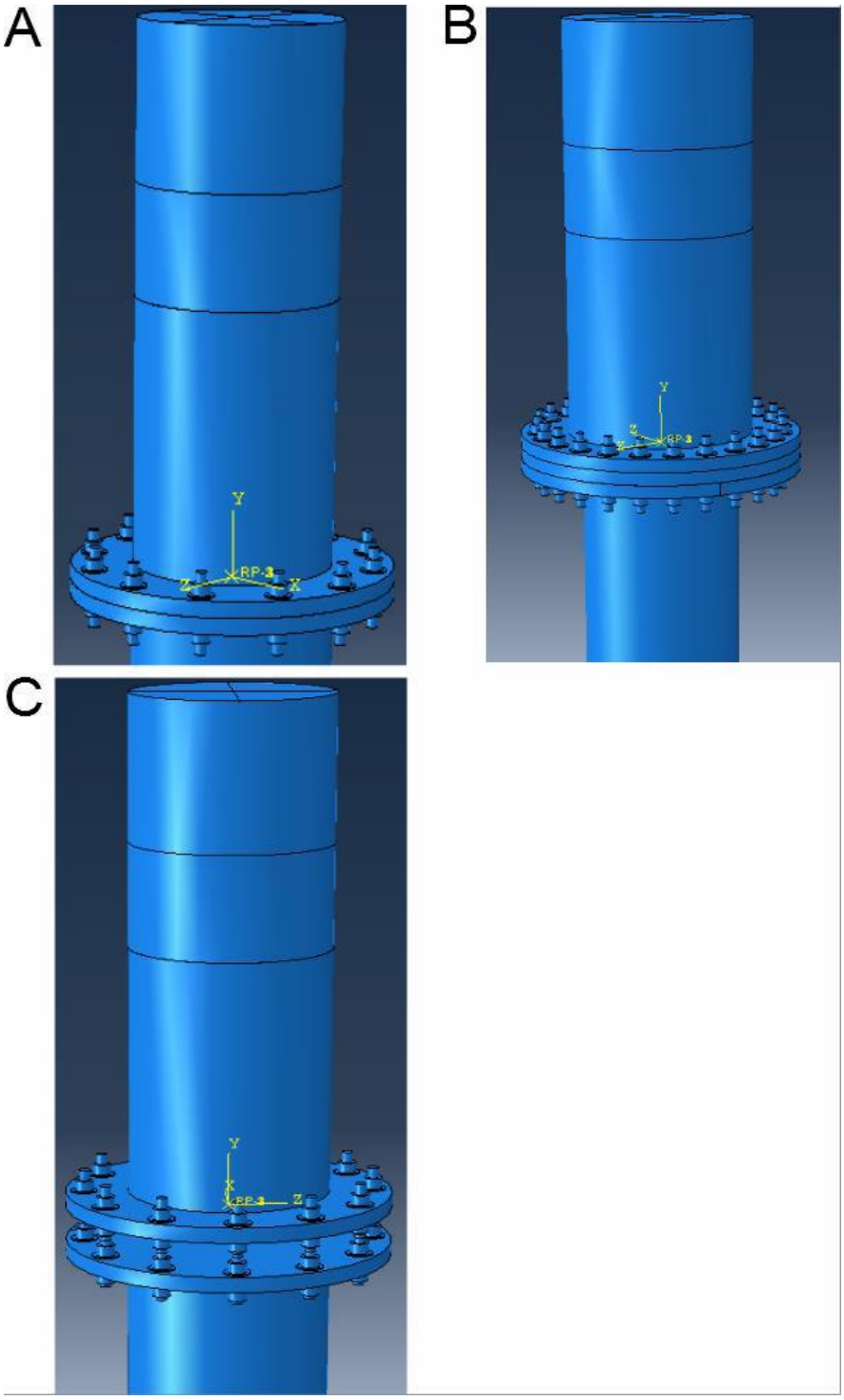

Figure 3.6: HMLP Assemblies

3.3.2 HMLP Geometry

The dimensions of the parts for each scenario are as follows:

Table 3-1: HMLP Dimensions for all Scenarios

	Dimensions (in)
Inner Nut Diameter	1.41
Outer Nut Diameter	2.4
Inner Washer Diameter	1.5
Outer Washer Diameter	3.5
Rod Diameter	1.41
Pile Diameter	27

Table 3-2: HMLP Dimensions for Specified FE Models

	Bolt Circle Diameter (in)	Plate Diameter (in)	Pole Diameter (in)
Scenario A	38	43	26.5
Scenario B	42	48	42
Scenario C	38	43	31.6

3.3.3 Material Behavior

The pole, pile, base plate, and flange plate were defined using linear-elastic, isotropic behavior with an elastic modulus E=29,000,000 ksi, and a Poisson's ratio . The F1554 Gr. 55 threaded rods had the same Poisson's ratio, but were defined using the stress-strain relationship shown in Figure 3.7. The stress-strain relationship approximates behavior that was experimentally determined by loading a specimen to failure via ASTM E8 (Appendix D). For model stability, the negative post yield slopes were replaced by slopes of zero. Figure 3.4 shows that separation can occur before the rod reaches the strain hardening zone during external loading. Because of this, the exact definition of the strain hardening curve of the material above the yield stress is not important in

determining clamp load loss; therefore it is approximated by two lines to reduce computation time.

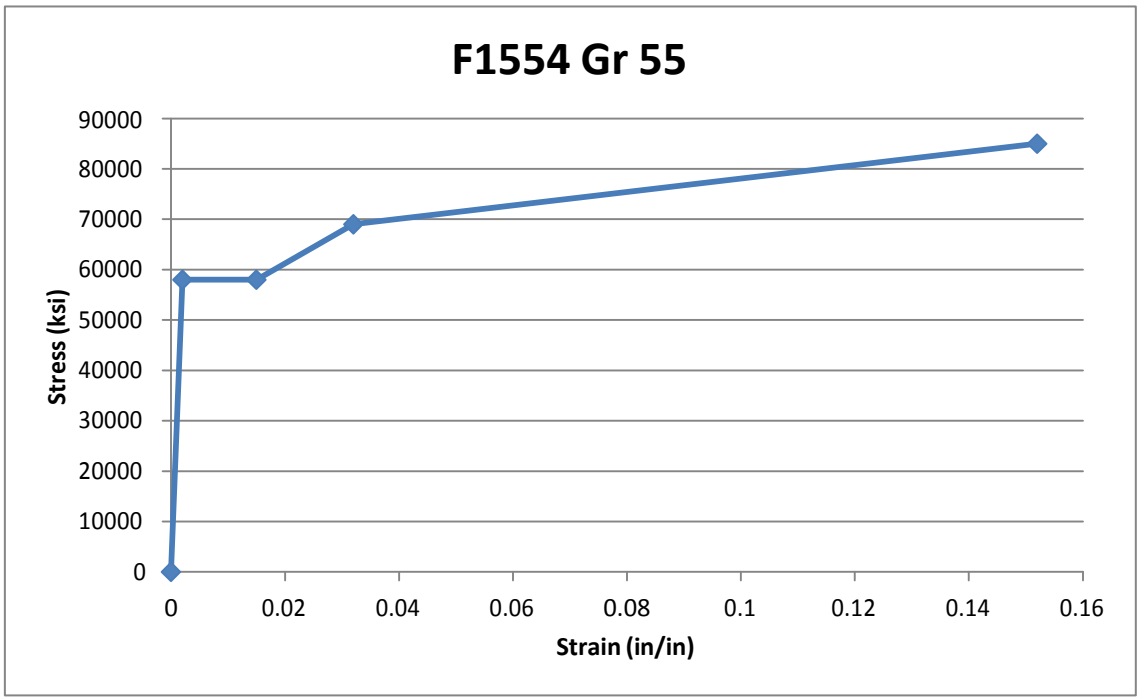

Figure 3.7: Stress-strain Relationship of F1554 Rods Used in FE Models

3.3.4 Element Description

All FE models used Abaqus element type C3D8R. This is an 8 node brick element with reduced integration and hourglass control. The analysis was conducted using Abaqus implicit. The approximate element size of each mesh was modified until the faces of most elements had a length/width ratio that didn't exceed 1.5 in the rods, washers, plates, and nuts. The sizes of these elements vary with each part. The approximate element size of the rods, washers, and nuts was set to 0.2 inches. The approximate element size of all plates was set to 0.5 inches, the pole was set to 3 inches and the pile was set to 6 inches.

3.3.5 Interaction Definitions

Table 3-3 contains the constraint and interaction property definitions for all scenarios.

Table 3-3: Abaqus Interaction Definitions for all Scenarios

Constraints		**Interaction Properties**	
Tie	Surface-Surface	Tangential Behavior	Penalty, μ=0.3
Position Tolerance	Use default	Shear Stress Limit	None
Adjust Slave Surface Initial Position?	Yes	Max. Elastic Slip	0.005 (Fraction of Characteristic Surface Dimension)
Tie Rotational DOFs if Applicable?	Yes	Normal Behavior	Pressure-Overclosure
Contact	Surface-Surface	Enforcement Method	Default
Sliding	Finite	Contact Stiffness	2.90E+08
Slave Adjustment	None		
Surface Smoothing	Automatic		

The interactions of following parts were considered surface-surface contact:

- Scenario A : Flange Plate-Base Plate
- Scenario B : Flange Plate-Spacer Plate, Base Plate-Spacer Plate
- Scenario C : Bottom Washer-Flange Plate, & Bottom Washer-Base Plate

All other part interactions were defined as tied.

3.3.6 Boundary Conditions

In both the flange-flange and the double moment nut scenarios, the bottom of the pile was fixed at a depth of 12'. The pile's depth of fixity was determined using the effective depth-to-maximum-moment method with the following equation by Chai & Hutchinson [10]:

(——

)

Where is the maximum moment applied to the pile, is the maximum lateral force applied to the pile, and H is the length of pile above ground.

In all scenarios, varying the depth of fixity had little effect on stresses in the plates or rods.

3.3.7 Applied Loads

There are three different load steps that were applied to each model: Pretension, Load, and Unload. These were applied sequentially in Load steps.

To apply pretension, a "bolt load" was applied to each rod. This bolt load is applied between two nuts that are clamping a plate or plates. Selecting "adjust length" for the loading method imposes a stretch in the bolt that mimics the displacement controlled pretension. The magnitude of the length adjustment is selected to reach a pretension equal to 60% of the minimum tensile stress in the rod. To accomplish this, the change in length is set equal to

Where:

is equal to 0.008 inches in the Scenario A, 0.011 inches in the Scenario B, 0.004 inches in both clamp zones in Scenario C. 60% of the rod's minimum tensile stress value was targeted in accordance with existing pretension recommendations by Garlich [1]. The plate(s) will be flattened by $\bar{\bar{\ }}$, where:

During the "Load" step, external load representing a 100 mph design wind speed is applied to the top pole stub as a moment couple. Unlike the real pole, a 36 inch portion of the pole stub is solid to prevent excessive deformation. The magnitude of this moment couple varies by pole configuration as follows:

A. Flange-Flange, 12 rods, 150' height: 6765k*in
B. Flange-Flange, 24 rods, 155' height: 8768 k*in
C. Double Nut Moment, 12 rods, 150' height: 6765 k*in

The moments used were taken from calculations done by the HMLP manufacturer. These calculations were done in accordance with the American Association of State Highway And Transportation Officials' *Standard Specifications for Structural Supports for Highway Signs, Luminaries, and Traffic Signals (2011)* [11]. They were verified with calculations according to the American Society of Civil Engineers' *Minimum Design Loads for Buildings and Other Structures (7-10)* [12]. These verification calculations can be seen in Appendix N. Scenario B has a higher design moment because the pole is both larger in diameter and taller than the pole in scenarios A & C.

In addition to moments due to design wind velocities, moments of varying magnitudes were applied to cause both small clamp load loss and complete separation.

After the “Load” step, there is an “Unload” step where this couple moment is reduced to 0 to represent the unloaded condition of the pole.

3.4 Results

The clamp load loss predicted by the FE models due to external wind loading is summarized below. The effect of the design wind moment on all configurations will be discussed, as will the minimum moment required to separate one rod in each scenario, and the minimum moment required to cause significant clamp load loss equal to 10% of initial pretension. The effect of high strength rods in scenarios A & C will be summarized, as will the effects of stiffeners and thicker plates on scenario A.

3.4.1 Flange-Flange Twelve 1.5 inch Rods

In Figure 3.8, 100 mph wind is being simulated by applying a 6800 k*in moment to the pole.

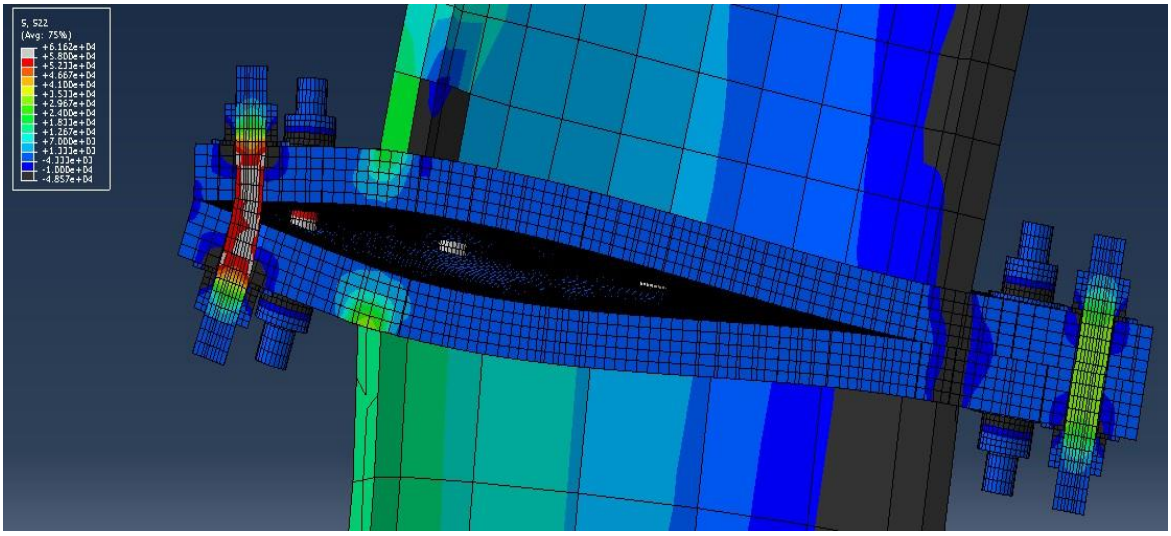

Figure 3.8: Scenario A Load (6800 k*in Moment)

The figure shows a section cut center parallel to the applied force, with the tension side of the moment on the left, and the compression on the right. Deformation is scaled by a

factor of 25. Elements that are darker than the blue color in the middle of the plates are in axial compression. Lighter colored elements are in axial tension. Red elements are carrying stresses approximately equal to yield (58,000 ksi). Grey elements are carrying stresses greater than yield. It was observed that yielding occurs in all seven of the rods that experience tension. They undergo permanent deflection while this moment is applied. Figure 3.9 shows the next step, after the moment is removed.

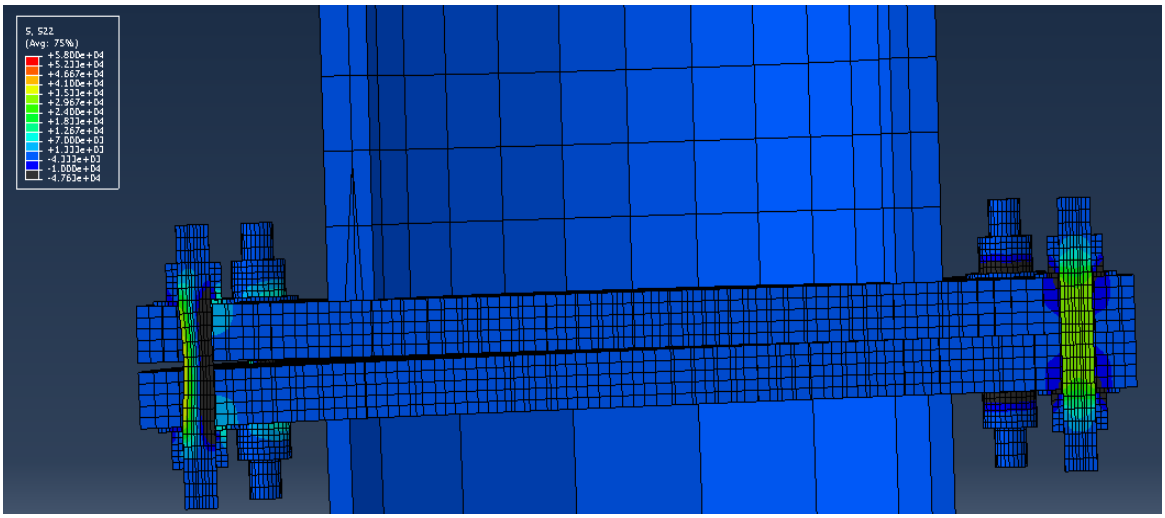

Figure 3.9: Scenario A Unload (6800 k*in Moment)

It can be observed that there is no stress in the middle of the leftmost tension rod, there are residual bending stresses of opposite sign on either side of this rod, and there is separation between the two flanges. This separation occurs at five of the tension rods. The permanent deflection the rods undergo during the applied moment exceeds the stretch that the bolts experience due to pretension in these rods. Because of this, when the moment is removed, the clamp load is zero in these five bolted joint interfaces. This is in agreement with section 3.4, which predicts that mild steel rods will separate if external loads of sufficiently large magnitude are applied. A moment of 6300 k*in (93% of design wind) is required for only one rod to separate in this configuration.

3.4.2 Flange-Flange Twenty-four 1.5 inch Rods

In scenario B, a 100 mph wind is simulated by applying an 8800 k*in moment to the pole.

During the unload step there is no clamp load loss due to permanent deformation. Since the foundation uses 24 rods, the system has the necessary capacity to absorb the moment without loss of clamp load. To cause separation of one rod, a moment of 11600 k*in (132% of design) is required.

3.4.3 Double Nut Moment Connection Twelve 1.5 inch Rods

In Figure 3.10, 100 mph wind is being simulated by applying a 6800 k*in moment to the pole.

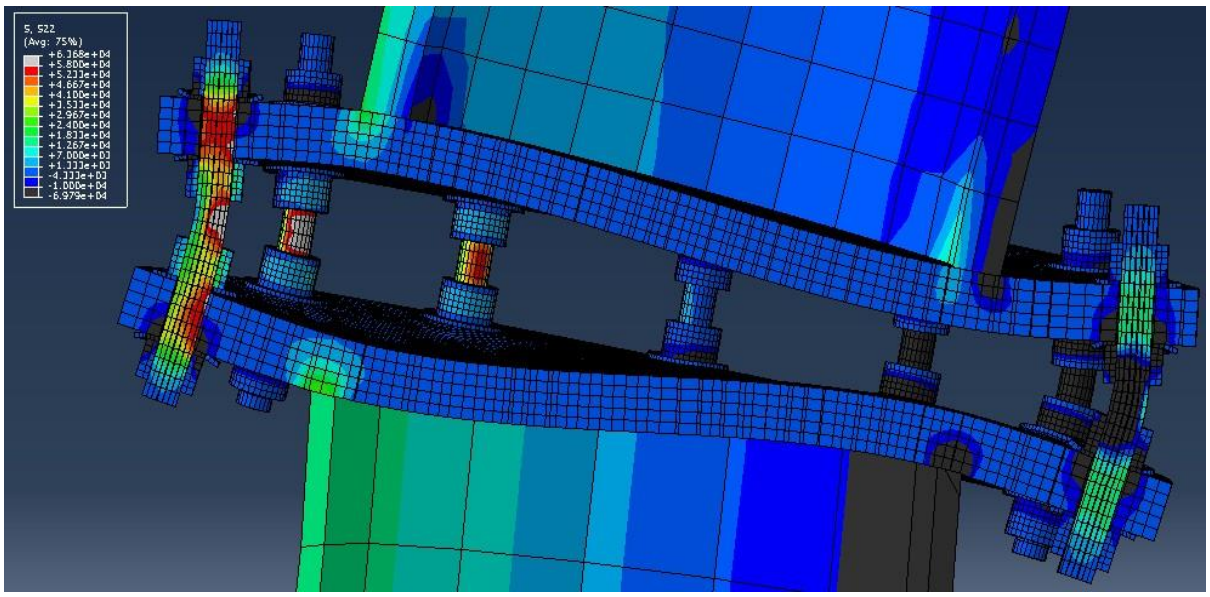

*Figure 3.10: Scenario C Load (6800 k*in Moment)*

The figure shows a section cut of the model at the center parallel to the applied moment with the tension side on the left, and the compression on the right. Five rods are absorbing the tension component of the moment, while five rods are absorbing the

compression component because there is no plate-plate contact. The other two rods carry negligible load because they lie on the plate's neutral axis during the applied moment. The deformation is scaled by a factor of 25. The colors indicate the same stresses as mentioned in section 3.3.1. There is some yielding in the tension rods due to bending, mostly between the two inside nuts. Figure 3.11 shows the step, in which the moment is removed. Because of the yielding, there are residual stresses between the inside nuts at three tension rods and three compression rods. However, because yielding of the rod occurs outside the areas where the rods are being clamped, the system has a much higher resistance to clamp loss. A moment of 10900 k*in (161% of design) is required for this configuration to separate.

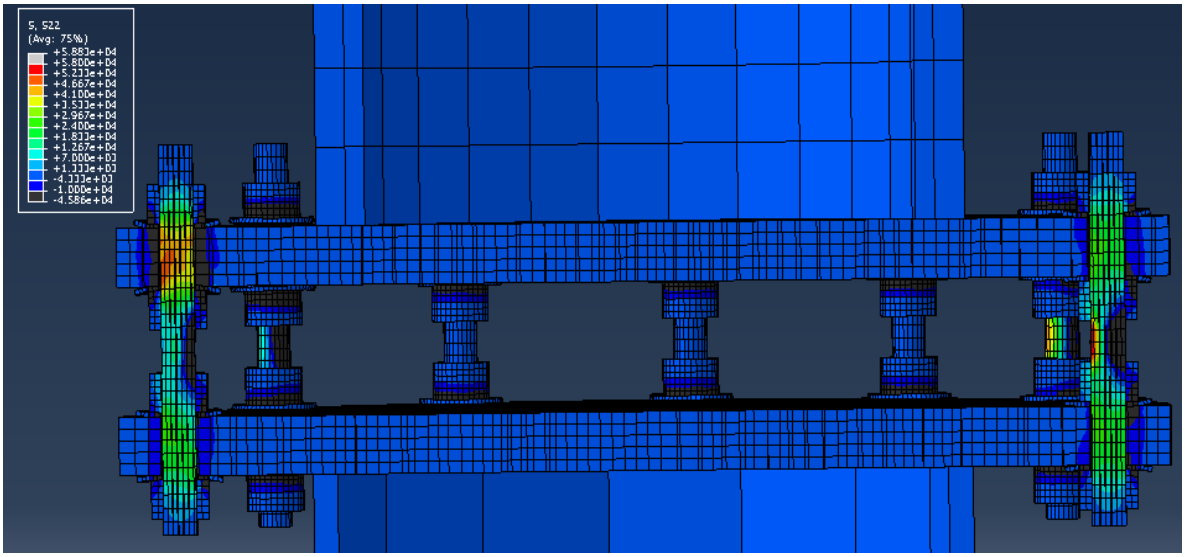

*Figure 3.11:Scenario C Unload (6800 k*in Moment)*

3.4.4 Effect of Pretension Magnitude

The magnitude of pretension was varied in scenario A by varying the value from 0.004 inches to 0.012 inches, and on scenario C by varying from 0.002 inches to 0.006 inches. This change in pretension had no effect on the moment required to separate either interface after unloading. This supports section 3.1.5 that shows that a mild steel

bolted joint interface undergoes clamp loss when an external load exceeds of the rods, regardless of pretension.

3.4.5 High Strength Rods

When high strength rods (F1554 Grade 105) were used instead of the mild steel rods, resistance to separation increased dramatically. In scenario A, the moment required for separation was 11560 k*in, an increase of 183% when compared to the 6300 k*in moment required to separate the mild steel configuration. When high strength rods were used in scenario C, the moment required for separation was 20500 k*in, an increase of 188% when compared to the 10900 k*in moment required to separate the mild steel configuration. Because the bolted joint interface undergoes clamp loss when an external load exceeds of the rods, increasing from 55ksi to 105ksi should have this effect. High strength rods weren't used in scenario B because the result would be similar to scenario A, and scenario B already requires 132% of design load to separate.

3.4.6 Clamp Load Losses due to Localized Stress

There are external loads of smaller magnitude that result in clamp load loss in the bolted joint interface. Figure 3.12 shows the unload step of Scenario A with a moment of 6000k*in which represents a 90mph, a load that does not cause plate separation. The bright blue color in the middle of the figure represents zero stress. Brighter colors represent axial tension, darker colors represent axial compression. It can be seen that elements on the inner face of the tension rod are in a state of zero stress. By observing the stresses in the elements of the centerline of the tension rod, and comparing them with the stresses in the compression rod, (both were tightened the same amount during the pretension step) it can be seen that the tension rod has undergone significant clamp load loss.

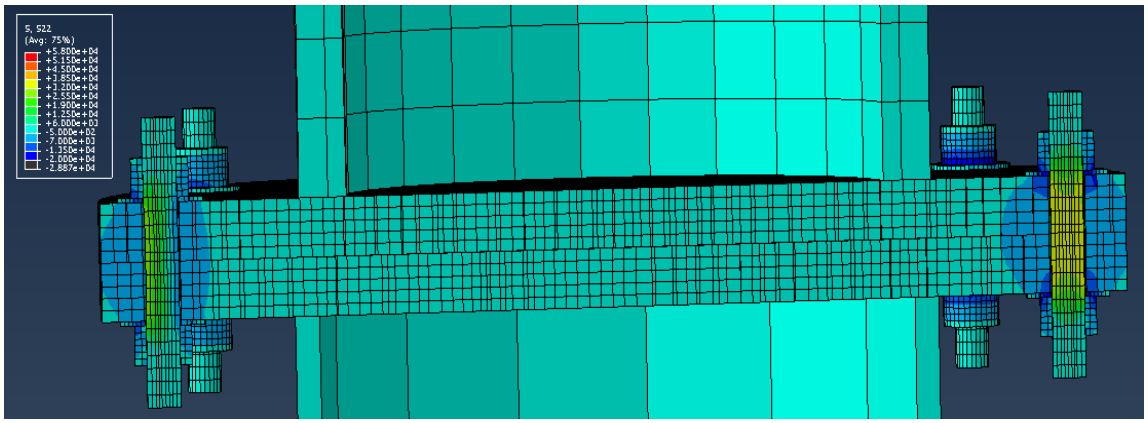

Figure 3.12:Scenario A Unload (6000 k*in)

When an external load of the same magnitude is re-applied and unloaded again, no additional clamp load loss occurs. Significant localized clamp load loss (at least 10% of initial clamp load along the centerline of the tension bolt) occurs at the following moments:

- Scenario A: 5100 k*in (75% of design wind)
- Scenario B: 8100 k*in (99% of design wind)
- Scenario C: 9200 k*in (136% of design wind)

3.4.7 Effect of Thicker Plates and Stiffeners

The effects of both adding stiffeners and increasing the thickness of the plates were analyzed on scenario A. Figure 3.13 shows scenario A with stiffeners attached undergoing the 6800 k*in design load. The maximum distance between the two plates is reduced by 40% when compared to scenario A without stiffeners. However, the clamp load loss is not significantly mitigated. It can be observed that the majority of elements in the leftmost tension rod are still yielded.

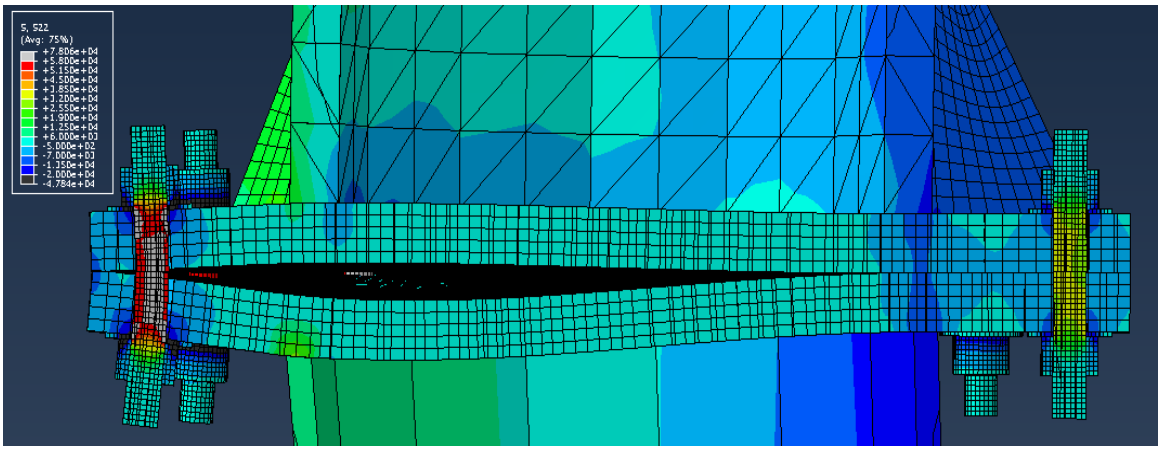

Figure 3.13:Scenario A with Stiffeners Load (6800 k*in)

In Figure 3.14, the base and flange plates are doubled in thickness from 2.25 inches to 4.5 inches. The pretension displacement was increased so that the stress due to pretension was the same as scenario A. In a design wind load, the maximum distance between the two plates is reduced by 80%. The clamp load loss is reduced to zero.

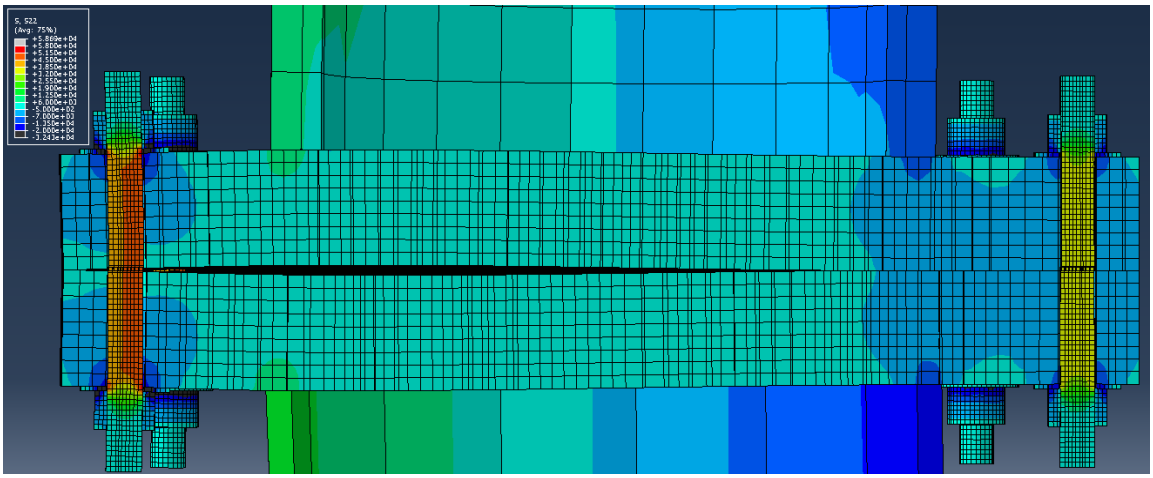

Figure 3.14:Scenario A with 4.5 Inch Thick Plates Load (6800 k*in)

3.4.8 Clamp Loss for all Configurations

The magnitude of moment required to cause significant clamp loss and the magnitude of moment required to cause separation in one rod can be seen in Table 3-4.

Table 3-4:Minimum Clamp Loss & Separation Moments (All Scenarios)

Configuration	Design Moment (k*in)	Moment Required for Significant Clamp Loss (k*in)	Moment Required for Separation (k*in)
Scenario A	6765	5100	6300
Scenario B	8800	8100	11600
Scenario C	6765	9200	10900
Scenario A, High Strength Rods	6765	9800	11500
Scenario C, High Strength Rods	6765	18200	20500

3.5 Summary and Conclusions

Finite element analysis was used to model three HMLP scenarios. Clamp load loss due to permanent fastener deformation was captured in models of each scenario at magnitudes of applied moments above and below the design wind speed. Significant localized clamp load loss was observed in scenarios A & B with applied moments below the design wind speed. Increasing the rod count from 12 to 24 increased the applied

moment required to cause separation by 84%. It also increased the applied moment required to cause significant clamp load loss by 59%. Using a double nut moment connection instead of a flange-flange configuration increased the applied moment required to cause separation by 73%. It also increased the applied moment required to cause significant clamp load loss by 80%. Using high strength rods increased the resistance to separation in scenario A by 83%, and increased the resistance to separation in scenario C by 88%. It also increased the resistance to significant clamp load loss by 92% in scenario A and 98% in scenario C.

Clamp load loss due to permanent rod deformation is not affected by pretension magnitude (in F1554 grade 55 rods). Pretension magnitudes were varied in all models, with no difference in clamp load loss. In F1554 Grade 105 rods or similar high strength rods, a higher pretension will result in more clamp load loss. However, if the high strength rod is at a higher initial pretension, the final pretension would be higher. This is similar to the conclusion that *Nassar & Matin* [8] reached, that the magnitude of pretension affects rods with high strain hardening stiffness more than rods with low strain hardening stiffness. Since F1554 Grade 55 rods have a zone with no strain hardening, the pretension has no effect on clamp load loss within that zone.

The difference between the magnitude of the external load required to separate one rod and the load required to separate several rods is relatively small. This is because the rods adjacent to the yielding critical rod are absorbing the force that the critical rod can no longer absorb. When those rods also yield and can no longer absorb load, separation can occur in many rods. This can be seen in HMLP scenario A, where a 6800 kip*in moment separates 5 rods, yet a 6000 k*in moment does not separate any rods.

Rods in double nut moment connections are less likely to experience clamp loss due to permanent deformation. The area of maximum strain in the rod due to external loads occurs between the two plates, which is outside the clamp zone. The FEA showed double nut moment connections require higher magnitude moments to cause both localized clamp load loss and separation. Grade 105 rods are less likely to permanently

deform than grade 55 rods. Adding stiffeners to scenario A decreased the maximum separation between the two plates during a design wind load 35%. It did not significantly increase the resistance to clamp load loss. Increasing the thickness of the flange and base plates to 4.5 inches in scenario A decreased the maximum distance between the two plates during a design wind load by 80%. More importantly, it significantly increased the configuration's resistance to clamp load loss.

3.6 References

[1] M. J. Garlich and J. W. Koonce, "Anchor Rod Tightening for Highmast Light Towers and Cantilever Sign Structures," in Transportation *Research Board 90th Annual Meeting*, Washington, D.C., 2011, vol. 11–2030.

[2] J. H. Bickford, *An Introduction to the Design and Behavior of Bolted Joints*. CRC Press, 1995.

[3] Research Council on Structural Connections, *Specification for Structural Joints Using High-Strength Bolts*. Chicago, Il: AISC, 2009.

[4] M. J. Garlich and E. R. Thorkildsen, "Guidelines for the Installation, Inspection, Maintenance and Repair of Structural Supports for Highway Signs, Luminaires, and Traffic Signals," Federal Highway Administration, Washington, D.C., Technical Report FHWA NHI 05-036, Mar. 2005.

[5] American Association of State Highway and Transportation Officials, *Standard Specifications for Structural Supports for* Highway *Signs, Luminaires, and Traffic Signals*. AASHTO, 2009.

[6] R. W. James, P. B. Keating, R. W. Bolton, F. C. Benson, D. E. Bray, R. C. Abraham, and J. B. Hodge, "Tightening Procedures for Large-Diameter Anchor Bolts," Texas Transportation Institute, Texas A&M University System, College Station, TX, Research Report 1472-1F, 1997.

[7] S. A. Nassar and P. H. Matin, "Clamp Load Loss due to Fastener Elongation Beyond its Elastic Limit," *J. Pressure Vessel Technol.*, vol. 128, no. 3, pp. 379–387, Aug. 2005.

[8] I. Giosan, "Vortex shedding induced loads on free standing structures," *Structural Vortex Shedding Response Estimation Methodology and Finite Element Simulation*.

[9] Montgomery, Jerome. "Methods for Modeling Bolts in the Bolted Joint." In *ANSYS User's Conference*.Vol. 5, 2002.

[10] Chai, Y. H., and Tara C. Hutchinson. "Flexural Strength and Ductility of Extended Pile-Shafts. II: Experimental Study." *Journal of Structural Engineering* 128, no. 5 (2002): 595–602.

[11] American Association of State Highway and Transportation Officials, *Standard Specifications for Structural Supports for Highway Signs, Luminaires, and Traffic Signals*. AASHTO, 2001.

[12] American Society of Civil Engineers, *Minimum Design Loads for Buildings and other Structures.* Reston, VA: ASCE, 2010

CHAPTER 4: GENERAL CONCLUSIONS

4.1 Conclusions

In Chapter 2, *Measured Anchor Rod Tightening of High Mast Lighting Poles in Alaska*, a FHWA tightening procedure was followed when tightening an HMLP. The axial force of each anchor rod in the HMLPs foundation was monitored during tightening. It was determined that several of the anchor rods yielded during the tightening procedure. Based on the foundation type, anchor rod geometry, and data acquired during this study, three primary conclusions were drawn:

- Large diameter fasteners with short grip lengths that are snug tightened without controlling the torque are likely to exceed the recommended snug tight pretension range.
- If the degree of rotation in the turn-of-the-nut method were adjusted for the grip length/rod diameter ratio, in addition to existing recommendations about bolt diameter and grade, then final bolt pretensions would be more likely to fall within the desired range.
- If the verification torque were reduced from 60% to 50% of the minimum tensile stress of F1554 Grade 55, as is the case with F1554 grade 36, the rods may be less likely to yield.

Chapter 3 contains a study to be submitted to the American Society of Civil Engineers Journal of Structural Engineering entitled *Evaluating the Behavior of Anchor Rod Foundations for High-Mast Light Poles (HMLPs) Using Nonlinear Finite-element Analysis.* In this study, finite element analysis was used to model three HMLP foundation configurations. In addition to these configurations, the effects of thickening the base plates, adding stiffeners to the poles, and using high strength anchor rods were analyzed. The study examined these scenarios to test for clamp load loss due to post-yield permanent fastener deformation. The following conclusions were drawn from this study:

- Clamp load loss due to permanent rod deformation is not affected by pretension magnitude (in F1554 grade 55 rods). Pretension magnitudes were varied in all models, with no difference in clamp load loss.
- The difference between the magnitude of the external load required to separate one rod, and the load required to separate several rods, is relatively small. This is because the rods adjacent to the yielding critical rod are absorbing the force that the critical rod can no longer absorb.
- Rods in double nut moment connections are less likely to experience clamp loss due to permanent deformation. Grade 105 rods are less likely to permanently deform than grade 55 rods. Adding stiffeners to scenario A did not significantly increase the resistance to clamp load loss. Doubling the thickness of the flange and base plates in scenario A did significantly increased the resistance to clamp load loss.

The inspection reports in Appendix K show that when a pole had a rod with no full clamp loss, there was an average of 3.1 such rods on that pole. Of poles with at least 2 loose rods, 56% of the rods were adjacent to at least one other loose rod.

Appendix B contains a modified tightening procedure for a 2nd HMLP that was developed from the conclusions reached in chapter 2. Appendix C contains the results from the application of that tightening procedure. Pretension scatter was significantly reduced during tightening.

4.2 Limitations

Strain gauges are not the ideal choice to record clamp load loss due to permanent rod deformation. In the best case scenario, if the DAQ monitoring the strain gauge was recording continuously, it would be capable of capturing an anchor rod's strain during any large wind event. If the wind event exerted an external load of sufficient magnitude to cause separation, the strain would increase, indicating that the rod had deformed. When the external load is no longer applied, the strain would decrease, but it would not

return to zero. There would be residual strain due to the permanent deformation of the rod. If the DAQ wasn't recording during the separation load, it would appear as if nothing happened because the pre-load strains and the post-load strains would be similar.

The epoxy used to bind the strain gauges to the inside of the rods was sensitive to temperature changes. Because thermal effects are different for each rod depending on the angle of the sun, the variations in strain don't necessarily correspond to the recorded temperature variations. Unless the temperature was recorded at each rod, this will continue to be a problem for strain gauges inserted in epoxy cores of threaded rods in field measurements.

If the pretension developed during tightening is too low, the rods absorbing the compression component of an external wind moment can lose their tension during the wind moment. If vibration is occurring during the wind load, the nuts may be free to rotate, resulting in traditional loosening. The FE model used captures static loading only, and is not capable of reproducing this type of loosening. The static FE model is also incapable of applying loads that cause small clamp load losses repeatedly until separation occurs.

4.3 Recommendations

Existing turn-of-the-nut tightening procedures should be modified. The existing top nut rotation beyond snug tight can be seen as a table in appendix M, taken from Garlich & Thorkildsen [2]. This rotation does not change between grades 55 and 105. It also is only for use in double-nut moment connections, but has been generalized and used in other configurations. A new value for top nut rotation should directly vary with the yield strength of the material and the grip length of the bolted joint interface.

It is recommended that future designs use F1554 grade 105 rods. The benefits of having anchor rods yield at nearly double the magnitude of stress are twofold. First, as discussed in section 3.1.7, clamp load loss occurs when an external load exerts a force onto a single bolted joint interface that exceeds of the rod. Increasing the yield strength of an

anchor rod by 90% should increase its resistance to post-yield clamp load loss by 90% as well. This is reflected in section 3.3.5, where one configuration gained an 83% increased resistance to post-yield clamp load loss, and another gained 85% increased resistance. The second benefit of using F1554 grade 105 rods is to combat traditional loosening. If F1554 grade 55 rods are tightened to their recommended minimum pretension magnitudes, traditional rotation of a nut during external wind loading shouldn't occur. However, it is impossible to completely get rid of pretension scatter. Some rods may have pretensions low enough that an external wind load can remove their load when the rods are on the compression side of the load. Grade 105 rods can be tightened to a pretension magnitude 90% higher than grade 55 rods, and still not yield. This would make it extremely unlikely that any rods undergoing external compression would lose their clamp load. Existing HMLPs in danger of anchor nut loosening should also replace their existing grade 55 rods with grade 105 rods.

It is recommended that future designs use double-nut moment connections. The configuration provides a larger resistance to post-yield clamp load loss because of the gap between the two plates. During an external wind load, the largest strains will occur in between these two plates. In a flange-flange connection, this means the largest strain occurs in the zone of clamp. In a double-nut moment connection, the largest strain occurs in the middle of the gap. If the rod were to permanently deform, it would do so primarily outside the zone of clamp. Section 3.3.3 shows that a double-nut moment connection has a 61% increased resistance to post-yield clamp load loss when compared to a similar flange-flange design.

It is recommended that future designs use a 1.5 inch rod HMLP foundation configuration with at least 16 rods. The use of a 24 rod system with a spacer plate resulted in a 71% increased resistance to post-yield clamp load loss when compared to a 12 rod system without a spacer plate. An HMLP with more rods can absorb higher magnitude loads without yielding, and when rods are closer together, they are more capable of absorbing additional load when a nearby rod has yielded.

In each future tightening procedure, at least two methods of determining pretension should be used. These methods include, but are not limited to:

- Using a Turn-of-the-Nut procedure that uses a torque wrench for the snug tight condition.
- Using a torque wrench to verify the final pretension
- Using direct tension indicating washers to verify final pretension.

4.4 Additional Research

A static FEA was used in this study. It is incapable of producing dynamic effects which may be occurring during the load and unload steps. A dynamic FEA could be capable of reproducing traditional loosening, when nuts rotate on the threads of the rod during an external load. A dynamic FEA could also determine if separation occurs when loads causing small clamp load loss are repeated.

Modeling the correct dynamic effects to represent a HMLP undergoing external wind loading is impossible without knowing the true behavior of a HMLP. The critical behavior may actually be a combination of wind buffeting and vortex shedding. *Giosan* [3] showed that tall cylindrical structures experience significant stresses due to vortex shedding, even if they are tapered. A study should be conducted to capture the dynamic effects of an HMLP. This study should record axial loads of the anchor rods, place strain gauges on the side of the pole to measure deformation, and place sensitive accelerometers on the pole to measure acceleration. This behavior could then be used as input in a FEM to predict the true magnitude of clamp load loss.

Instead of strain gauges, future research should include the use of load cell washers to record axial load of the rods. They would directly display the tension existing in the rod at any point. While expensive, they're the only way to capture clamp load loss due to permanent fastener deformation.

References

[1] Michael J. Garlich, and Eric R. Thorkildsen. *Guidelines for the Installation, Inspection, Maintenance and Repair of Structural Supports for Highway Signs, Luminaires, and Traffic Signals*. Publication FHWA NHI 05-036. Federal Highway Administration, Washington, D.C., Mar. 2005.

[2] S. A. Nassar and P. H. Matin, "Clamp Load Loss due to Fastener Elongation Beyond its Elastic Limit," *J. Pressure Vessel Technol.*, vol. 128, no. 3, pp. 379–387, Aug. 2005.

[3] I. Giosan, "Vortex shedding induced loads on free standing structures," *Structural Vortex Shedding Response Estimation Methodology and Finite Element Simulation*.

Appendix A

Weighstation Tightening Procedure

The following procedure shall be used for the WS1 High-mast Light Pole (Weight Station NB) during installation of strain-gaged bolts. This was taken from the HT Special Provisions contract dated 6/14/2010. It has been modified slightly to account for the strain gage wires and accelerometers. The rod assembly type used on this HMLP is type B. Figure A.1 shows the order in which type B rod assemblies are to be tightened. Figure A.2 shows the type B configuration, which is a flange-flange connection.

A. General. For ALL High Tower nut retightening use the following procedures:

- Tighten nuts only on days when the ground wind speed is less than 15 mph.
- Once the tightening procedure is started, tighten all Rod Assemblies without pause or delay.
- Field numbered Rod Assemblies may NOT match the "Tightening Sequence" shown.
- DO NOT use vise grips, channel locks, adjustable end or pipe wrenches.
- Use the appropriately sized hydraulic wrench system. Submit hydraulic wrench system information to the Engineer for review and acceptance. Include a pressure-torque curve.
- Place a smooth beveled washer in contact with the sloped surface, when the outer edge of the assembly has a slope greater than 1:20.

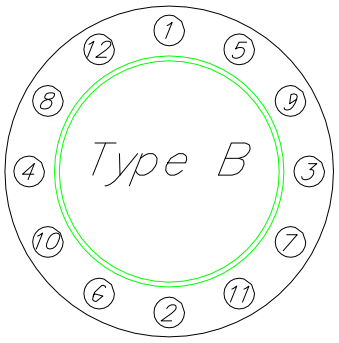

Figure A.1: Type ‘B’ Tightening Sequence

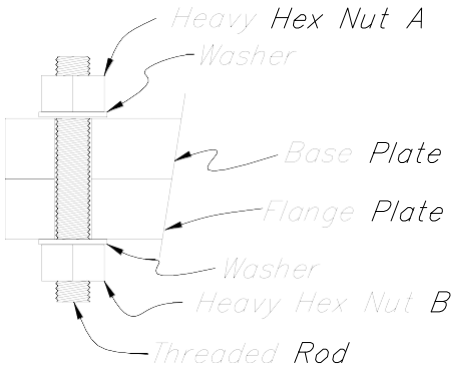

Figure A.2: Type ‘B’ Rod Assembly

B. For ‘Type B’ foundation, bolt replacement and nut tightening use the following procedure:

1) Clean exposed threads on all existing bolt assemblies.

2) Tighten all nuts “Snug tight”.

a. Wherever mentioned, “Snug tight” is defined as 600 ft-lbs of torque. Use a hydraulic torque wrench to bring nuts to snug tight torque. Consult manufacturer documentation to determine delivery pressure required to

achieve specified torque. -or-

b. If torque wrench cannot be used, “Snug tight” is the full effort of one person on an open-end wrench close to the end with a length equal to 14 times the rod diameter but not less than 18 inches.

3) Bolt assembly replacement and nut retightening begins with Rod Assembly labeled #1 in the “Type ‘B’ Tightening Sequence” above and continues sequentially until all bolts are replaced and new Rod Assemblies are tightened. **Remove only one bolt assembly at a time.**

   a. Remove existing bolt assembly and discard. DO NOT reuse existing bolts, washers or nuts.

   b. Clean plate bearing areas immediately before tightening.

   c. Install threaded rod, washer and ‘A’ nut.

   d. Install washer and ‘B’ nut

   e. Snug tight both nuts. Ensure that a minimum of three threads stick through at each ‘A’ nut and ‘B’ nut.

4) Repeat step 3 until all Bolt Assemblies are sequentially replaced and all Rod Assembly nuts are snug tight.

5) Initial Turn of the Nut.

   a. Beginning with Rod Assembly labeled #1 in the Type ‘B’ Tightening Sequence,

   b. Mark nut ‘A’, base plate, flange plate, nut ‘B’ and threaded rod with a permanent felt tipped pen or crayon as a reference for determining the relative rotation of the nut and threaded rod during the tightening.

   c. Rotate nut ‘A’ 20 degrees. **Prevent nut ‘B’ and threaded rod from moving whenever turning nut ‘A’.**

6) Repeat step 5 above until all 12 ‘A’ nuts are sequentially tightened 20 degrees.

a. After all Rod Assemblies are tightened 20 degrees, re-check snug tightness of the ‘B’ nuts. If nut ‘B’ or threaded rod moves then, loosen ‘A’ nut, snug tight both nuts and repeat step 5 on that Rod Assembly.

7) Intermediate Turn of the Nut.

   a. Continue tightening ‘A’ nuts beginning with Rod Assembly labeled #1 in the Type ‘B’ Tightening Sequence,

   b. Rotate nut ‘A’ an additional 20 degrees for a total rotation of 40 degrees.

8) Repeat step 7 above until all 12 ‘A’ nuts are sequentially tightened 40 degrees.

   a. After all Rod Assemblies are tightened to 40 degrees, re-check snug tightness of all ‘B’ nuts. If nut ‘B’ or threaded rod moves then, loosen ‘A’ nut, snug tight both nuts and repeat steps 5 and 7 on that Rod Assembly.

9) Final Turn of the Nut.

   a. Complete tightening ‘A’ nuts beginning with the Rod Assembly labeled #1 in the Type ‘B’ Tightening Sequence,

   b. Rotate nut ‘A’ an additional 20 degrees for a total rotation of 60 degrees.

   c. Do not over torque. If the delivered torque reaches 2,500 ft-lbs without achieving the required turn of the nut then on that Rod Assembly:

      (1) Remove nut ‘B’ nut then, loosen nut ‘A’,

      (2) Clean and re-lubricate all contact surfaces,

      (3) Snug tight nuts ‘A’ and ‘B’.

      (4) Mark nuts, base plate, flange plate, threaded rod and rotate nut ‘A’ 60 degrees.

      (5) If required rotation is not achieved at 2,500 ft-lb torque then, notify the Engineer and proceed with Final Turn of the Nut on remaining ‘A’ nuts.

10) Repeat step 9 above until final tightening is sequentially completed on all 12 Rod Assemblies.

11) After all Rod Assemblies are tightened to 60 degrees, re-check snug tightness of all ‘B’ nuts. If nut ‘B’ or the rod moves during snug tight check then loosen ‘A’ nut, snug tight both nuts and repeat steps 5, 7 and 9 on that Rod Assembly.

12) A minimum of 1 week and a maximum of 2 weeks after re-tightening apply a 1,300 ft-lb torque to ‘A’ nuts and check snug tightness of ‘B’ nuts. If any nut or threaded rod moves, mark the nut and notify the Engineer.

Appendix B

Tightening Procedure for Peter's Creek HMLP

The following procedure shall be used for High-mast Light Pole #1 at Peter's Creek (GSPC1) during installation of strain-gaged bolts. This was taken from the HT Special Provisions contract dated 6/14/2010. It has been modified slightly to account for the strain gage wires. It has been updated based on the results of the rod tightening at the Glenn Highway Weigh Station in February 2013. Figure B.1 shows the tightening sequence for a 24 rod system. Figure B.2 shows the modified flange-spacer-flange HMLP configuration.

A. General. For ALL High Tower nut retightening use the following procedures:

- Tighten nuts only on days when the ground wind speed is less than 15 mph.
- Once the tightening procedure is started, tighten all Rod Assemblies without pause or delay.
- Field numbered Rod Assemblies may NOT match the "Tightening Sequence" shown.
- DO NOT use vise grips, channel locks, adjustable end or pipe wrenches.
- Use the appropriately sized hydraulic wrench system. Submit hydraulic wrench system information to the Engineer for review and acceptance. Include a pressure-torque curve.
- Place a smooth beveled washer in contact with the sloped surface, when the outer edge of the assembly has a slope greater than 1:20.

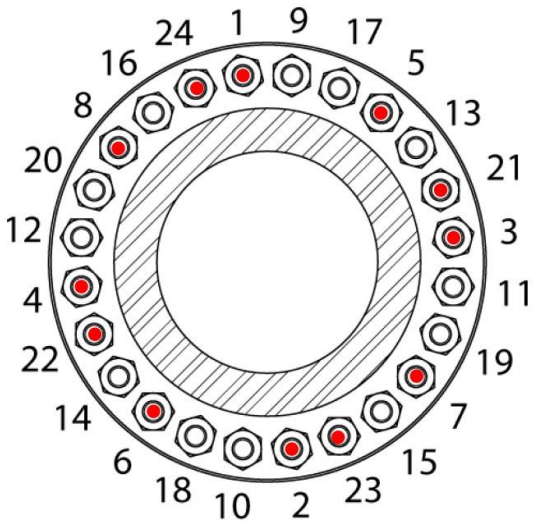

Figure B.1: Tightening Sequence

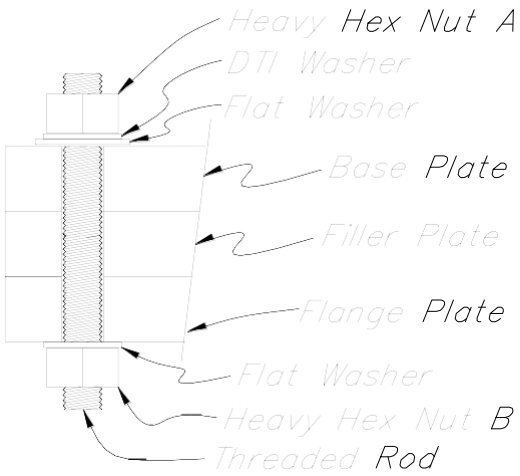

Figure B.2: Rod Assembly

B. For 24-bolt rod replacement and nut tightening use the following procedure:

1) Clean exposed threads on all existing bolt assemblies.

2) Tighten all nuts “Snug tight”. “Snug tight” is defined as 600 ft-lbs of torque. Either a Torque multiplier or a hydraulic torque wrench may be used to bring

nuts to snug tight torque. Consult manufacturer documentation to determine delivery pressure required to achieve specified torque for the hydraulic wrench.

3) Bolt assembly replacement and nut retightening begins with Rod Assembly labeled #1 in Figure 1 and continues sequentially until all bolts are replaced and new Rod Assemblies are tightened. **Remove only one bolt assembly at a time.** Rods that have an embedded axial strain gage (SG Rod) shall be installed in locations 1, 2, 3, 4, 5, 6, 7, 8, 21, 22, 23, 24, as shown in Figure 1.

    f. Remove existing bolt assembly and discard. DO NOT reuse existing bolts, washers or nuts.

    g. Clean plate bearing areas immediately before tightening.

    h. Install threaded rod, washer and 'A' nut.

    i. Install washer and 'B' nut

    j. Snug tight both nuts. Ensure that a minimum of three threads stick through at each 'A' nut and 'B' nut.

4) Repeat step 3 until all Rod Assemblies are sequentially replaced and all Rod Assembly nuts are snug tight.

5) Initial Turn of the Nut.

    a. Beginning with Rod Assembly labeled #1 in *Figure B.1* Tightening Sequence,

    b. Mark nut 'A', base plate, flange plate, nut 'B' and threaded rod with a permanent felt tipped pen or crayon as a reference for determining the relative rotation of the nut and threaded rod during the tightening.

    c. Rotate nut 'A' 20 degrees. **Prevent nut 'B' and threaded rod from moving whenever turning nut 'A'.**

6) Repeat step 5 above until all 24 ‘A’ nuts are sequentially tightened 20 degrees.

   a. After all Rod Assemblies are tightened 20 degrees, re-check snug tightness of the ‘B’ nuts. If nut ‘B’ or threaded rod moves then, loosen ‘A’ nut, snug tight both nuts and repeat step 5 on that Rod Assembly.

7) Repeat step 5 above three times until all 24 ‘A’ nuts are sequentially tightened 80 degrees.

8) Final Turn of the Nut.

   a. Complete tightening ‘A’ nuts beginning with the Rod Assembly labeled #1 in Figure 1,

   b. Rotate nut ‘A’ as follows:

      I. For SG Rods, stop rotation if any of the following conditions occur:

         (1) DTI washers display full volume of orange silicone

         (2) Strain gage instrumentation indicate 68 kips of axial force (70% of nominal yield)

         (3) Nut A rotates an additional 20 degrees for a total rotation of 100 degrees

         (4) Delivered torque reaches 2,500 ft-lbs

      II. For rods without strain gage instrumentation, stop rotation if any of the following conditions occur:

         (1) DTI washers display full volume of orange silicone

         (2) Nut A rotates an additional 20 degrees for a total rotation of 100 degrees

         (3) Delivered torque reaches 2,500 ft-lbs

   c. Record the final applied torque for each Rod Assembly

d. If the delivered torque reaches 2,500 ft-lbs without achieving the required turn of the nut, the required axial force, or full indication from the DTI washers, then on that Rod Assembly:

(1) Remove nut ‘B’ nut then, loosen nut ‘A’,

(2) Clean and re-lubricate all contact surfaces,

(3) Snug tight nuts ‘A’ and ‘B’.

(4) Mark nuts, base plate, flange plate, threaded rod and rotate nut ‘A’ 100 degrees.

(5) If required rotation is not achieved at 2,500 ft-lb torque then, notify the Engineer and proceed with Final Turn of the Nut on remaining ‘A’ nuts.

9) Repeat step 8 above until final tightening is sequentially completed on all 24 Rod Assemblies.

10) After all Rod Assemblies are tightened to their final rotation, re-check snug tightness of all ‘B’ nuts. If nut ‘B’ or the rod moves during snug tight check then loosen ‘A’ nut, snug tight both nuts and repeat steps 6, 7 and 8 on that Rod Assembly.

11) Utilizing the recorded final applied torque for each Rod Assembly, apply a Verification Torque to ‘A’ nut on each Rod Assembly in the sequence shown in Figure 1.

12) A minimum of 1 week and a maximum of 2 weeks after tightening, re-apply the Verification Torque to ‘A’ nuts and check snug tightness of ‘B’ nuts. If any nut or threaded rod moves, mark the nut and notify the Engineer.

Appendix C

Results of Peter's Creek Tightening

The tightening procedure used in *Measured Anchor Rod Tightening of High-mast Light Poles in Alaska* (Hoisington, Hoffman, Hamel) resulted in large pretension scatter. A few special provisions were adopted to try to reduce pretension scatter. They include the following changes:

- The inclusion of DTI washers. DTI washers are deformable washers that contain pockets of silicon. As the washers are flattened, the pockets of silicon are crushed, and squirt out of the side of the washers. Once all the cells have squirted, a feeler gauge is inserted between the connection plate and pockets of silicon. If the feeler gauge is not allowed to penetrate between the washer and the plate, the washer is carrying a load specified by the manufacturer +-1.5kips. The DTI washers used on this HMLP were set to fully indicate at 54 kips. The feeler gauge was not used for this tightening procedure.
- 'Snug Tight' condition includes the use of a torque wrench. The existing definition: "Snug tight" is the full effort of one person on an open-end wrench close to the end with a length equal to 14 times the rod diameter but not less than 18 inches. Instead, snug tight was taken only as the maximum rotation achieved by a torque wrench outputting 600 ft*lbs of torque.
- The degree of turn for turn-of-the-nut method was varied with grip length of threaded rods. The grip length of this HMLP is 6.75" because it has a spacer plate in between its flange and base plates. Instead of three 20 degree rotations, five 20 degree rotations were used in the turn-of-the-nut method.
- A final tightening step was added. After finishing the rotation of all nuts by the turn-of-the-nut method, a separate condition was added. Any of the rods that had DTI washers which didn't indicate were tightened with a hydraulic wrench. The

torque on this hydraulic wrench was set equal to the value required to rotate the nut on a rod whose DTI washer fully indicated.

There were 24 1.5 inch diameter rods on this HMLP, 12 of which were strain gauged. Figure C.1 & Figure C.2 below show the load monitored in ten of the strain gauges over the duration of the tightening procedure.

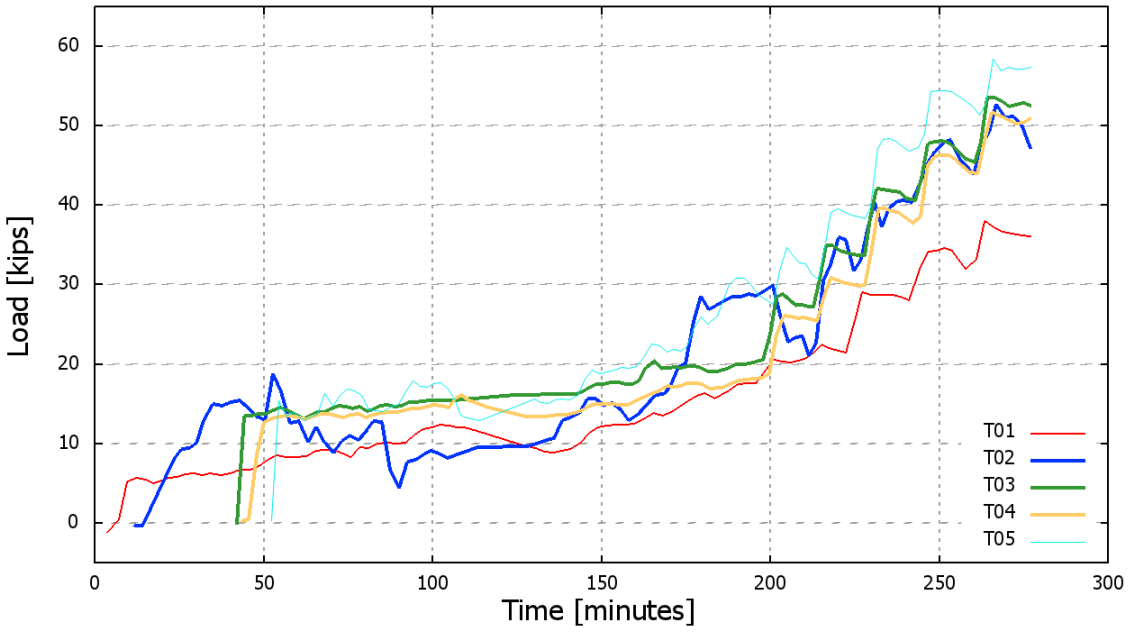

Figure C.1: Peters Creek Tightening of Strain Gauges(1*)*

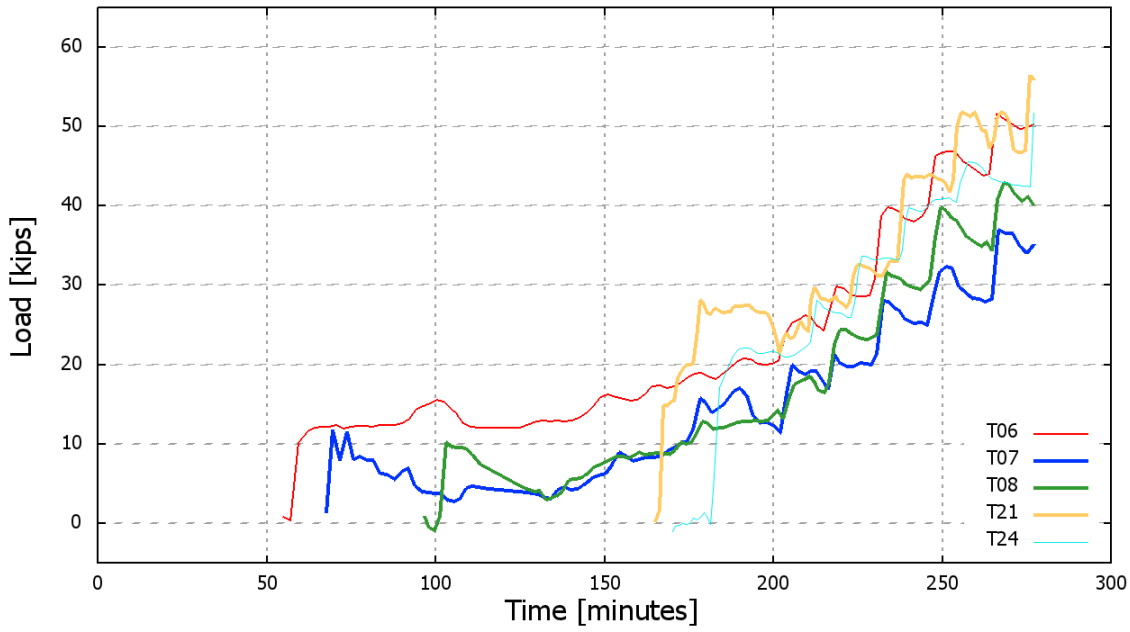

Figure C.2: Peters Creek Tightening of Strain Gauges(2)

From the above figures, it can be observed that there is significant noise in all of the strain gauges. This is due to electromagnetic interference thought to be originating from a nearby transformer.

The final pretension values for each strain gauge are summarized below in Table C-1.

Table C-1: Pretensions in SG Rods

Bolt #	Snug Tight	20 degrees	40 degrees	60 degrees	80 degrees	100 degrees	Squirt Status
1	12	21	25	30	35	40	+
2	14	24	33	38	43	48	*
3	15	28	35	42	49	54	-
4	15	26	32	40	47	53	-
5	16	30	38	47	53	58	-
6	14	25	30	39	45	51	-
7	--	--	--	25	30	36	*
8	12	18	25	31	36	42	+
21	15	25	32	41	48	54	-
24	17	27	33	39	44	52	-
Avg	14.4	24.9	31.4	37.2	43.0	48.8	
S.D.	1.67	3.62	4.28	6.56	7.18	7.15	

*No DTI indication, torqued until squirt.
+Partial indication, no further torque.

-Full Indication, no further torque.
all measurements considering +/- 2 kips error

The pretension scatter was greatly minimized when compared to the weigh-station tightening procedure. This is especially the case in the snug tight condition, which had a standard deviation of only 1.67 kips. The DTI washers performed especially well, even without the feeler gauge. The recorded pretension range of rods with DTI washers that were deemed fully indicated by observation alone was 51-58kips.

Appendix D

Long Term Monitoring Data

In addition to monitoring axial force during the tightening procedures, strain gauges were used to monitor data over time in both HMLPs. For the weigh-station HMLP, the same cRIO DAQ used during the tightening procedure was used to record strain gauge voltages until it experienced a catastrophic failure on day 50. The data acquisition system can be seen in Figure D.1 below. The system was powered by a 250W solar panel and a 12v battery.

Figure D.1: Weigh Station HMLP cRIO DAQ

The source of this failure is unknown. Figure D.2 & Figure D.3 show the data collected from strain gauges. Wind and temperature were being monitored on a nearby radio tower.

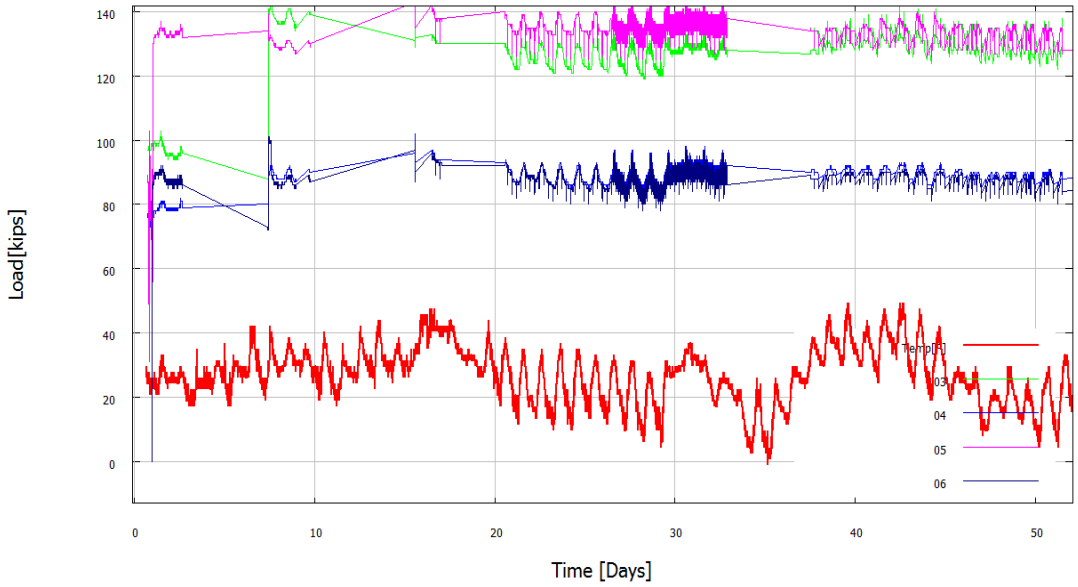

Figure D.2: Weigh Station cRIO Long Term Data(1)

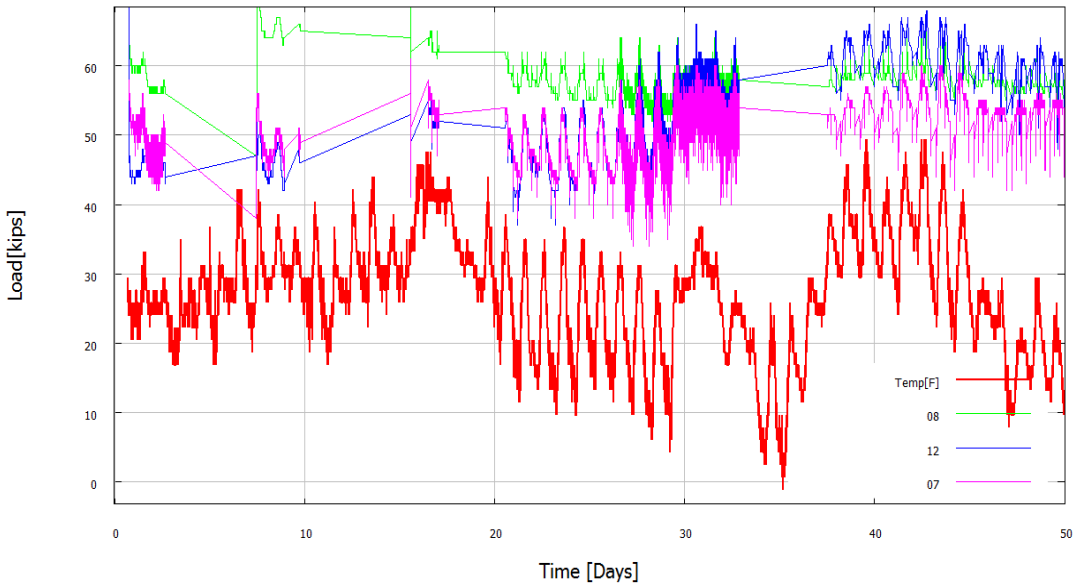

Figure D.3: Weigh Station cRIO Long Term Data(2)

The change in the axial load in the strain gauges closely matches the change in air temperature over the duration of data collection. No drastic change in axial load was observed after re-tightening on day 7. Note that strain gauges 3-6 indicate yielded rods.

After the failure, a new DAQ needed. Due to budgetary constraints, a new system was built instead of using an off-the-shelf model. The team elected to use Labjack® modules to monitor voltages which were output to a BeagleBone© miniature computer. A Python program was written that received, displayed, and stored the voltages on the BeagleBone. The system can be seen below in Figure D.4.

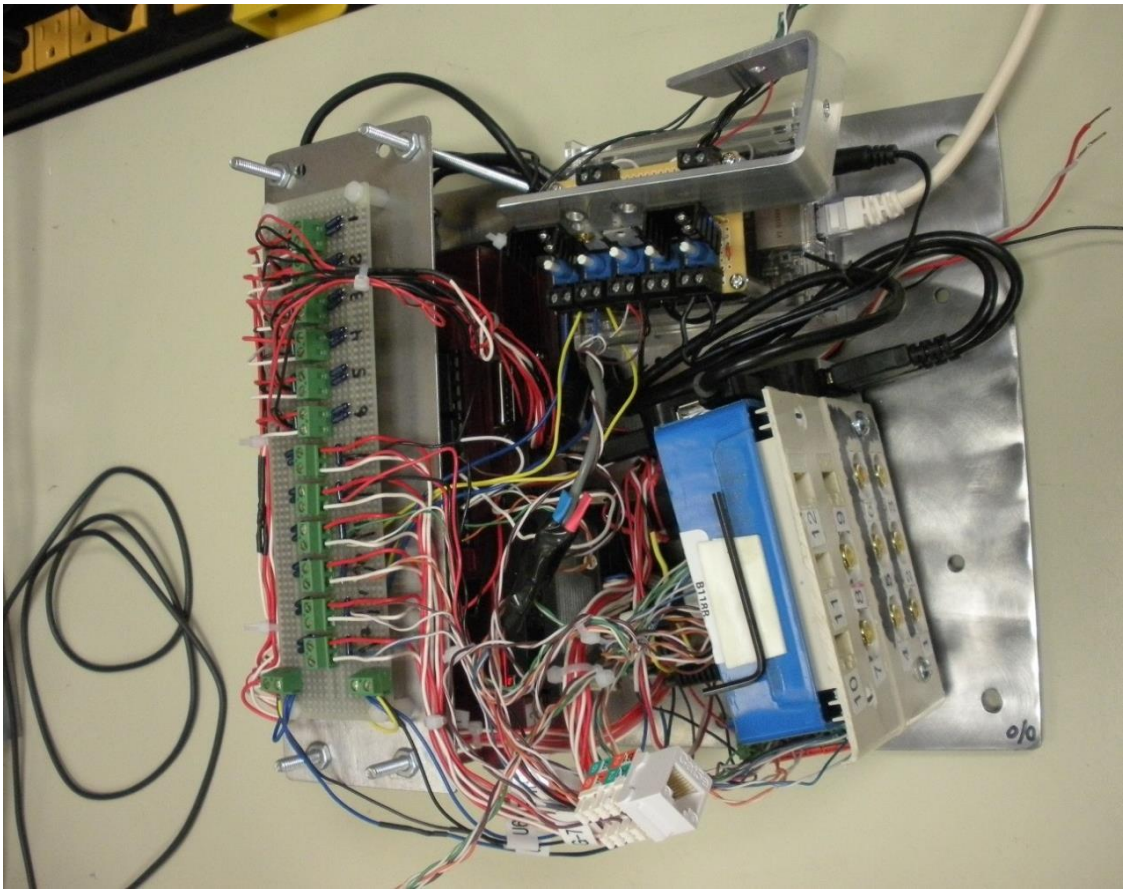

Figure D.4: Weigh Station Custom DAQ Build

This system ran into a few problems. The first of which was overheating. The BeagleBone requires 5V, but was being powered with a 12V battery. Initially, the

voltage step-down was executed using a linear regulator. The large amount of heat given off by the regulator combined with a small enclosure and little ventilation resulted in the BeagleBone quickly powering down. After unsuccessfully trying to dissipate the heat with aluminum and copper heat sinks, the regulators were replaced with a buck converter. The buck converter steps down the 12V into 5V, meaning voltage potential won't be wasted and turn into heat at the BeagleBone's power socket. After a few weeks of running smoothly, another catastrophic failure occurred. A spider was able to get into the box and span a positive and negative terminal, which rendered the BeagleBone inoperable. A new BeagleBone was purchased, and the DAQ was reassembled.

For the Peter's Creek HMLP, a DAQ system seen in Figure D.5 using Labjack OEM boards and a Beaglebone was used. A smaller 50W solar panel and three 12v deep cycle batteries were used; calculations showed the solar panel should generate enough charge to power the DAQ system.

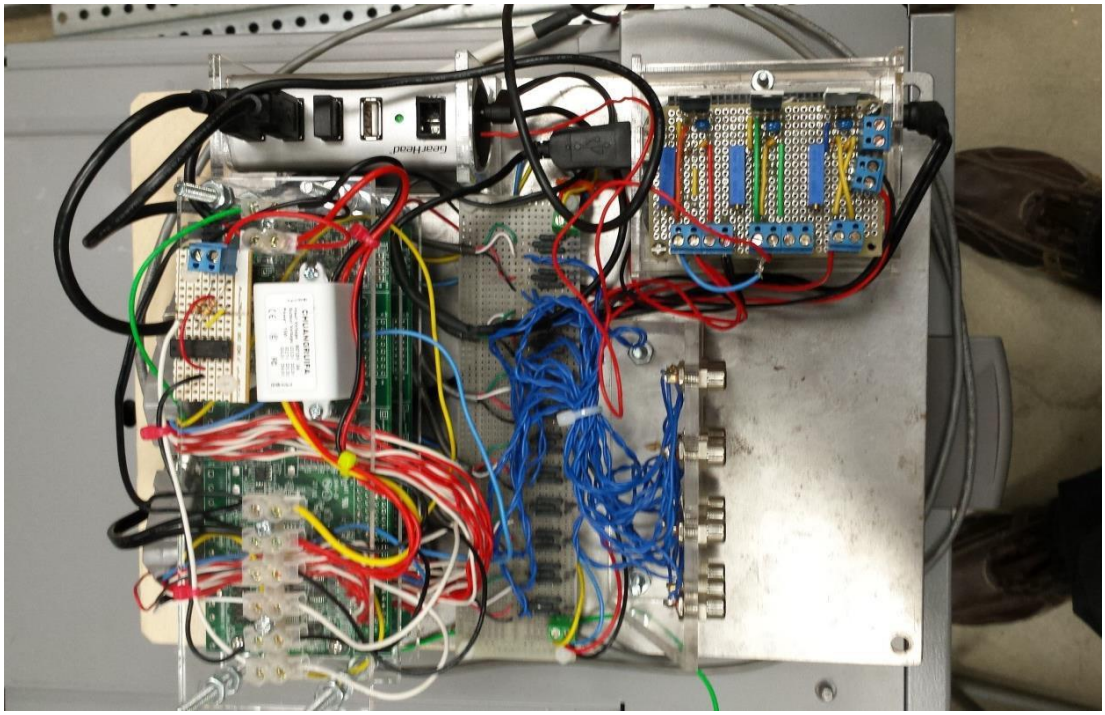

Figure D.5: Peter's Creek HMLP Custom DAQ Build

In the field, the solar panel didn't generate enough power to keep the DAQ from draining the batteries. The solution was to create a digital relay to shut down the USB hub, which would also turn off the Labjack boards that record the voltage from the strain gauges. This function significantly reduced power consumption and was successfully used in the lab for several days before the DAQ was returned to the Peter's Creek HMLP. However, the program only ran for 24 hours in the field due to an error. Further development of the Labjack-Beaglebone DAQ system is needed to create a reliable system. Figure D.6 & Figure D.7 below show the data recorded from the Peter's Creek system.

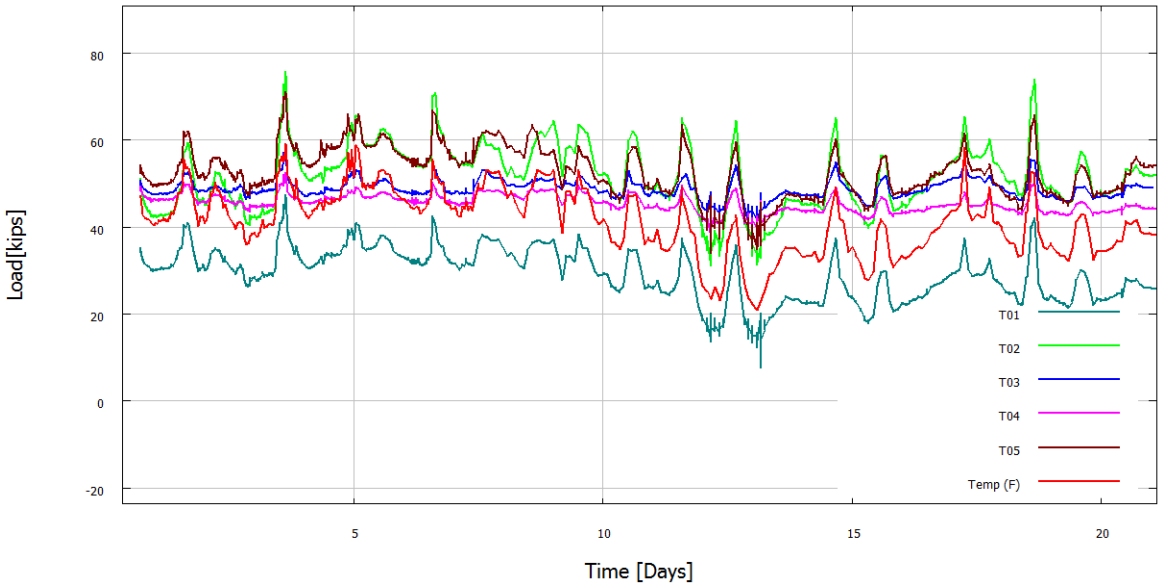

Figure D.6: Peter's Creek Time Data (1)

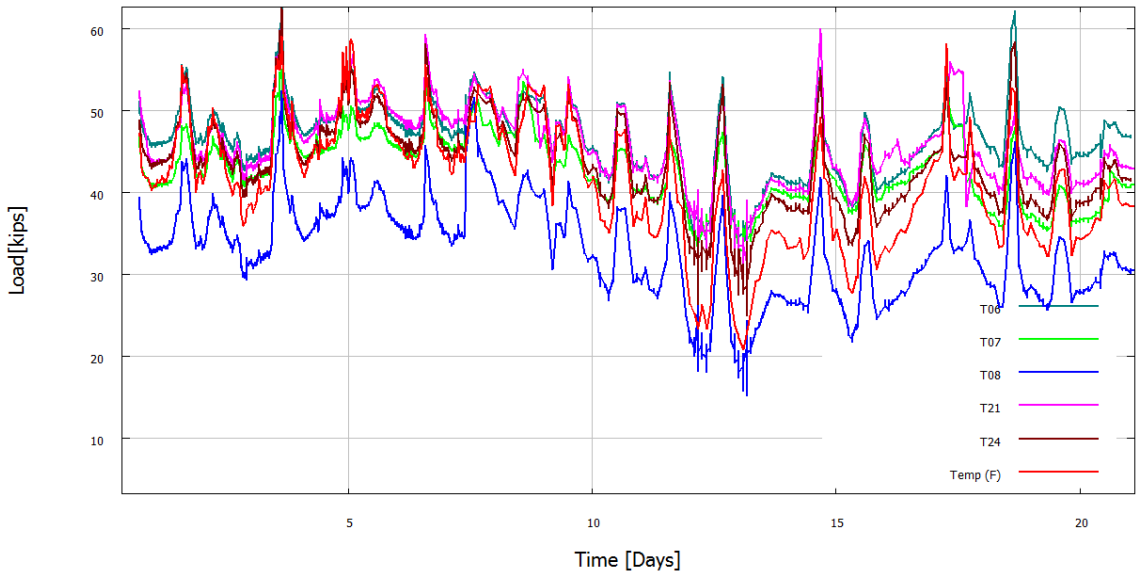

Figure D.7: Peter's Creek Time Data (2)

Appendix E

FEA of CIP Concrete HMLP Sixteen 2 Inch Rods

This FE model represents a HMLP configuration that is widely used in Alaska. The sixteen rods are embedded in concrete, which is represented by a rigid solid. The nuts clamp the base plate of the pole.

In Figure E.1, the anchor rods are pre-tensioned with a .

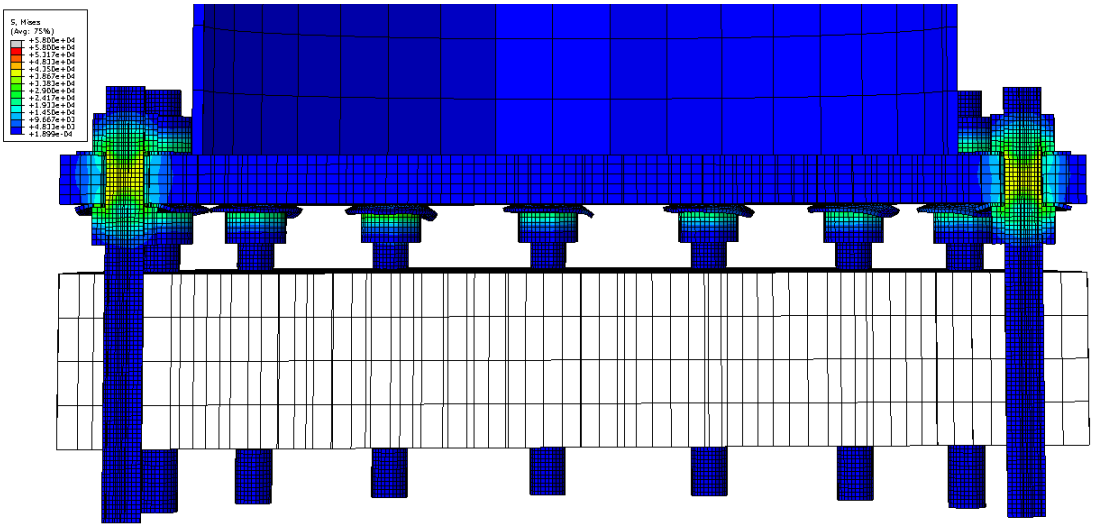

Figure E.1: CIP Concrete Pretension (

In Figure E.2, 110 mph wind is being simulated by applying a 9500 k*in moment to the pole.

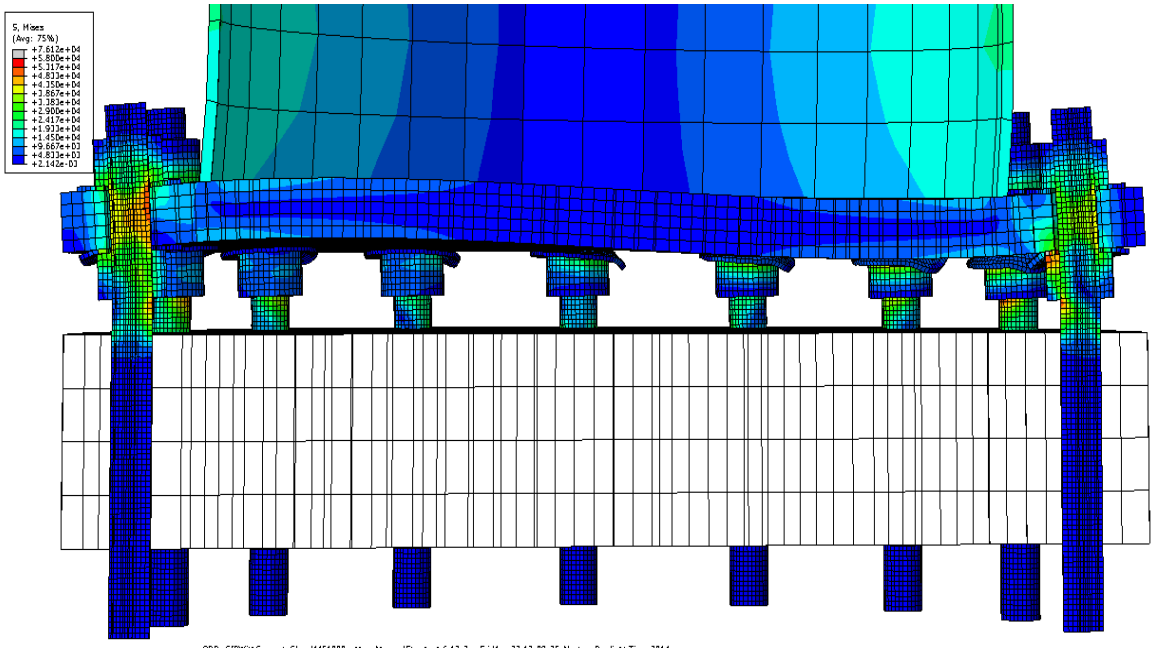

Figure E.2: CIP Concrete Load (9500 k*in Moment)

The model is cut down the middle of the X axis with the tension side of the moment on the left, and the compression on the right. Five rods are absorbing the tension component of the moment, while five rods are absorbing the compression component because there is no plate-plate contact. The deformation is scaled by a factor of 25. In Figure E.3, the load is removed.

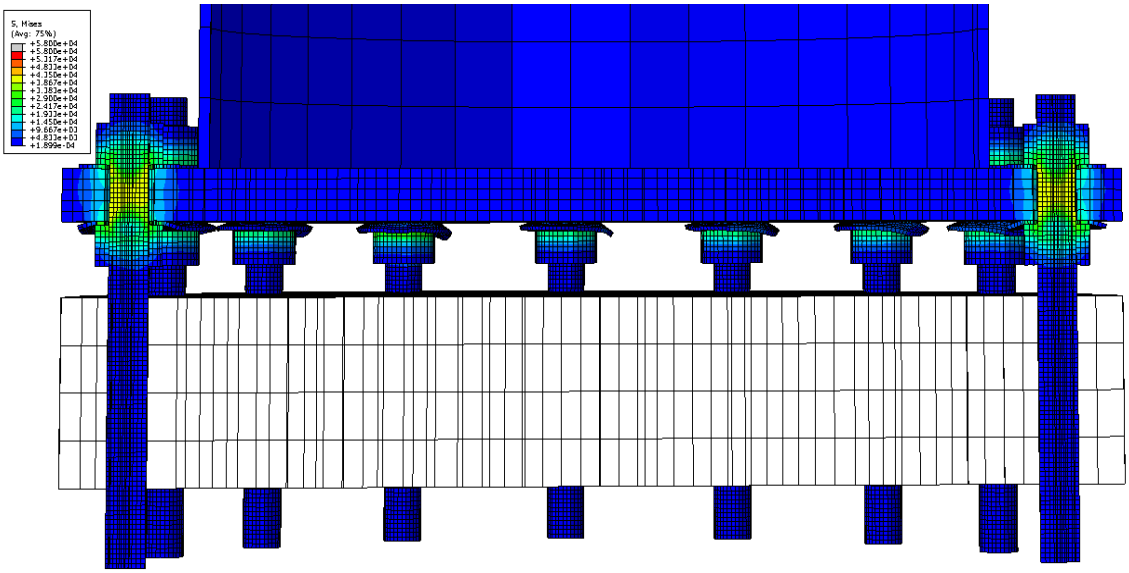

Figure E.3: CIP Concrete Unload (9500 k*in Moment)

It can be observed that there is not significant clamp loss. In Figure E.4 & Figure E.5, a moment of 18000 k*in lowers clamp load below “snug tight” levels.

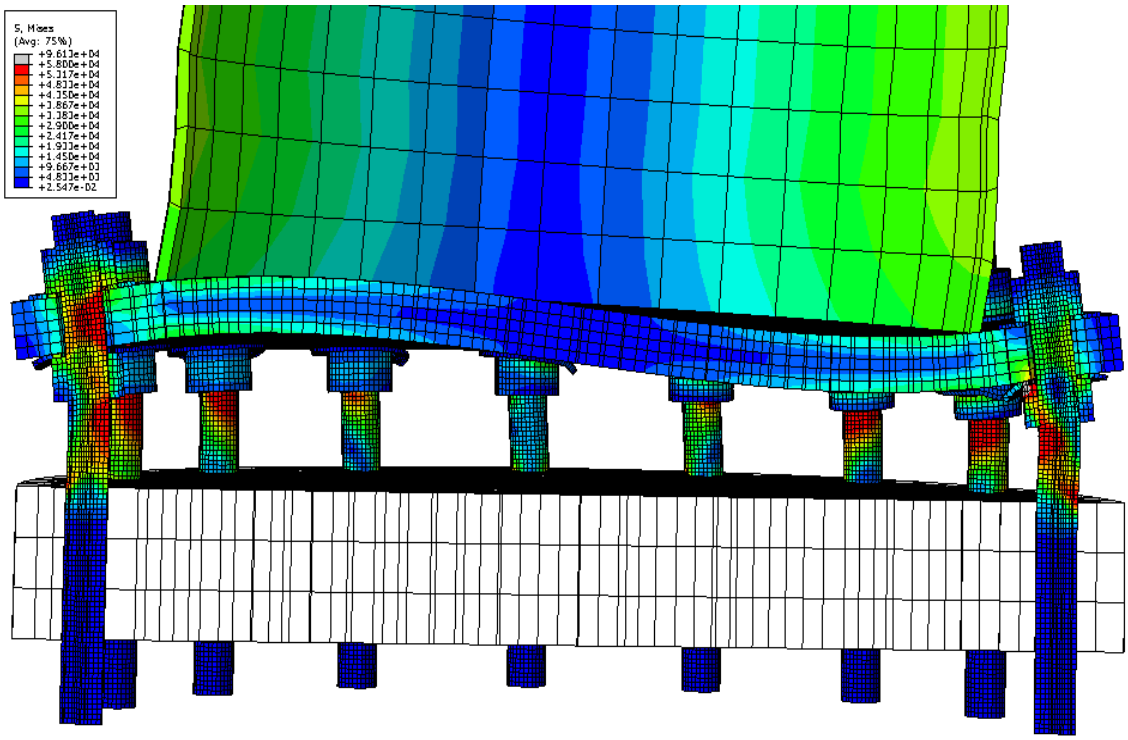

Figure E.4: CIP Concrete Load (18000 k*in Moment)

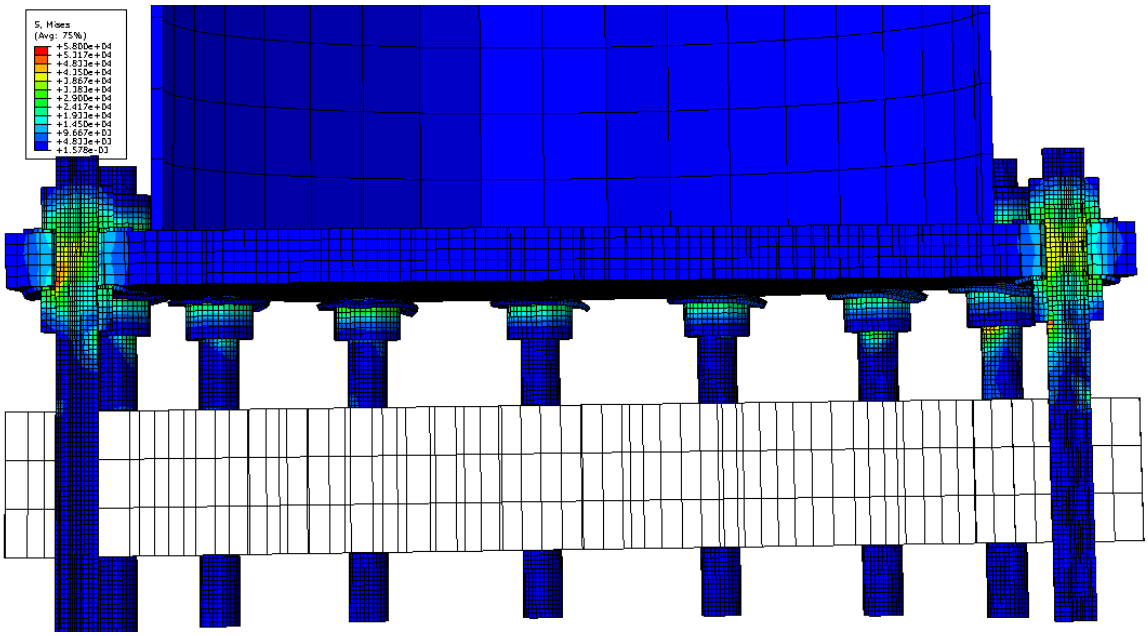

Figure E.5: CIP Concrete Unload (18000 k*in Moment)

The CIP Concrete foundation type separates at 20000 k*in. The design wind moment is equal to 9500 k*in. If the pretension is in the correct range, the FEA model shows that this foundation has a high resistance to clamp load loss. However, this model is static, and doesn't capture the effects of dynamic loads like vortex shedding. This actual maximum wind load may be much higher than the design wind load. Also, the model's geometry is perfect, and doesn't include variations in the angle of nuts which may be occurring in configurations with very short grip lengths. As seen in Figure E.4, rods on the compression side of the moment temporarily lose some of their tension during an external wind load. If the pretension in these rods in low enough, the rods will carry no load during the external wind load. If vibration occurs in the nut, it would be free to spin, and traditional loosening may occur. To make sure this bolted-joint interface utilizes its maximum resistance to clamp load loss due to traditional loosening, pre-tension needs to be kept in an acceptable range.

Appendix F

ASTM E8 Specimen Test to Fracture

A F1554 grade 55 specimen was fractured according to ASTM E8. The force and strain were monitored with an external strain gauge, an extensometer, and an internal strain gauge. Figure F.1 shows the stress-strain relationship recorded during the test.

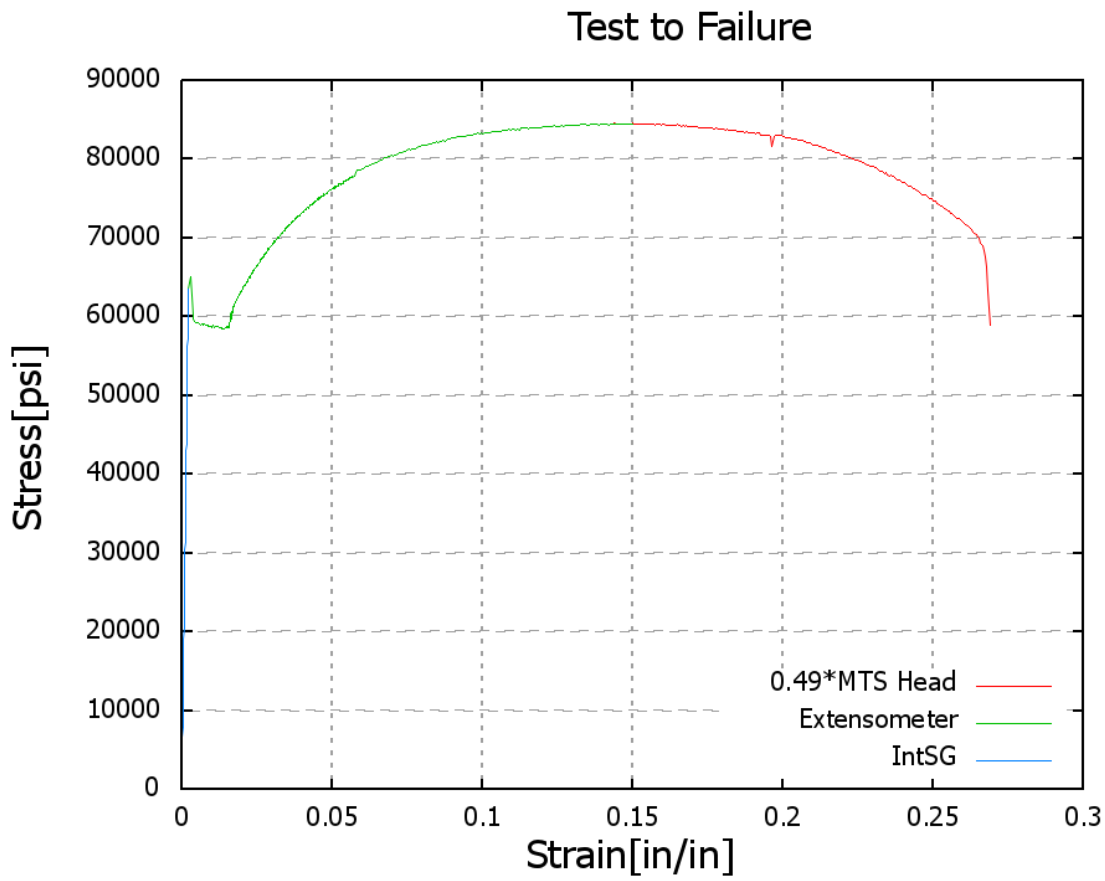

Figure F.1: F1554 Specimen Tested to Fracture

Appendix G

RCSC Suggested Minimum Pretension & Rotation for High Strength Bolts

The Research Council for Structural Connections has published minimum pretensions for high strength bolts according to their minimum tensile strength and diameter, seen in Table G-1. Table G-2 shows the recommended nut rotation to achieve these minimum pretensions based on the bolt lengths of the interface.

Table G-1: RCSC Table 8.1, Minimum Bolt Pretension for High Strength Bolts

Table 8.1. Minimum Bolt Pretension, *Pretensioned* and *Slip-Critical* Joints

Nominal Bolt Diameter, d_b, in.	Specified Minimum Bolt Pretension, T_m, kips [a]	
	ASTM A325 and F1852	ASTM A490 and F2280
½	12	15
⅝	19	24
¾	28	35
⅞	39	49
1	51	64
1⅛	56	80
1¼	71	102
1⅜	85	121
1½	103	148

[a] Equal to 70 percent of the specified minimum tensile strength of bolts as specified in ASTM Specifications for tests of full-size ASTM A325 and A490 bolts with UNC threads loaded in axial tension, rounded to the nearest kip.

Table G-2: RSCS Table 8.2, Turn-of-the-Nut Rotation for High Strength Bolts

Table 8.2. Nut Rotation from Snug-Tight Condition for Turn-of-Nut Pretensioning [a,b]

Bolt Length [c]	Disposition of Outer Faces of Bolted Parts		
	Both faces normal to bolt axis	One face normal to bolt axis, other sloped not more than 1:20 [d]	Both faces sloped not more than 1:20 from normal to bolt axis [d]
Not more than $4d_b$	⅓ turn	½ turn	⅔ turn
More than $4d_b$ but not more than $8d_b$	½ turn	⅔ turn	⅚ turn
More than $8d_b$ but not more than $12d_b$	⅔ turn	⅚ turn	1 turn

[a] Nut rotation is relative to bolt regardless of the element (nut or bolt) being turned. For required nut rotations of ½ turn and less, the tolerance is plus or minus 30 degrees; for required nut rotations of ⅔ turn and more, the tolerance is plus or minus 45 degrees.

[b] Applicable only to *joints* in which all material within the *grip* is steel.

[c] When the bolt length exceeds $12d_b$, the required nut rotation shall be determined by actual testing in a suitable *tension calibrator* that simulates the conditions of solidly fitting steel.

[d] Beveled washer not used.

Appendix H

FEA Element Descriptions

The options used to generate the elements in the three Finite-Element Modelling scenarios in chapter 3 and the one scenario in Appendix E (Scenario D) are tabulated below. Table H-1 contains the options used to generate the elements in Scenario A. Table H-2 contains the options used to generate the elements in Scenario B. Table H-3 contains the options used to generate the elements in Scenario C. Table H-4 contains the options used to generate the elements in Scenario D.

Table H-1: Scenario A Nodes/Element

Instance	Threaded Rod	Base Plate	Flange Plate	Pile
Approximate Size	0.2	0.5	0.5	6
Curvature Control	0.1	0.1	0.1	0.1
Minimum Size (% global size)	0.1	0.1	0.1	0.1
# Nodes (Per Instance)	4047	44022	43080	588
# Nodes (Total)	48564	44022	43080	588
# Elements (Per Instance)	3304	35765	34890	280
# Elements (Total)	39648	35765	34890	280
Instance	Washer	Nut	Pole (Top)	Pole (Bottom)
Approximate Size	0.2	0.2	5	3
Curvature Control	0.1	0.1	0.1	0.1
Minimum Size (% global size)	0.1	0.1	0.1	0.1
# Nodes (Per Instance)	646	1125	520	806
# Nodes (Total)	15504	27000	520	806
# Elements (Per Instance)	283	760	385	432
# Elements (Total)	6792	18240	385	432

Table H-2: Scenario B Nodes/Elements

Instance	Anchor Rod	Base Plate	Washer
Approximate Size	0.2	0.5	0.2
Curvature Control	0.1	0.1	0.1
Minimum Size (% global size)	0.1	0.1	0.1
# Nodes (Per Instance)	5992	55230	902
# Nodes (Total)	95872	55230	28864
# Elements (Per Instance)	5060	44785	398
# Elements (Total)	80960	44785	12736
Instance	Nut	Pole (Top)	Pole (Bottom)
Approximate Size	0.25	5	3
Curvature Control	0.1	0.1	0.1
Minimum Size (% global size)	0.1	0.1	0.1
# Nodes (Per Instance)	1008	560	988
# Nodes (Total)	32256	560	988
# Elements (Per Instance)	672	399	456
# Elements (Total)	21504	399	456

Table H-3: Scenario C Nodes/Elements

Instance	Threaded Rod	Base Plate	Flange Plate	Spacer Plate	Pile
Approximate Size	0.2	0.5	0.5	6	6
Curvature Control	0.1	0.1	0.1	0.1	0.1
Minimum Size (% global size)	0.1	0.1	0.1	0.1	0.1
# Nodes (Per Instance)	4690	57546	57546	57546	588
# Nodes (Total)	112560	57546	57546	57546	588
# Elements (Per Instance)	3828	46715	46715	46715	280
# Elements (Total)	91872	46715	46715	46715	280

Instance	Washer	Nut	Pole (Top)	Pole (Bottom)
Approximate Size	0.2	0.25	5	3
Curvature Control	0.1	0.1	0.1	0.1
Minimum Size (% global size)	0.1	0.1	0.1	0.1
# Nodes (Per Instance)	646	574	520	806
# Nodes (Total)	31008	27552	520	806
# Elements (Per Instance)	283	348	385	432
# Elements (Total)	13584	16704	385	432

Table H-4: Scenario D Nodes/Elements

Instance	Threaded Rod	Base Plate	Flange Plate	Pile
Approximate Size	0.2	0.5	0.5	6
Curvature Control	0.1	0.1	0.1	0.1
Minimum Size (% global size)	0.1	0.1	0.1	0.1
# Nodes (Per Instance)	5390	44022	43080	588
# Nodes (Total)	64680	44022	43080	588
# Elements (Per Instance)	4408	35765	34890	280
# Elements (Total)	52896	35765	34890	280
Instance	Washer	Nut	Pole (Top)	Pole (Bottom)
Approximate Size	0.2	0.25	5	3
Curvature Control	0.1	0.1	0.1	0.1
Minimum Size (% global size)	0.1	0.1	0.1	0.1
# Nodes (Per Instance)	646	574	520	806
# Nodes (Total)	31008	27552	520	806
# Elements (Per Instance)	283	348	385	432
# Elements (Total)	13584	16704	385	432

Appendix I

Weighstation DAQ Python Code

This appendix contains the Python code used to record the voltages from the strain gauges, and create a program that both converts the voltages into equivalent elastic force and displays that information for real time monitoring. This was the code used in the HMLP at the Weighstation, designated WS-1.

```
1.  from PyQt4.QtCore import *
2.  from PyQt4.QtGui import *
3.  import sys
4.  from math import *
5.  import time
6.  import datetime
7.  import numpy as np
8.  import pyqtgraph as pg
9.  import u6
10. import os
11.
12. try:
13.         import platform
14.         if platform.system() == 'Windows':
15.                 print "Running on Windows " + platform.release()
16.         elif platform.system() == "Linux":
17.                 import Adafruit_BBIO.GPIO as GPIO
18.                 GPIO.setup("P9_12", GPIO.OUT)
19.                 GPIO.output("P9_12", GPIO.HIGH)
20.                 print "Running on Linux " + platform.release()
21. except Exception, e: print "Error: "+str(e)
22. else: None
23.
24. try:
25.         u6_1 = u6.U6(serial = 360009278)
26.         u6_2 = u6.U6(serial = 360009319)
27.
28.         u6_1.getCalibrationData()
```

```
29.             u6_2.getCalibrationData()
30.
31. except Exception, e:
32.             print "Labjack Error: "+str(e)
33. else: None
34.
35. DAC0_REGISTER = 5000
36.
37. p_channels = 16
38. t_channels = 32
39.
40. v_labels = []
41. time_array = []
42.
43. v_arrays = []
44. for i in range(p_channels):
45.             v_arrays.append([])
46.
47. GAIN_INDEX = 2 #0 = 10v, 1 = 1v, 2 = 0.1v, 3 = 0.01v
48.
49. feedbackArguments = []
50. for i in range(0, p_channels, 2):
51.             feedbackArguments.append(u6.AIN24(PositiveChannel=i,
52. ResolutionIndex=8, GainIndex = GAIN_INDEX, Differential =  True))
53.
54. f = 1
55.
56. force_cal_array = [77420., 88210., 86260., 87520., 88640., 81905., 1., 1.,
57.                                                 85330., 84340., 85290., 84950., 84580.,
    87230., 1., 1.,]
58.
59. class Window(QMainWindow):
60.
61.             def     init    (self):
62.                         super(Window, self).    init    ()
63.
64.                         self.setWindowTitle('Labjack Voltage Monitor : Cold Room
    Creations')
65.
66.                         self.create_main_frame()
67.                         self.create_status_bar()

68.
```

```
69.                 self.running = False
70.
71.                 self.run_button()
72.
73.         def create_main_frame(self):
74.
75.                 bold = QFont()
76.                 bold.setBold(True)
77.
78.                         #row 1
79.                 self.gridLayout = QGridLayout()
80.                 self.gridLayout.setMargin(1)
81.                 self.gridLayout.setSpacing(3)
82.
83.                 self.gauge_title = QLabel('Gauge')
84.                 self.gauge_title.setFont(bold)
85.                 self.gridLayout.addWidget(self.gauge_title, 0,0,1,1)
86.
87.                 self.voltage_title = QLabel('Reading')
88.                 self.voltage_title.setFont(bold)
89.                 self.gridLayout.addWidget(self.voltage_title, 0,1,1,1)
90.
91.                 self.plot_title = QLabel('Plot')
92.                 self.plot_title.setFont(bold)
93.                 self.gridLayout.addWidget(self.plot_title, 0,2,1,1)
94.
95.                 self.offset_title = QLabel('Offset')
96.                 self.offset_title.setFont(bold)
97.                 self.gridLayout.addWidget(self.offset_title, 0,3,1,1)
98.
99.                         #column 1
100.                        for i in range(p_channels/2-2):
101.                                vT = QLabel('%i'%(i+1))
102.                                self.gridLayout.addWidget(vT, i+1,0,1,1) #pos 2 - 7
103.
104.                        eT = QLabel('E+ U6-1')
105.                        self.gridLayout.addWidget(eT, p_channels/2-1,0,1,1)
        #pos 8
106.
107.                        batt = QLabel('Battery')
108.                        self.gridLayout.addWidget(batt, p_channels/2,0,1,1) #pos 9
109.
110.                        for i in range(p_channels/2-2):
```

```
111.                                    vT = QLabel('%i'%(i+p_channels/2-1))
112.                                    self.gridLayout.addWidget(vT,
    i+p_channels/2+1,0,1,1) #pos 10 - 15
113.
114.                            eT = QLabel('E+ U6-2')
115.                            self.gridLayout.addWidget(eT, p_channels-1,0,1,1) #pos 16
116.
117.                            tT = QLabel('TEMP')
118.                            self.gridLayout.addWidget(tT, p_channels,0,1,1) #pos 17
119.
120.                                    #column 2
121.                            for i in range(p_channels):
122.                                    self.vL = QLabel('0.000000', self)
123.                                    self.vL.my_index = i
124.                                    v_labels.append(self.vL)
125.                                    self.gridLayout.addWidget(self.vL, i+1,1,1,1)
126.
127.                                    #column 3
128.                            self.checkboxes = []
129.                            self.plots = []
130.                            self.plot_data = []
131.                            for i in range(p_channels):
132.                                    cb = QCheckBox()
133.                                    cb.my_index = i
134.                                    self.checkboxes.append(cb)
135.                                    self.plots.append(None)
136.                                    self.plot_data.append(None)
137.                                    cb.toggled.connect(self.check_toggled)
138.                                    self.gridLayout.addWidget(cb, i+1,2,1,1)
139.
140.                                    #column 4
141.
142.                            self.offsets = []
143.                            for i in range(p_channels):
144.                                    cb = QLineEdit()
145.                                    cb.setValidator(QDoubleValidator(-
    9999999,9999999, 5))
146.                                    cb.setFixedWidth(50)
147.                                    cb.setText('0.0')
148.                                    cb.my_index = i
149.                                    self.offsets.append(cb)
150.                                    self.gridLayout.addWidget(cb, i+1,3,1,1)
151.
```

```
152.                    #vertical layout (left column, grid, spacer)
153.                    self.verticalLayout_1 = QVBoxLayout()
154.
155.                    #set sampling frequency, duration, & wait
156.                    self.freq1_hlayout = QHBoxLayout()
157.                    self.freq_1 = QSpinBox()
158.                    self.freq_1.setValue(10)
159.                    self.freq_1.setRange(1,99999)
160.                    self.freq_1_title = QLabel('Frequency (Hz):')
161.                    self.freq_1_title.setFont(bold)
162.                    self.freq1_hlayout.addWidget(self.freq_1_title)
163.                    self.freq1_hlayout.addWidget(self.freq_1)
164.                    self.verticalLayout_1.addLayout(self.freq1_hlayout)
165.
166.                    self.collect_dur_hlayout = QHBoxLayout()
167.                    self.collect_dur = QSpinBox()
168.                    self.collect_dur.setRange(1,9999)
169.                    self.collect_dur.setValue(999)
170.                    self.collect_dur_title = QLabel('Duration (s):')
171.                    self.collect_dur_title.setFont(bold)
172.                    self.collect_dur_hlayout.addWidget(self.collect_dur_title)
173.                    self.collect_dur_hlayout.addWidget(self.collect_dur)
174.                    self.verticalLayout_1.addLayout(self.collect_dur_hlayout)
175.
176.                    self.wait_dur_hlayout = QHBoxLayout()
177.                    self.wait_dur = QSpinBox()
178.                    self.wait_dur.setValue(5)
179.                    self.wait_dur.setRange(1,9999)
180.                    self.wait_dur_title = QLabel('Wait (s):')
181.                    self.wait_dur_title.setFont(bold)
182.                    self.wait_dur_hlayout.addWidget(self.wait_dur_title)
183.                    self.wait_dur_hlayout.addWidget(self.wait_dur)
184.                    self.verticalLayout_1.addLayout(self.wait_dur_hlayout)
185.
186.                    self.verticalLayout_1.addLayout(self.gridLayout)
187.
188.                    self.spacerItem_1 = QSpacerItem(20, 40,
    QSizePolicy.Minimum,
189.                            QSizePolicy.Expanding)
190.                    self.verticalLayout_1.addItem(self.spacerItem_1)
191.
192.                    # horizontal layout 1 (grid layout + plot window)
193.                    self.horizontalLayout_1 = QHBoxLayout()
```

```
194.
195.                         self.horizontalLayout_1.addLayout(self.verticalLayout_1)
196.
197.                         self.v_plot_layout = QVBoxLayout()
198.                         self.win = pg.GraphicsLayoutWidget()
199.                         self.plotter = self.win
200.                         self.v_plot_layout.addWidget(self.plotter)
201.
202.                         # display value type
203.
204.                         self.volts_chkbox = QRadioButton()
205.                         self.volts_chkbox_title = QLabel('Volts')
206.                         self.volts_chkbox.setChecked(True)
207.
208.                         self.force_chkbox = QRadioButton()
209.                         self.force_chkbox_title = QLabel('Force')
210.
211.                         self.display_type_layout = QHBoxLayout()
212.                         self.display_type_layout.addWidget(self.volts_chkbox)
213.
        self.display_type_layout.addWidget(self.volts_chkbox_title)
214.                         self.display_type_layout.addWidget(self.force_chkbox)
215.
        self.display_type_layout.addWidget(self.force_chkbox_title)
216.
217.                         self.display_type_spacer = QSpacerItem(40, 20,
    QSizePolicy.Expanding,
218.                                 QSizePolicy.Minimum)
219.                         self.display_type_layout.addItem(self.display_type_spacer)
220.
221.                         self.v_plot_layout.addLayout(self.display_type_layout)
222.
223.                         self.horizontalLayout_1.addLayout(self.v_plot_layout)
224.
225.                         # horizontal layout 2 (time title + time label + spacer)
226.
227.                         self.horizontalLayout_2 = QHBoxLayout()
228.
229.                         self.time_title = QLabel('Time:')
230.                         self.time_title.setFont(bold)
231.                         self.horizontalLayout_2.addWidget(self.time_title)
232.
233.     self.time_label = QLabel('0.00', self)
```

```
234.                    self.horizontalLayout_2.addWidget(self.time_label)
235.
236.                    spacerItem_2 = QSpacerItem(40, 20,
    QSizePolicy.Expanding,
237.                            QSizePolicy.Minimum)
238.                    self.horizontalLayout_2.addItem(spacerItem_2)
239.
240.                    # horizontal layout 3 (file title + file label + spacer)
241.                    self.horizontalLayout_3 = QHBoxLayout()
242.
243.                    self.file_title = QLabel('File:')
244.                    self.file_title.setFont(bold)
245.
246.                    self.write_cb = QCheckBox()
247.
248.                    self.horizontalLayout_3.addWidget(self.write_cb)
249.                    self.horizontalLayout_3.addWidget(self.file_title)
250.
251.                    self.file_label = QLabel('"Check to write to file"', self)#
252.                    self.horizontalLayout_3.addWidget(self.file_label)
253.
254.                    spacerItem_3 = QSpacerItem(40, 20,
    QSizePolicy.Expanding,
255.                            QSizePolicy.Minimum)
256.                    self.horizontalLayout_3.addItem(spacerItem_3)
257.
258.                    # horizontal layout 4 (run button + file dialog button +
    spacer)
259.                    self.horizontalLayout_4 = QHBoxLayout()
260.
261.                    self.button = QPushButton('Start', self)
262.                    self.button.clicked.connect(self.run_button)
263.                    self.horizontalLayout_4.addWidget(self.button)
264.
265.                    spacerItem_4 = QSpacerItem(40, 20,
    QSizePolicy.Expanding,
266.                            QSizePolicy.Minimum)
267.                    self.horizontalLayout_4.addItem(spacerItem_4)
268.
269.                    # vertical layout (encompassing)
270.
271.                    self.verticalLayout_2 = QVBoxLayout()
272.
```

```
273.                    self.verticalLayout_2.addLayout(self.horizontalLayout_4)
274.                    self.verticalLayout_2.addLayout(self.horizontalLayout_3)
275.                    self.verticalLayout_2.addLayout(self.horizontalLayout_2)
276.                    self.verticalLayout_2.addLayout(self.horizontalLayout_1)
277.
278.                    # main layout
279.                    self.main_frame = QWidget()
280.
281.                    self.setCentralWidget(self.main_frame)
282.                    self.main_frame.setLayout(self.verticalLayout_2)
283.
284.                    self.checkboxes[0].setChecked(False) #set first checkbox to
    checked
285.
286.            def create_status_bar(self):
287.
288.                    self.status_text = QLabel('Monitor idle')
289.                    self.statusBar().addWidget(self.status_text, 1)
290.
291.            def run_button(self):
292.
293.                    if self.running == False:
294.                            self.running = True
295.
296.                            self.show_dialog()
297.
298.                            self.time_on_press = time.time()
299.
300.                            self.timer = QTimer()
301.                            self.timer.timeout.connect(self.run_loop)
302.
303.                            self.on_start()
304.
305.                            self.freq_1.setEnabled(False)
306.                            self.collect_dur.setEnabled(False)
307.                            self.wait_dur.setEnabled(False)
308.                            self.write_cb.setEnabled(False)
309.
310.                            self.button.setText('Stop')
311.
312.                    elif self.running == True:
313.                            self.running = False
314.
```

```
315.                                    self.on_stop()
316.
317.                                    self.freq_1.setEnabled(True)
318.                                    self.collect_dur.setEnabled(True)
319.                                    self.wait_dur.setEnabled(True)
320.                                    self.write_cb.setEnabled(True)
321.
322.                                    self.button.setText('Start')
323.
324.                    def show_dialog(self):
325.                            #if self.write_cb.isChecked():
326.                                    #self.file_name =
    QFileDialog.getSaveFileName(self, 'Save file', '.raw')
327.
328.                            self.file_name = './test_file.raw'
329.                            open(self.file_name, 'w').close()
330.
331.                            with open(self.file_name, "w") as file:
332.
333.                                    file.write(str(datetime.datetime.now(
334.                                            ).strftime("#%Y-%m-%d
    %H:%M:%S"))+'\n')
335.                                    file.write('#PC'+'\n')
336.                                    file.write('#freq: '+str(self.freq_1.value())+'\n')
337.                                    file.write('#collect dur:
    '+str(self.collect_dur.value())+'\n')
338.                                    file.write('#wait dur:
    '+str(self.wait_dur.value())+'\n'+'#\n')
339.
340.                                    file.write('#Day'+'\t')
341.
342.                                    file.write('Time (s)'+'\t')
343.
344.                                    for i in range(p_channels/2-2):
345.                                            file.write('Voltage_%i (V)'%(i+1)+'\t')
346.
347.                                    file.write('E+(u6_1) (V)'+'\t')
348.                                    file.write('Battery (V)'+'\t')
349.
350.                                    for i in range(p_channels/2-2):
351.                                            file.write('Voltage_%i (V)'%(i+8)+'\t')
352.
353.                                    file.write('E+(u6_1) (V)'+'\t')
```

```
354.                                    file.write('Temp (V)')
355.                                    s
356.                                    file.write('\n')
357.                                    file.close()
358.
359.                            self.file_label.setText(self.file_name)
360.                            self.file = open(self.file_name, "a")
361.
362.                            #else:
363.                                    #None
364.
365.             def     excitation(self):
366.                            # d.writeRegister(DAC0_REGISTER, 4.5)
367.
368.                            if platform.system() == 'Linux':
369.                                    GPIO.output("P9_12", GPIO.LOW)
370.
371.
372.             def on_start(self):
373.                            self.excitation()
374.
375.                            self.timer.start(1000/self.freq_1.value())
376.
377.                            self.wait_timer = QTimer()
378.                            self.wait_timer.setSingleShot(True)
379.                            self.wait_timer.setInterval(self.collect_dur.value()*1000)
380.                            self.wait_timer.timeout.connect(self.on_pause)
381.                            self.wait_timer.start()
382.
383.                            self.status_text.setText('Monitor running...')
384.
385.             def on_stop(self):
386.                            if platform.system() == 'Linux':
387.                                    GPIO.output("P9_12", GPIO.HIGH)
388.
389.                            self.timer.stop()
390.                            self.wait_timer.stop()
391.
392.                            for i in range(p_channels):
393.                                    del v_arrays[i][:]
394.
395.                            del time_array[:]
396.
```

```
397.                        self.status_text.setText('Monitor stopped')
398.
399.                        if self.write_cb.isChecked():
400.                                self.file.close()
401.
402.                def on_pause(self):
403.                        if platform.system() == 'Linux':
404.                                GPIO.output("P9_12", GPIO.HIGH)
405.
406.                        self.timer.stop()
407.
408.                        self.wait_timer = QTimer()
409.                        self.wait_timer.setSingleShot(True)
410.                        self.wait_timer.setInterval(self.wait_dur.value()*1000)
411.                        self.wait_timer.timeout.connect(self.on_start)
412.                        self.wait_timer.start()
413.
414.                        self.status_text.setText('Monitor waiting...')
415.
416.                def run_loop(self):
417.                        t = time.time() - 1348272000 #WS datum: 9/22/2012
    00:00:00, AK time (no DST)
418.                        days = int(t/86400)
419.                        secs = '{0:.2f}'.format(t - days * 86400)
420.                        clock_time = round((time.time() - self.time_on_press), 3)
421.
422.                        self.time_label.setText(str(days)+' ('+str(secs)+')')
423.
424.                        time_array.append(clock_time)
425.                        if len(time_array) > 100:
426.                                time_array.pop(0)
427.
428.                        if self.write_cb.isChecked():
429.                                self.file.write(str(days)+'\t')
430.                                self.file.write(str(secs)+'\t')
431.
432.                        for i in range(p_channels):
433.
434.                                if i < p_channels/2-2:
435.                                        ainBits =
    u6_1.getFeedback(feedbackArguments[i])
436.                                        v =
    u6_1.binaryToCalibratedAnalogVoltage(gainIndex=GAIN_INDEX,
```

```
437.                                                 bytesVoltage=ainBits[0],
    is16Bits=False)
438.
439.                                 elif i == p_channels/2-2:
440.                                     ainBits =
    u6_1.getFeedback(u6.AIN24(PositiveChannel=12,
441.                                                 ResolutionIndex=8, GainIndex = 0,
    Differential = False))
442.                                     v =
    u6_1.binaryToCalibratedAnalogVoltage(gainIndex=0,
443.                                                 bytesVoltage=ainBits[0],
    is16Bits=False)
444.
445.                                 elif i == p_channels/2-1:
446.                                     ainBits =
    u6_1.getFeedback(u6.AIN24(PositiveChannel=13,
447.                                                 ResolutionIndex=8, GainIndex = 0,
    Differential = False))
448.                                     v =
    u6_1.binaryToCalibratedAnalogVoltage(gainIndex=0,
449.                                                 bytesVoltage=ainBits[0],
    is16Bits=False)
450.
451.                                 elif i == p_channels-2:
452.                                     ainBits =
    u6_2.getFeedback(u6.AIN24(PositiveChannel=12,
453.                                                 ResolutionIndex=8, GainIndex = 0,
    Differential = False))
454.                                     v =
    u6_1.binaryToCalibratedAnalogVoltage(gainIndex=0,
455.                                                 bytesVoltage=ainBits[0],
    is16Bits=False)
456.
457.                                 elif i == p_channels-1:
458.                                     ainBits =
    u6_2.getFeedback(u6.AIN24(PositiveChannel=13,
459.                                                 ResolutionIndex=8, GainIndex = 0,
    Differential = False))
460.                                     v =
    u6_1.binaryToCalibratedAnalogVoltage(gainIndex=0,
461.                                                 bytesVoltage=ainBits[0],
    is16Bits=False)
462.
```

```
463.                                 elif i > p_channels/2-1:
464.                                         ainBits =
    u6_2.getFeedback(feedbackArguments[i-p_channels/2])
465.                                         v =
    u6_2.binaryToCalibratedAnalogVoltage(gainIndex=GAIN_INDEX,
466.                                                 bytesVoltage=ainBits[0],
    is16Bits=False)
467.
468.                                 if i < p_channels-1:
469.                                         if self.force_chkbox.isChecked():
470.                                                 if not v_arrays[6]:
471.                                                         ex = 1
472.                                                 else:
473.                                                         ex = v_arrays[6].pop()
474.
475.
            v_labels[i].setText(str((v*force_cal_array[i]/ex+float(self.offsets[i].text()
    ))))
476.
            v_arrays[i].append(v*force_cal_array[i]/ex+float(self.offsets[i].text() ))
477.                                         else:
478.
            v_labels[i].setText(str(v+float(self.offsets[i].text() )))
479.
            v_arrays[i].append(v+float(self.offsets[i].text() ))
480.
481.                                 elif i == p_channels-1:
482.                                         temp = v#((100*v)-273.15)*1.8+32
483.                                         v_labels[i].setText(str(temp))
484.                                         v_arrays[i].append(v)
485.
486.                                 if self.write_cb.isChecked():
487.                                         self.file.write(str(v)+'\t')
488.
489.                                 if len(v_arrays[i]) > 100:
490.                                         v_arrays[i].pop(0)
491.
492.                         if self.write_cb.isChecked():
493.                                         self.file.write('\n')
494.
495.                         self.update_plot()
496.
497.                 def check_toggled(self):
```

```
498.                            cb = self.sender()
499.                            i = cb.my_index
500.                            if cb.isChecked():
501.                                    if i < p_channels/2-1:
502.                                            plot = self.win.addPlot(title="%d"%(i+1),
    col=1, row=i+1)
503.                                    elif i == p_channels/2-1 or i == p_channels-1:
504.                                            plot = self.win.addPlot(title="%d"%(i+1),
    col=1, row=i+1)
505.                                    elif i > p_channels/2-1:
506.                                            plot = self.win.addPlot(title="%d"%(i),
    col=1, row=i+1)
507.
508.                                    if self.force_chkbox.isChecked():
509.                                            plot.setLabel('bottom', 'Time', units='s')
510.                                            plot.setLabel('left', 'Force', units ='  kip')
511.                                    else:
512.                                            plot.setLabel('bottom', 'Time', units='s')
513.                                            plot.setLabel('left', 'Volts', units ='V')
514.
515.                                    self.plots[i] = plot
516.                                    self.plot_data[i] = plot.plot()
517.                            else:
518.                                    self.win.removeItem(self.plots[i])
519.
520.                    def update_plot(self):
521.                            for i in range(p_channels):
522.                                    if self.checkboxes[i].isChecked():
523.                                            self.plot_data[i].setData(time_array,
    v_arrays[i])
524.
525.
526.            def main():
527.                    app = QApplication(sys.argv)
528.                    window = Window()
529.                    window.show()
530.                    app.exec_()
531.
532.
533.            if    name__== "    main    ":
534.               main()
```

Appendix J

Peter's Creek Daq Python Code

This appendix contains the Python code used to record the voltages from the strain gauges, and create a program that both converts the voltages into equivalent elastic force and displays that information for real time monitoring. This was the code used in the HMLP at Peter's Creek, designated SPC-01.

```
from PyQt4.QtCore import *
from PyQt4.QtGui import *
import sys
from math import *
import time
import datetime
#import numpy as np
import pyqtgraph as pg
import u6
import os

try:
    import platform
    if platform.system() == 'Windows':
        print "Running on Windows " + platform.release()
    elif platform.system() == "Linux":
        import Adafruit_BBIO.GPIO as GPIO
        GPIO.setup("P9_12", GPIO.OUT)
        GPIO.output("P9_12", GPIO.LOW)
        print "Running on Linux " + platform.release()
except Exception, e: print "Error: "+str(e)
else: None

time.sleep(5)

try:
    u6_1 = u6.U6(serial = 360008508)
    u6_2 = u6.U6(serial = 360009180)
```

```
29.
30.       u6_1.getCalibrationData()
31.       u6_2.getCalibrationData()
32.
33. except Exception, e:
34.       print "Labjack Error: "+str(e)
35. else: None
36.
37. #DAC0_REGISTER = 5000
38.
39. p_channels = 16
40. t_channels = 32
41.
42. v_labels = []
43. time_array = []
44.
45. v_arrays = []
46. for i in range(p_channels):
47.       v_arrays.append([])
48.
49. GAIN_INDEX = 2 #0 = 10v, 1 = 1v, 2 = 0.1v, 3 = 0.01v
50.
51. feedbackArguments = []
52. for i in range(0, p_channels, 2):
53.       feedbackArguments.append(u6.AIN24(PositiveChannel=i,
54.                 ResolutionIndex=8, GainIndex = GAIN_INDEX, Differential = True))
55.
56. f = 1
57.
58. force_cal_array = [77420., 88210., 86260., 87520., 88640., 81905., 1., 1.,
59.                                         85330., 84340., 85290., 84950., 84580., 87230., 1.,
    1.,]
60.
61. class Window(QMainWindow):
62.
63.       def     init    (self):
64.                 super(Window, self).    init    ()
65.
66.                 self.setWindowTitle('Labjack Voltage Monitor : Cold Room Creations')
67.
68.                 self.create_main_frame()
69.                 self.create_status_bar()
70.
```

```
71.             self.running = False
72.
73.     def create_main_frame(self):
74.
75.             bold = QFont()
76.             bold.setBold(True)
77.
78.                     #row 1
79.             self.gridLayout = QGridLayout()
80.             self.gridLayout.setMargin(1)
81.             self.gridLayout.setSpacing(3)
82.
83.             self.gauge_title = QLabel('Gauge')
84.             self.gauge_title.setFont(bold)
85.             self.gridLayout.addWidget(self.gauge_title, 0,0,1,1)
86.
87.             self.voltage_title = QLabel('Reading')
88.             self.voltage_title.setFont(bold)
89.             self.gridLayout.addWidget(self.voltage_title, 0,1,1,1)
90.
91.             self.plot_title = QLabel('Plot')
92.             self.plot_title.setFont(bold)
93.             self.gridLayout.addWidget(self.plot_title, 0,2,1,1)
94.
95.             self.offset_title = QLabel('Offset')
96.             self.offset_title.setFont(bold)
97.             self.gridLayout.addWidget(self.offset_title, 0,3,1,1)
98.
99.                     #column 1
100.                    for i in range(p_channels/2-2):
101.                            vT = QLabel('%i'%(i+1))
102.                            self.gridLayout.addWidget(vT, i+1,0,1,1) #pos 2 - 7
103.
104.                    eT = QLabel('E+ U6-1')
105.                    self.gridLayout.addWidget(eT, p_channels/2-1,0,1,1)          #pos 8
106.
107.                    batt = QLabel('Battery')
108.                    self.gridLayout.addWidget(batt, p_channels/2,0,1,1) #pos 9
109.
110.                    for i in range(p_channels/2-2):
111.                            vT = QLabel('%i'%(i+p_channels/2-1))
112.                            self.gridLayout.addWidget(vT, i+p_channels/2+1,0,1,1)
    #pos 10 - 15
```

```
113.
114.                 eT = QLabel('E+ U6-2')
115.                 self.gridLayout.addWidget(eT, p_channels-1,0,1,1) #pos 16
116.
117.                 tT = QLabel('TEMP')
118.                 self.gridLayout.addWidget(tT, p_channels,0,1,1) #pos 17
119.
120.                         #column 2
121.                 for i in range(p_channels):
122.                         self.vL = QLabel('0.000000', self)
123.                         self.vL.my_index = i
124.                         v_labels.append(self.vL)
125.                         self.gridLayout.addWidget(self.vL, i+1,1,1,1)
126.
127.                         #column 3
128.                 self.checkboxes = []
129.                 self.plots = []
130.                 self.plot_data = []
131.                 for i in range(p_channels):
132.                         cb = QCheckBox()
133.                         cb.my_index = i
134.                         self.checkboxes.append(cb)
135.                         self.plots.append(None)
136.                         self.plot_data.append(None)
137.                         cb.toggled.connect(self.check_toggled)
138.                         self.gridLayout.addWidget(cb, i+1,2,1,1)
139.
140.                         #column 4
141.
142.                 self.offsets = []
143.                 for i in range(p_channels):
144.                         cb = QLineEdit()
145.                         cb.setValidator(QDoubleValidator(-9999999,9999999, 5))
146.                         cb.setFixedWidth(50)
147.                         cb.setText('0.0')
148.                         cb.my_index = i
149.                         self.offsets.append(cb)
150.                         self.gridLayout.addWidget(cb, i+1,3,1,1)
151.
152.                 #vertical layout (left column, grid, spacer)
153.                 self.verticalLayout_1 = QVBoxLayout()
154.
155.                 #set sampling frequency, duration, & wait
```

```
156.            self.freq1_hlayout = QHBoxLayout()
157.            self.freq_1 = QSpinBox()
158.            self.freq_1.setValue(10)
159.            self.freq_1.setRange(1,100)
160.            self.freq_1_title = QLabel('Frequency (Hz):')
161.            self.freq_1_title.setFont(bold)
162.            self.freq1_hlayout.addWidget(self.freq_1_title)
163.            self.freq1_hlayout.addWidget(self.freq_1)
164.            self.verticalLayout_1.addLayout(self.freq1_hlayout)
165.
166.            self.collect_dur_hlayout = QHBoxLayout()
167.            self.collect_dur = QSpinBox()
168.            self.collect_dur.setRange(1,9999)
169.            self.collect_dur.setValue(999)
170.            self.collect_dur_title = QLabel('Duration (s):')
171.            self.collect_dur_title.setFont(bold)
172.            self.collect_dur_hlayout.addWidget(self.collect_dur_title)
173.            self.collect_dur_hlayout.addWidget(self.collect_dur)
174.            self.verticalLayout_1.addLayout(self.collect_dur_hlayout)
175.
176.            self.wait_dur_hlayout = QHBoxLayout()
177.            self.wait_dur = QSpinBox()
178.            self.wait_dur.setValue(5)
179.            self.wait_dur.setRange(1,9999)
180.            self.wait_dur_title = QLabel('Wait (s):')
181.            self.wait_dur_title.setFont(bold)
182.            self.wait_dur_hlayout.addWidget(self.wait_dur_title)
183.            self.wait_dur_hlayout.addWidget(self.wait_dur)
184.            self.verticalLayout_1.addLayout(self.wait_dur_hlayout)
185.
186.            self.verticalLayout_1.addLayout(self.gridLayout)
187.
188.            self.spacerItem_1 = QSpacerItem(20, 40, QSizePolicy.Minimum,
189.                    QSizePolicy.Expanding)
190.            self.verticalLayout_1.addItem(self.spacerItem_1)
191.
192.            # horizontal layout 1 (grid layout + plot window)
193.            self.horizontalLayout_1 = QHBoxLayout()
194.
195.            self.horizontalLayout_1.addLayout(self.verticalLayout_1)
196.
197.            self.v_plot_layout = QVBoxLayout()
198.            self.win = pg.GraphicsLayoutWidget()
```

```
199.                    self.plotter = self.win
200.                    self.v_plot_layout.addWidget(self.plotter)
201.
202.                    # display value type
203.
204.                    self.volts_chkbox = QRadioButton()
205.                    self.volts_chkbox_title = QLabel('Volts')
206.                    self.volts_chkbox.setChecked(True)
207.
208.                    self.force_chkbox = QRadioButton()
209.                    self.force_chkbox_title = QLabel('Force')
210.
211.                    self.display_type_layout = QHBoxLayout()
212.                    self.display_type_layout.addWidget(self.volts_chkbox)
213.                    self.display_type_layout.addWidget(self.volts_chkbox_title)
214.                    self.display_type_layout.addWidget(self.force_chkbox)
215.                    self.display_type_layout.addWidget(self.force_chkbox_title)
216.
217.                    self.display_type_spacer = QSpacerItem(40, 20,
    QSizePolicy.Expanding,
218.                            QSizePolicy.Minimum)
219.                    self.display_type_layout.addItem(self.display_type_spacer)
220.
221.                    self.v_plot_layout.addLayout(self.display_type_layout)
222.
223.                    self.horizontalLayout_1.addLayout(self.v_plot_layout)
224.
225.                    # horizontal layout 2 (time title + time label + spacer)
226.
227.                    self.horizontalLayout_2 = QHBoxLayout()
228.
229.                    self.time_title = QLabel('Time:')
230.                    self.time_title.setFont(bold)
231.                    self.horizontalLayout_2.addWidget(self.time_title)
232.
233.                    self.time_label = QLabel('0.00', self)
234.                    self.horizontalLayout_2.addWidget(self.time_label)
235.
236.                    spacerItem_2 = QSpacerItem(40, 20, QSizePolicy.Expanding,
237.                            QSizePolicy.Minimum)
238.                    self.horizontalLayout_2.addItem(spacerItem_2)
239.
240.                    # horizontal layout 3 (file title + file label + spacer)
```

```
241.            self.horizontalLayout_3 = QHBoxLayout()
242.
243.            self.file_title = QLabel('File:')
244.            self.file_title.setFont(bold)
245.
246.            self.write_cb = QCheckBox()
247.
248.            self.horizontalLayout_3.addWidget(self.write_cb)
249.            self.horizontalLayout_3.addWidget(self.file_title)
250.
251.            self.file_label = QLabel('"Check to write to file"', self)
252.            self.horizontalLayout_3.addWidget(self.file_label)
253.
254.            spacerItem_3 = QSpacerItem(40, 20, QSizePolicy.Expanding,
255.                    QSizePolicy.Minimum)
256.            self.horizontalLayout_3.addItem(spacerItem_3)
257.
258.            # horizontal layout 4 (run button + file dialog button + spacer)
259.            self.horizontalLayout_4 = QHBoxLayout()
260.
261.            self.button = QPushButton('Start', self)
262.            self.button.clicked.connect(self.run_button)
263.            self.horizontalLayout_4.addWidget(self.button)
264.
265.            spacerItem_4 = QSpacerItem(40, 20, QSizePolicy.Expanding,
266.                    QSizePolicy.Minimum)
267.            self.horizontalLayout_4.addItem(spacerItem_4)
268.
269.            # vertical layout (encompassing)
270.
271.            self.verticalLayout_2 = QVBoxLayout()
272.
273.            self.verticalLayout_2.addLayout(self.horizontalLayout_4)
274.            self.verticalLayout_2.addLayout(self.horizontalLayout_3)
275.            self.verticalLayout_2.addLayout(self.horizontalLayout_2)
276.            self.verticalLayout_2.addLayout(self.horizontalLayout_1)
277.
278.            # main layout
279.            self.main_frame = QWidget()
280.
281.            self.setCentralWidget(self.main_frame)
282.            self.main_frame.setLayout(self.verticalLayout_2)
283.
```

```
284.                    self.checkboxes[0].setChecked(True) #set first checkbox to
    checked
285.
286.            def create_status_bar(self):
287.
288.                    self.status_text = QLabel('Monitor idle')
289.                    self.statusBar().addWidget(self.status_text, 1)
290.
291.            def run_button(self):
292.
293.                    if self.running == False:
294.                            self.running = True
295.
296.                            self.show_dialog()
297.
298.                            self.time_on_press = time.time()
299.
300.                            self.timer = QTimer()
301.                            self.timer.timeout.connect(self.run_loop)
302.
303.                            self.on_start()
304.
305.                            self.freq_1.setEnabled(False)
306.                            self.collect_dur.setEnabled(False)
307.                            self.wait_dur.setEnabled(False)
308.                            self.write_cb.setEnabled(False)
309.
310.                            self.button.setText('Stop')
311.
312.                    elif self.running == True:
313.                            self.running = False
314.
315.                            self.on_stop()
316.
317.                            self.freq_1.setEnabled(True)
318.                            self.collect_dur.setEnabled(True)
319.                            self.wait_dur.setEnabled(True)
320.                            self.write_cb.setEnabled(True)
321.
322.                            self.button.setText('Start')
323.
324.    def show_dialog(self):
325.                    if self.write_cb.isChecked():
```

```
326.                                self.file_name = QFileDialog.getSaveFileName(self, 'Save
    file', '.raw')
327.
328.                                with open(self.file_name, "w") as file:
329.
330.                                        file.write(str(datetime.datetime.now(
331.                                                ).strftime("#%Y-%m-%d
    %H:%M:%S"))+'\n')
332.                                        file.write('#PC'+'\n')
333.                                        file.write('#freq: '+str(self.freq_1.value())+'\n')
334.                                        file.write('#collect dur:
    '+str(self.collect_dur.value())+'\n')
335.                                        file.write('#wait dur:
    '+str(self.wait_dur.value())+'\n'+'#\n')
336.
337.                                        file.write('#Day'+'\t')
338.
339.                                        file.write('Time (s)'+'\t')
340.
341.                                        for i in range(p_channels/2-2):
342.                                                file.write('Voltage_%i (V)'%(i+1)+'\t')
343.
344.                                        file.write('E+(u6_1) (V)'+'\t')
345.                                        file.write('Battery (V)'+'\t')
346.
347.                                        for i in range(p_channels/2-2):
348.                                                file.write('Voltage_%i (V)'%(i+8)+'\t')
349.
350.                                        file.write('E+(u6_1) (V)'+'\t')
351.                                        file.write('Temp (V)')
352.
353.                                        file.write('\n')
354.                                        file.close()
355.
356.                                self.file_label.setText(self.file_name)
357.                                self.file = open(self.file_name, "a")
358.
359.                        else:
360.                                None
361.
362.                def     excitation(self):
363.                        # d.writeRegister(DAC0_REGISTER, 4.5)
364.
```

```
365.                    if platform.system() == 'Linux':
366.                            GPIO.output("P9_12", GPIO.LOW)
367.
368.            def on_start(self):
369.                    self.excitation()
370.
371.                    self.timer.start(1000/self.freq_1.value())
372.
373.                    self.wait_timer = QTimer()
374.                    self.wait_timer.setSingleShot(True)
375.                    self.wait_timer.setInterval(self.collect_dur.value()*1000)
376.                    self.wait_timer.timeout.connect(self.on_pause)
377.                    self.wait_timer.start()
378.
379.                    self.status_text.setText('Monitor running...')
380.
381.            def on_stop(self):
382.
383.                    if platform.system() == 'Linux':
384.                            GPIO.output("P9_12", GPIO.LOW)
385.
386.                    self.timer.stop()
387.                    self.wait_timer.stop()
388.
389.                    for i in range(p_channels):
390.                            del v_arrays[i][:]
391.
392.                    del time_array[:]
393.
394.                    self.status_text.setText('Monitor stopped')
395.
396.                    if self.write_cb.isChecked():
397.                            self.file.close()
398.
399.            def on_resume(self):
400.
401.                    if platform.system() == 'Linux':
402.                            GPIO.output("P9_12", GPIO.LOW)
403.
404.                    time.sleep(5)
405.
406.                    #u6_1.open()
407.                    #u6_2.open()
```

```
408.
409.                     u6_1 = u6.U6(serial = 360008508)
410.                     u6_2 = u6.U6(serial = 360009180)
411.
412.                     time.sleep(1)
413.
414.
415.                     self.timer.start(1000/self.freq_1.value())
416.
417.                     self.wait_timer = QTimer()
418.                     self.wait_timer.setSingleShot(True)
419.                     self.wait_timer.setInterval(self.collect_dur.value()*1000)
420.                     self.wait_timer.timeout.connect(self.on_pause)
421.                     self.wait_timer.start()
422.
423.                     self.status_text.setText('Monitor running...')
424.
425.             def on_pause(self):
426.                     self.timer.stop()
427.
428.                     #u6_1.close()
429.                     #u6_2.close()
430.
431.                     if platform.system() == 'Linux':
432.                             GPIO.output("P9_12", GPIO.HIGH)
433.
434.
435.
436.                     self.wait_timer = QTimer()
437.                     self.wait_timer.setSingleShot(True)
438.                     self.wait_timer.setInterval(self.wait_dur.value()*1000)
439.                     self.wait_timer.timeout.connect(self.on_resume)
440.                     self.wait_timer.start()
441.
442.                     self.status_text.setText('Monitor waiting...')
443.
444.
445.
446.
447.             def run_loop(self):
448.                     t = time.time() - 1348272000 #WS datum: 9/22/2012 00:00:00, AK
    time (no DST)
449.                     days = int(t/86400)
```

```
450.                    secs = '{0:.2f}'.format(t - days * 86400)
451.                    clock_time = round((time.time() - self.time_on_press), 3)
452.
453.                    self.time_label.setText(str(days)+' ('+str(secs)+')')
454.
455.                    time_array.append(clock_time)
456.                    if len(time_array) > 100:
457.                            time_array.pop(0)
458.
459.                    if self.write_cb.isChecked():
460.                            self.file.write(str(days)+'\t')
461.                            self.file.write(str(secs)+'\t')
462.
463.                    for i in range(p_channels):
464.
465.                            if i < p_channels/2-2:
466.                                    ainBits = u6_1.getFeedback(feedbackArguments[i])
467.                                    v =
    u6_1.binaryToCalibratedAnalogVoltage(gainIndex=GAIN_INDEX,
468.                                            bytesVoltage=ainBits[0], is16Bits=False)
469.
470.                            elif i == p_channels/2-2:
471.                                    ainBits =
    u6_1.getFeedback(u6.AIN24(PositiveChannel=12,
472.                                            ResolutionIndex=8, GainIndex = 0,
    Differential = False))
473.                                    v =
    u6_1.binaryToCalibratedAnalogVoltage(gainIndex=0,
474.                                            bytesVoltage=ainBits[0], is16Bits=False)
475.
476.                            elif i == p_channels/2-1:
477.                                    ainBits =
    u6_1.getFeedback(u6.AIN24(PositiveChannel=13,
478.                                            ResolutionIndex=8, GainIndex = 0,
    Differential = False))
479.                                    v =
    u6_1.binaryToCalibratedAnalogVoltage(gainIndex=0,
480.                                            bytesVoltage=ainBits[0], is16Bits=False)
481.
482.                            elif i == p_channels-2:
483.                                    ainBits =
    u6_2.getFeedback(u6.AIN24(PositiveChannel=12,
```

```
484.                                        ResolutionIndex=8, GainIndex = 0,
    Differential = False))
485.                                v =
    u6_1.binaryToCalibratedAnalogVoltage(gainIndex=0,
486.                                        bytesVoltage=ainBits[0], is16Bits=False)
487.
488.                            elif i == p_channels-1:
489.                                ainBits =
    u6_2.getFeedback(u6.AIN24(PositiveChannel=13,
490.                                        ResolutionIndex=8, GainIndex = 0,
    Differential = False))
491.                                v =
    u6_1.binaryToCalibratedAnalogVoltage(gainIndex=0,
492.                                        bytesVoltage=ainBits[0], is16Bits=False)
493.
494.                            elif i > p_channels/2-1:
495.                                ainBits = u6_2.getFeedback(feedbackArguments[i-
    p_channels/2])
496.                                v =
    u6_2.binaryToCalibratedAnalogVoltage(gainIndex=GAIN_INDEX,
497.                                        bytesVoltage=ainBits[0], is16Bits=False)
498.
499.                            if i < p_channels-1:
500.                                if self.force_chkbox.isChecked():
501.                                    if not v_arrays[6]:
502.                                        ex = 1
503.                                    else:
504.                                        ex = v_arrays[6].pop()
505.
506.
        v_labels[i].setText(str((v*force_cal_array[i]/ex+float(self.offsets[i].text() ))))
507.
        v_arrays[i].append(v*force_cal_array[i]/ex+float(self.offsets[i].text() ))
508.                                else:
509.
        v_labels[i].setText(str(v+float(self.offsets[i].text() )))
510.
        v_arrays[i].append(v+float(self.offsets[i].text() ))
511.
512.                            elif i == p_channels-1:
513.                                temp = ((100*v)-273.15)*1.8+32
514.                                v_labels[i].setText(str(temp))
515.                                v_arrays[i].append(v)
```

```
516.
517.                             if self.write_cb.isChecked():
518.                                     self.file.write(str(v)+'\t')
519.
520.                             if len(v_arrays[i]) > 100:
521.                                     v_arrays[i].pop(0)
522.
523.                     if self.write_cb.isChecked():
524.                             self.file.write('\n')
525.
526.                     self.update_plot()
527.
528.             def check_toggled(self):
529.                     cb = self.sender()
530.                     i = cb.my_index
531.                     if cb.isChecked():
532.                             if i < p_channels/2-1:
533.                                     plot = self.win.addPlot(title="%d"%(i+1), col=1,
    row=i+1)
534.                             elif i == p_channels/2-1 or i == p_channels-1:
535.                                     plot = self.win.addPlot(title="%d"%(i+1), col=1,
    row=i+1)
536.                             elif i > p_channels/2-1:
537.                                     plot = self.win.addPlot(title="%d"%(i), col=1,
    row=i+1)
538.
539.                             if self.force_chkbox.isChecked():
540.                                     plot.setLabel('bottom', 'Time', units='s')
541.                                     plot.setLabel('left', 'Force', units ='  kip')
542.                             else:
543.                                     plot.setLabel('bottom', 'Time', units='s')
544.                                     plot.setLabel('left', 'Volts', units ='V')
545.
546.                             self.plots[i] = plot
547.                             self.plot_data[i] = plot.plot()
548.                     else:
549.                             self.win.removeItem(self.plots[i])
550.
551.             def update_plot(self):
552.                     for i in range(p_channels):
553.                             if self.checkboxes[i].isChecked():
554.                                     self.plot_data[i].setData(time_array, v_arrays[i])
555.
```

```
556.
557.    def main():
558.            app = QApplication(sys.argv)
559.            window = Window()
560.            window.show()
561.            app.exec_()
562.
563.
564.    if    name__== "    main    ":
565.       main()
```

Appendix K

Inspection Reports

Table K-1 contains the HMLP inspection reports the AK Department of Transportation and Public Facilities gathered from 2007-2011.

Table K-1: AKDOT&PF HMLP Inspection Reports, 2007-2011

Tower Title	Height (ft)	Anchor Rod Diameter (in)	Rod Material	# Rods	# of Nuts Loose	Foundation Type
Glenn Artillery 1	165	1.875	F1554	16	3	Base Plate
Glenn Artillery 2	165	1.875	F1554	16		Base Plate
Glenn Boniface 1	170	1.875	F1554	16		CIP Cap
Glenn Boniface 2	150	1.875	F1554	16		CIP Cap
Glenn Boniface 3	170	1.875	F1554	16		CIP Cap
Glenn Boniface 4	170	1.875	F1554	16		CIP Cap
Glenn Bragaw 1-1	120	2	F1554	12	10	CIP Cap
Glenn Bragaw 1-2	120	2	F1554	12		CIP Cap
Glenn Bragaw 1-3	120	2	F1554	12		CIP Cap
Glenn Bragaw 2-1	120	2		12	11	CIP Cap
Glenn Bragaw 2-2	120	2		12		CIP Cap
Glenn Bragaw 2-3	120	2		12		CIP Cap
Glenn Bragaw 3-1	120	2		12	8	CIP Cap
Glenn Bragaw 3-2	120	2		12		CIP Cap
Glenn Bragaw 3-3	120	2		12		CIP Cap
Glenn Hiland 1	170	2	F1554	16		CIP Cap
Glenn Hiland 2	170	2	F1554	16		CIP Cap
Glenn Hiland 3	170	2	F1554	16		CIP Cap
Glenn Hiland 4	170	2	F1554	16		CIP Cap
Glenn Muldoon 1	170	1.875	F1554	16		CIP Cap
Glenn Muldoon 2	170	1.875	F1554	16		CIP Cap
Glenn Muldoon 3	170	1.875	F1554	16		CIP Cap

Glenn Muldoon 4	170	1.875	F1554	16		CIP Cap
Glenn Muldoon 5	170	1.875	F1554	16		CIP Cap
Glenn Muldoon 6	165	1.5	A325	12	1	Base Plate
Glenn Muldoon 7	165	1.5	A325	12	1	Base Plate
Glenn Neagle 1	170	1.875	F1554	16		CIP Cap
Glenn Neagle 2	170	1.875	F1554	16	14	CIP Cap
Glenn Neagle 3	170	1.875	F1554	16	8	CIP Cap
Glenn Neagle 4	170	1.875	F1554	16	4	CIP Cap
Glenn Neagle 5	170	1.875	F1554	16	6	CIP Cap
Glenn Neagle 6	170	1.875	F1554	16	7	CIP Cap
Glenn-Parks 1	150	1.875		16	3	Base Plate
Glenn-Parks 2	150	1.875		12	3	Base Plate
Glenn-Parks 3	150	1.875		12	2	Base Plate
Glenn-Parks 4	150	1.875		12		Base Plate
Glenn-Parks 5	150	1.875		12	1	Base Plate
Glenn-Parks 6	150	1.875		12	1	Base Plate
Glenn-Parks 7	150	1.875		12	1	Base Plate
Glenn-Parks 8	150	1.875		12	2	Base Plate
Glenn-SBirchwood 1	170	2	F1554	16		CIP Cap
Glenn-SBirchwood 2	170	2	F1554	16		CIP Cap
Glenn-SBirchwood 3	170	2	F1554	16		CIP Cap
Glenn-SBirchwood 4	170	2	F1554	16		CIP Cap
Glenn-SBirchwood 5	150	2	F1554	16	1	CIP Cap
Glenn-SBirchwood 6	150	2	F1554	16		CIP Cap
Glenn-Weighsta 1	150	1.5		12	1	Base Plate
Glenn-Weighsta 2-1	150	1.5		12		Base Plate
Glenn-Weighsta 2-2	150	1.5		12	1	Base Plate
Minn-Dimond 1-1	165	2	F1554	16	2	CIP Cap
Minn-Dimond 1-2	165	2	F1554	16	1	CIP Cap
Minn-Dimond 1-3	165	2	F1554	16		CIP Cap
Minn-Dimond 2-1	150	2	F1554	16	2	CIP Cap
Minn-Dimond 2-2	150	2	F1554	16		CIP Cap
Minn-Dimond 2-3	150	2	F1554	16		CIP Cap
Minn-Dimond 3-1	150	2	F1554	16	2	CIP Cap

Minn-Dimond 3-2	150	2	F1554	16		CIP Cap
Minn-Dimond 3-3	150	2	F1554	16		CIP Cap
Minn-Dimond 4-1	170	2	F1554	16	1	CIP Cap
Minn-Dimond 4-2	170	2	F1554	16		CIP Cap
Minn-Dimond 4-3	170	2	F1554	16		CIP Cap
Minn-Dimond 5-1	175	2	F1554	16	3	CIP Cap
Minn-Dimond 5-2	175	2	F1554	16		CIP Cap
Minn-Dimond 5-3	175	2	F1554	16		CIP Cap
Minn-Intern 1-1	170	1.875	F1554	16		CIP Cap
Minn-Intern 1-2	170	1.875	F1554	16		CIP Cap
Minn-Intern 2-1	170	1.875	F1554	16	8	CIP Cap
Minn-Intern 2-2	170	1.875	F1554	16	8	CIP Cap
Minn-Rasp 1-1	170	1.875	F1554	16		CIP Cap
Minn-Rasp 1-2	170	1.875	F1554	16		CIP Cap
Minn-Rasp 2-1	150	1.875	F1554	16		CIP Cap
Minn-Rasp 2-2	150	1.875	F1554	16		CIP Cap
Minn-Rasp 3-1	170	1.875	F1554	16		CIP Cap
Minn-Rasp 3-2	170	1.875	F1554	16		CIP Cap
Minn-Rasp 4-1	170	1.875	F1554	16		CIP Cap
Minn-Rasp 4-2	170	1.875	F1554	16		CIP Cap
Minn-Rasp 5-1	170	1.875	F1554	16		CIP Cap
Minn-Rasp 5-2	170	1.875	F1554	16		CIP Cap
Minn-W100 1-1	170	1.875	F1554	16		CIP Cap
Minn-W100 1-2	170	1.875	F1554	16		CIP Cap
Minn-W100 2-1	160	1.875	F1554	16	2	CIP Cap
Minn-W100 2-2	160	1.875	F1554	16		CIP Cap
Minn-W100 3-1	160	1.875	F1554	16		CIP Cap
Minn-W100 3-2	160	1.875	F1554	16		CIP Cap
Minn-W100 4-1	170	1.875		16	1	CIP Cap
Minn-W100 4-2	170	1.875		16	1	CIP Cap
Omalley-C 1-1	165	2	F1554	16		CIP Cap
Omalley-C 1-2	165	2	F1554	16		CIP Cap
Omalley-C 2-1	165	2	F1554	16		CIP Cap
Omalley-C 2-2	165	2	F1554	16		CIP Cap
Omalley-C 3-1	165	2	F1554	16		CIP Cap
Omalley-C 3-2	165	2	F1554	16		CIP Cap
Omalley-C 4-1	165	2	F1554	16		CIP Cap
Omalley-C 4-2	165	2	F1554	16		CIP Cap

Omalley-C 5-1	150	2	F1554	16		CIP Cap
Omalley-C 5-2	150	2	F1554	16		CIP Cap
Omalley-C 6-1	150	2	F1554	16	1	CIP Cap
Omalley-C 6-2	150	2	F1554	16	1	CIP Cap
Parks-Hyer 1	153	2		16		Base Plate
Parks-Hyer 2	153	2		16		Base Plate
Parks-Hyer 3	151	2		16	1	Base Plate
Parks-Hyer 4	154	2		16	2	Base Plate
Parks-Hyer 5	161	2		16		Base Plate
Parks-Smeridian 1	175	1.875		16		Base Plate
Parks-Smeridian 2	175	1.875		16		Base Plate
Parks-Smeridian 3	175	1.875		16	5	Base Plate
Parks-Smeridian 4	175	1.875		16		Base Plate
Parks-Smeridian 5	175	1.875		16	6	Base Plate
Parks-Trunk 1	120	1.875	F1554	16		Base Plate
Parks-Trunk 2	120	1.875	F1554	16		Base Plate
Rich-Badger 1-1	165	2	F1554	16		CIP Cap
Rich-Badger 1-2	165	2	F1554	16		CIP Cap
Rich-Badger 2-1	165	2	F1554	16	1	CIP Cap
Rich-Badger 2-2	165	2	F1554	16		CIP Cap
Rich-Badger 3-1	165	2	F1554	16		CIP Cap
Rich-Badger 3-2	165	2	F1554	16		CIP Cap
Rich-Badger 4-1	165	2	F1554	16		CIP Cap
Rich-Badger 4-2	165	2	F1554	16	1	CIP Cap
Sew-Dimond 1-1	175	2	F1554	16	4	CIP Cap
Sew-Dimond 1-2	175	2	F1554	16		CIP Cap
Sew-Dimond 2-1	175	2	F1554	16	8	CIP Cap
Sew-Dimond 2-2	175	2	F1554	16		CIP Cap
Sew-Dimond 3-1	175	2	F1554	16		CIP Cap
Sew-Dimond 4-1	175	2	F1554	16	4	CIP Cap
Sew-Dimond 4-2	175	2	F1554	16	2	CIP Cap
Sew-Dimond 5-1	175	2	F1554	16	8	CIP Cap
Sew-Dimond 5-2	175	2	F1554	16		CIP Cap
Sew-Dearmoun 1-1	170	2	F1554	16	1	CIP Cap
Sew-Dearmoun	170	2	F1554	16		CIP Cap

1-2						
Sew-Dearmoun 1-3	170	2	F1554	16		CIP Cap
Sew-Dearmoun 2-1	170	2	F1554	16		CIP Cap
Sew-Dearmoun 2-2	170	2	F1554	16		CIP Cap
Sew-Dearmoun 2-3	170	2	F1554	16		CIP Cap
Sew-Dowling 1-1	170	2	F1554	16		CIP Cap
Sew-Dowling 1-2	170	2	F1554	16	2	CIP Cap
Sew-Dowling 2-1	170	2	F1554	16		CIP Cap
Sew-Dowling 2-2	170	2	F1554	16		CIP Cap
Sew-Dowling 3-1	170	2	F1554	16		CIP Cap
Sew-Dowling 3-2	170	2	F1554	16		CIP Cap
Sew-Dowling 4-1	170	2	F1554	16	2	CIP Cap
Sew-Dowling 4-2	170	2	F1554	16		CIP Cap
Sew-Huffman 1-1	170	1.875	F1554	16	6	CIP Cap
Sew-Huffman 1-2	170	1.875	F1554	16		CIP Cap
Sew-Huffman 2-1	170	1.875	F1554	16	1	CIP Cap
Sew-Huffman 2-2	170	1.875	F1554	16		CIP Cap
Sew-Huffman 3-1	150	1.875	F1554	16		CIP Cap
Sew-Huffman 3-2	150	1.875	F1554	16		CIP Cap
Sew-Huffman 4-1	170	1.875	F1554	16	2	CIP Cap
Sew-Huffman 4-2	170	1.875	F1554	16		CIP Cap
Sew-Huffman 5-1	170	1.875	F1554	16		CIP Cap
Sew-Huffman 5-2	170	1.875	F1554	16	1	CIP Cap
Seward-Omalley 1-1	170	2	F1554	16		CIP Cap
Seward-Omalley 1-2	170	2	F1554	16		CIP Cap
Seward-Omalley 2-1	170	2	F1554	16		CIP Cap
Seward-Omalley 2-2	170	2	F1554	16		CIP Cap
Seward-Omalley 3-1	170	2	F1554	16		CIP Cap
Seward-Omalley 3-2	170	2	F1554	16		CIP Cap
Seward-Omalley 4-1	170	2	F1554	16		CIP Cap
Seward-Omalley 4-2	170	2	F1554	16		CIP Cap
Seward-Omalley	170	2	F1554	16	1	CIP Cap

5-1					
Seward-Omalley 5-2	170	2	F1554	16	CIP Cap
Seward-Omalley 5-3	170	2	F1554	16	CIP Cap
Seward-Rabbit 1-1	165	2	F1554	16	CIP Cap
Seward-Rabbit 1-2	165	2	F1554	16	CIP Cap
Seward-Rabbit 2-1	165	2	F1554	16	CIP Cap
Seward-Rabbit 2-2	165	2	F1554	16	CIP Cap
Seward-Rabbit 3-1	165	2	F1554	16	CIP Cap
Seward-Rabbit 3-2	165	2	F1554	16	CIP Cap
Seward-Rabbit 4-1	165	2	F1554	16	CIP Cap
Seward-Rabbit 4-2	165	2	F1554	16	CIP Cap
Seward-Tudor 1-1	170	2	F1554	16	CIP Cap
Seward-Tudor 1-2	170	2	F1554	16	CIP Cap
Seward-Tudor 2-1	170	2	F1554	16	CIP Cap
Seward-Tudor 2-2	170	2	F1554	16	CIP Cap
Seward-Tudor 3-1	170	2	F1554	16	CIP Cap
Seward-Tudor 3-2	170	2	F1554	16	CIP Cap

:

Appendix L

Strain gauging Procedure

The steps taken to ensure the strain gauges were installed properly in the anchor rods and the items used are summarized below.

M-Bond AE 10 strain gage epoxy (resin, curing agent)

2mm diameter hole 6" deep has a volume of 0.5cc.

Needle is 5.5" long.

Uncoil at least 6" of strain gage wire. Mark 5.5" distance from the bottom of the strain gage on the wire. (0.5" minimum clearance from the bottom) Insert uncoiled strain gage into hole until the mark is flush with the opening.

Remove resin and curing agent from refrigerator, let warm at room temperature for 30 minutes. Fill dropper to "10" mark with curing agent. Insert into bottle of resin. Mix for 3 minutes (not 5). Glass jar bottom should be hot to the touch. If bottom is not hot, mix for 2 more minutes (5 total).

Once epoxy is mixed fully, its workability for this procedure is 10-15 minutes.

Remove plunger from syringe/needle. Funnel 2.0cc mixed resin/curing agent into the syringe. (Syringes used had 3.0cc max volume, leave at least 1.0cc of volume left for plunger.)

Slide needle into hole along wall opposite of strain gage. Take care not to puncture the strain gage wire. Needle should not contact the bottom of the hole, it should be at least 0.5" from the bottom. To push epoxy into the hole, apply enough force onto the plunger that its bottom is in constant contact with the epoxy mixture. Once 0.30cc of mixture has been freed from the syringe, pull the needle up so that the bottom sits 1" below the

surface of the hole. Continue inserting epoxy until epoxy can be visibly seen extruding from the hole's surface onto the flat of the bolt. Once this is done, repeat this procedure for the remaining bolts.

Appendix M

Turn-of-the-Nut Rotation Table

Table M-1 contains the FHWA recommended Turn-of-The-Nut rotation for mild steel bolts in double-nut-moment connection HMLP configurations.

Table M-1: FHWA Recommended Turn-of-the-Nut Rotation

TABLE 8

Nut Rotation for Turn-Of-Nut Pretensioning

Anchor Rod Diameter, in*.	Nut Rotation from Snug-Tight Condition a, b, c	
	F1554 Grade 36	F1554 Grades 55 and 105 A615 and A706 Grade 60
<1 1/2	1/6 Turn	1/3 Turn
>1 1/2	1/12 Turn	1/6 Turn

a. Nut rotation is relative to anchor rod. The tolerance is plus 20 degrees.
b. Applicable only to double-nut-moment joints.
c. Beveled washer should be used if: a) the nut is not in firm contact with the base plate; or b) the outer face of the base plate is sloped more than 1:40.

Appendix N

ASCE 7-10 Design Wind Calculations

The design wind moments applied to HMLPs were based off of 100 mph wind velocities in each configuration. They were calculated using the requirements in section 29.5, Design Wind Loads on Other Structures in *Minimum Design Loads for Buildings and Other Structures* [15]. They are determined by the following equation:

$$(\quad)\qquad\qquad \text{(Tables N-1 and N-2)}$$
(Exposure C Assumed)

Giosan [9] showed HMLPs have first mode natural frequencies between 0.88-1.20Hz. Section 26.9 of *Minimum Design Loads* [15] allows for a G of 0.85 when a tall slender structure has a natural period of 1 second or less. Since the natural period is very close to 1 second, G is taken as 0.85.

(Table N-1 and N-2)

Table N-1 shows the calculation for the total moment applied to the pole used in scenarios A & C in Chapter 3.

Table N-1: ASCE 7-10 Moment Calculation Scenarios A & C

HMLP A & C	Min Height (ft)	Max Height (ft)	Avg. Pole Diameter (in)	Af (ft^2)	Kz	qz (lb/ft^2)	F (lb)	Moment (k*in)
Section 1	0	5	26.15	16.30	0.85	20.67	200.49	6.01
Section 2	5	10	25.45	15.86	0.85	20.67	195.12	29.27
Section 3	10	15	24.75	15.43	0.85	20.67	189.76	51.23
Section 4	15	20	24.05	14.99	0.90	21.89	195.23	76.14
Section 5	20	25	23.35	14.55	0.94	22.86	197.98	100.97
Section 6	25	30	22.65	14.12	0.98	23.83	200.21	126.13
Section 7	30	35	21.95	13.68	0.98	23.83	194.03	145.52
Section 8	35	40	21.25	13.25	1.04	25.29	199.34	173.42
Section 9	40	45	20.55	12.81	1.04	25.29	192.77	190.84
Section 10	45	50	19.85	12.37	1.09	26.51	195.16	216.63
Section 11	50	55	19.15	11.94	1.09	26.51	188.28	231.58
Section 12	55	60	18.45	11.50	1.13	27.48	188.05	253.87
Section 13	60	65	17.75	11.06	1.13	27.48	180.92	265.95
Section 14	65	70	17.05	10.63	1.17	28.45	179.93	286.09
Section 15	70	75	16.35	10.19	1.17	28.45	172.55	295.05
Section 16	75	80	15.65	9.76	1.21	29.43	170.80	312.57
Section 17	80	85	14.95	9.32	1.21	29.43	163.16	318.17
Section 18	85	90	14.25	8.88	1.24	30.16	159.38	329.92
Section 19	90	95	13.55	8.45	1.24	30.16	151.55	331.90
Section 20	95	100	12.85	8.01	1.26	30.64	146.04	337.35
Section 21	100	105	12.15	7.57	1.26	30.64	138.09	335.55
Section 22	105	110	11.45	7.14	1.26	30.64	130.13	331.83
Section 23	110	115	10.75	6.70	1.26	30.64	122.17	326.20
Section 24	115	120	10.05	6.26	1.31	31.86	118.75	331.32
Section 25	120	125	9.35	5.83	1.31	31.86	110.48	321.50
Section 26	125	130	8.65	5.39	1.31	31.86	102.21	309.69
Section 27	130	135	7.95	4.96	1.31	31.86	93.94	295.90
Section 28	135	140	7.25	4.52	1.36	33.08	88.94	290.82
Section 29	140	145	6.55	4.08	1.36	33.08	80.35	272.38
Section 30	145	150	5.85	3.65	1.36	33.08	71.76	251.88
Sum							4717.56	7145.71

The total moment calculated using this method is equal to 7145 k*in. This is similar to the manufacturer's moment calculation of 6765 k*in.

Table N-2 shows the calculation for the total moment applied to the pole used in scenario B in Chapter 3.

Table N-2: ASCE 7-10 Moment Calculation Scenario B

HMLP B	Min Height (ft)	Max Height (ft)	Avg. Pole Diameter (in)	Af (ft^2)	Kz	qz (lb/ft^2)	F (lb)	Moment (k*in)
Section 1	0	5	31.25	17.79	0.85	20.67	218.76	6.56
Section 2	5	10	30.55	17.39	0.85	20.67	213.86	32.08
Section 3	10	15	29.85	16.99	0.85	20.67	208.96	56.42
Section 4	15	20	29.15	16.59	0.90	21.89	216.06	84.26
Section 5	20	25	28.45	16.19	0.94	22.86	220.24	112.32
Section 6	25	30	27.75	15.79	0.98	23.83	223.97	141.10
Section 7	30	35	27.05	15.39	0.98	23.83	218.32	163.74
Section 8	35	40	26.35	15.00	1.04	25.29	225.69	196.35
Section 9	40	45	25.65	14.60	1.04	25.29	219.69	217.49
Section 10	45	50	24.95	14.20	1.09	26.51	223.97	248.61
Section 11	50	55	24.25	13.80	1.09	26.51	217.69	267.75
Section 12	55	60	23.55	13.40	1.13	27.48	219.16	295.87
Section 13	60	65	22.85	13.00	1.13	27.48	212.65	312.59
Section 14	65	70	22.15	12.61	1.17	28.45	213.43	339.35
Section 15	70	75	21.45	12.21	1.17	28.45	206.68	353.43
Section 16	75	80	20.75	11.81	1.21	29.43	206.77	378.40
Section 17	80	85	20.05	11.41	1.21	29.43	199.80	389.61
Section 18	85	90	19.35	11.01	1.24	30.16	197.60	409.04
Section 19	90	95	18.65	10.61	1.24	30.16	190.45	417.10
Section 20	95	100	17.95	10.22	1.26	30.64	186.26	430.27
Section 21	100	105	17.25	9.82	1.26	30.64	179.00	434.97
Section 22	105	110	16.55	9.42	1.26	30.64	171.74	437.93
Section 23	110	115	15.85	9.02	1.26	30.64	164.47	439.14
Section 24	115	120	15.15	8.62	1.31	31.86	163.45	456.02
Section 25	120	125	14.45	8.22	1.31	31.86	155.89	453.65
Section 26	125	130	13.75	7.83	1.31	31.86	148.34	449.48
Section 27	130	135	13.05	7.43	1.31	31.86	140.79	443.49
Section 28	135	140	12.35	7.03	1.36	33.08	138.32	452.32
Section 29	140	145	11.65	6.63	1.36	33.08	130.48	442.34
Section 30	145	150	10.95	6.23	1.36	33.08	122.64	430.48
Section 31	150	155	10.25	5.83	1.36	33.08	114.80	416.74
Sum							5651.17	9702.29

The total moment calculated for scenario B is equal to 9700 k*in. This is 12% larger than the manufacturer's moment calculation of 8768 k*in.